

Dynamics of galaxy cores and supermassive black holes

David Merritt

Department of Physics, Rochester Institute of Technology, Rochester, NY 14623, USA

E-mail: merritt@astro.rit.edu

Abstract. Recent work on the dynamical evolution of galactic nuclei containing supermassive black holes is reviewed. Topics include galaxy structural properties; collisionless and collisional equilibria; loss-cone dynamics; and dynamics of binary and multiple supermassive black holes.

1. Introduction

Galaxy cores are the hosts of supermassive black holes (SBHs), the engines of quasars and of active galactic nuclei. There is increasing evidence that SBHs play an important role in the formation and global evolution of galaxies and of the intergalactic medium (IGM) (Merloni et al. 2005). The energy released by the formation and growth of SBHs must have had a major impact on how gas cooled to form galaxies and galaxy clusters (Silk & Rees 1998). While the detailed history of SBH growth is still being debated, much work has focused on the possibility that the seeds of SBHs were black holes of much smaller mass—either remnants of the first generation of stars, so-called “Population III black holes” (Madau & Rees 2001), or the (still speculative) “intermediate-mass black holes” (IMBHs), remnants of massive stars that form in dense star cluster via physical collisions between stars (Portegies Zwart et al. 2004).

These exciting developments have led to a renewed interest in the dynamics and evolution of galactic nuclei. Early theoretical studies (Spitzer & Saslaw 1966, Spitzer & Stone 1967, Colgate 1967, Sanders 1970) emphasized stellar encounters and collisions as the dominant physical processes. In these models, the density of a compact ($\rho \gtrsim 10^6 M_\odot \text{pc}^{-3}$) stellar system gradually increases as energetic stars are scattered into elongated orbits via two-body (star-star) gravitational encounters. The increase in density leads to a higher rate of physical collisions between stars; when collision velocities exceed $\sim 10^3 \text{ km s}^{-1}$, roughly the escape velocity from a star, collisions liberate gas that falls to the center of the system and condenses into new stars which undergo further collisions. Begelman & Rees (1978) argued that the evolution of a dense nucleus would lead inevitably to the formation of a massive black hole at the center, either by runaway stellar mergers or by creation of a massive gas cloud which collapses. Subsequent studies (Duncan & Shapiro 1983, Quinlan & Shapiro 1987, Quinlan & Shapiro 1989, David et al. 1987*a*, David et al. 1987*b*) included “seed” BHs which grow via accretion of stars or gas liberated by stellar collisions or tidal disruptions.

A fundamental time scale in these models is the relaxation time determined by the stars, or

$$T_r \approx \frac{v_{rms}^3}{G^2 m_* \rho \ln \Lambda} \quad (1)$$

(Spitzer 1987), where v_{rms} is the stellar velocity dispersion, m_* and ρ are the stellar mass and mass density, and $\ln \Lambda \approx 10^1$ is the Coulomb logarithm. In a time T_r , gravitational (not physical) encounters between stars can exchange orbital energy and angular momentum, and stars in the high-velocity tail of the distribution will be ejected. The result, after a time $T_{cc} \approx 10^2 T_r$, is “core collapse”: the core shrinks to zero size and infinite density. In order for many of the evolutionary models cited above to be viable, T_{cc} must be shorter than the age of the universe, i.e. T_r must be less than $\sim 10^8 \text{ yr}$, implying very high stellar densities. Physical collisions between stars also feature prominently in many of the early models. Collisions occur on a time scale that is longer than T_r by a factor $(\ln \Lambda) \Theta^2 / (1 + \Theta) \approx 10^1$ where Θ , the “Safronov number”

(Safronov 1960), is of order unity for stars in a galactic nucleus.

The necessity of attaining high densities in order for these evolutionary models to work – much higher densities than could be confirmed via direct observation at the time (or indeed now) – was clearly recognized. For instance, Saslaw (1973) noted that

It is an extrapolation from the observations of galaxies we have discussed to the idea that even more dense stellar systems exist...Yet this follows naturally enough from the observations of quasars and the realization that the central density of massive compact stellar systems increases with age.

Spitzer (1971) remarked

...the rate of dynamical evolution will depend on how compact is the stellar system resulting from initial gas inflow. If this rate of evolution is slow, activity will not begin for a long time. In fact, in some systems there might be a wait of 10^{12} years before the fireworks begin.

A number of developments since the 1970s have led to a qualitatively different picture of the dynamics and evolution of galactic nuclei.

- SBHs are now known to be ubiquitous components of galactic nuclei, and, at least in the most massive galaxies, to have been present with roughly their current masses ($\sim 10^9 M_\odot$) since very early times, as soon as $\sim 10^9$ yr after the Big Bang (Fan et al. 2001, Fan et al. 2003). Evolution of galactic nuclei during and after the era of peak quasar activity therefore took place with the SBHs already in place, and processes like core collapse and the buildup of massive stars via collisions could not have occurred after this time due to the inhibiting effect of the SBH's gravitational field.
- Observations with the Hubble Space Telescope have elucidated the run of stellar density and velocity dispersion near the centers of nearby galaxies (Crane et al. 1993, Ferrarese et al. 1994, Lauer et al. 1995). In the majority of galaxies massive enough to contain SBHs, the implied central relaxation time is much greater than the age of the universe, due both to the (relatively) low stellar densities and also to the presence of a SBH, which increases v_{rms} (Faber et al. 1997, Ferrarese et al. 2006). Only the smallest galaxies known to harbor SBHs have nuclear relaxation times shorter than 10^{10} yr. The bulge of the Milky Way is in this category, as is the nearby dwarf elliptical galaxy M32; both have nuclear relaxation times $T_r \approx 10^{9.5}$ yr, short enough that gravitational encounters between stars could have influenced the stellar distribution near the SBH. But in the majority of galaxies, the long relaxation times imply that nuclear structure will still reflect to a large extent the details of the nuclear formation process.
- Since the 1980s, the dominant model for the formation of elliptical galaxies and bulges – the stellar systems that contain SBHs – has been the merger model (Toomre 1977). Galaxy mergers are complex phenomena, but an almost certain consequence of a merger is the infall of the progenitor galaxies' SBHs into the

nucleus of the merged system, resulting in the formation of a binary SBH (Begelman et al. 1980). Such a massive binary would inject a substantial amount of energy into the stellar motions, enough to determine the structure of the remnant core. Indeed this process is probably responsible for the low densities, and long relaxation times, at the centers of the brighter elliptical galaxies.

- Quasars and active nuclei are now believed to be powered by infall of gas onto a pre-existing SBH. The bulk of the gas is believed to originate far from the nucleus and to be driven inward by gravitational torques (e.g. Shlosman et al. 1990). The fact that quasar activity peaks at approximately the same epoch as galaxy mergers is seen as strong support for this picture, since mergers are efficient at driving gas into a nucleus (e.g. Kauffmann & Haehnelt 2000). Capture or disruption of stars by the SBH are now generally believed to be energetically insignificant, at least in a time-averaged sense.

A recurring theme of this article will be the distinction between *collisionless* nuclei – which have central relaxation times longer than 10^{10} yr – and *collisional* nuclei in which $T_r \lesssim 10^{10}$ yr (§3). As noted above, the majority of observed nuclei are “collisionless” in this sense. The morphology of a collisionless nucleus is constrained only by the requirement that the stellar phase-space density f satisfy Jeans’s theorem, i.e. that f be constant along orbits, as they are defined in the combined gravitational potential of the SBH and the stars. This weak condition is consistent with a wide variety of possible equilibrium configurations (§4), including non-axisymmetric nuclei, and nuclei in which the majority of orbits are chaotic. In a nucleus with $T_r \lesssim 10^{10}$ yr, on the other hand, the stellar distribution will have had time to evolve to a more strongly constrained, collisionally relaxed steady state (§5). For a single-mass population of stars moving in the Keplerian potential of a black hole, the steady-state density profile is $\rho(r) \approx \rho_0 r^{-7/4}$, the so-called Bahcall-Wolf (1976) solution. The distribution of stars near the Milky Way SBH appears to be consistent with this collisionally-relaxed form (Schödel et al. 2006) but there is no evidence for Bahcall-Wolf cusps in any other galaxies.

The recent explosion of data from the Galactic center has motivated a large and ever-expanding number of theoretical studies of the central star cluster and its evolution due to collisional processes (as reviewed by Alexander 2005). It is important to keep in mind that the Galactic center is extreme, not only in the sense of harboring the nearest SBH, but also in the sense of having the *smallest* SBH with a well-determined mass (Ferrarese & Ford 2005). The bulge of the Milky Way is also one of the faintest systems known to contain a SBH, and its atypically high central density and short relaxation time are consistent with its low luminosity given the parameter correlations defined by more luminous systems (§3). As important as the Galactic center is, it is not typical of the majority of nuclei known to contain SBHs.

The distinction between collisionless and collisional nuclei is important in the context of star-SBH interactions. The “loss cone” of a SBH, i.e. the set of orbits that intersect its event horizon or tidal disruption sphere, is rapidly depopulated in a

spherical or axisymmetric nucleus, and continued feeding of stars to the SBH requires some mechanism for loss-cone repopulation; typically this is assumed to be gravitational encounters between stars. Classical loss cone theory (Frank & Rees 1976, Lightman & Shapiro 1977, Cohn & Kulsrud 1978) was worked out in the late 1970s in the context of massive black holes in globular clusters. Globular clusters are many relaxation times old, and loss cone dynamics was approached from the point of view that the distribution of stars would reach a steady state under the competing effects of gravitational scattering and capture. The same theory was later applied, with only minor modifications, to galactic nuclei, most of which however are far too young for this steady state to have been achieved. In a collisionless nucleus, SBH feeding rates can be much higher than in a relaxed nucleus, e.g. if the nucleus is triaxial and many of the orbits are “centrophilic;” or much lower, e.g. if orbits around the loss cone were substantially depleted by a binary SBH before its coalescence. Considerations like these have prompted a reinvestigation of the nuclear loss cone problem, as reviewed in §6.

In a collisionless nucleus, the distribution of stars around the SBH should still reflect the energy input from the binary SBH that preceded the current, single hole. (Some nuclei might contain *uncoalesced* binaries, particularly if they experienced a recent merger, although the observational evidence for binary SBHs is still largely circumstantial; see Komossa 2003.) The effect of binary SBHs on the morphology and kinematics of galactic nuclei is discussed in §7. An important success of the binary SBH model is its ability to quantitatively explain the low central densities of bright elliptical galaxies, i.e. the “cusp-core dichotomy.” Previously, this dichotomy had been widely interpreted to mean that dwarf and giant elliptical galaxies experienced very different formation histories (e.g. Kormendy 1985).

The literature on galactic nuclei and SBHs is enormous and exponentially expanding, and the writing of this review article was greatly facilitated by the recent appearance of a number of other articles that emphasize different aspects of this broad topic. A comprehensive review of observational evidence for SBHs is given by Ferrarese & Ford (2005). Alexander (2003, 2005) reviews the physics of star-star and star-SBH interactions, with an emphasis on dissipative processes and on the nucleus of the Milky Way; as noted above, such processes are of less importance in the nuclei of most galaxies known to contain SBHs. Komossa (2002, 2003) reviews the observational evidence for interaction of single and binary SBHs with stars and gas in galactic nuclei. (For a more theoretically oriented review of binary SBHs, see Merritt & Milosavljević 2005.) While intermediate mass black holes (IMBHs) are still seen as speculative by many astrophysicists, many of the models proposed for their formation are closely similar to early models for the dissipative evolution of galactic nuclei, as discussed by Miller & Colbert (2004) and van der Marel (2004). The prospect of detecting gravitational waves from coalescing black holes in galactic nuclei is a prime motivation behind much recent work on nuclear dynamics. While no single article can do justice to this exciting topic, the reviews by Schutz (2002) and Hughes (2003) are excellent places to start. Dark matter is almost certainly not a dominant component of galactic nuclei, but its

density there is likely to be higher than elsewhere in galaxies, making galactic nuclei ideal targets for so-called “indirect-detection” studies, as reviewed by Bertone & Merritt (2005). Finally, some early review articles on the evolution of galactic nuclei, while outdated in some respects, are still very much worth reading today, including those by Spitzer (1971), Saslaw (1973), Rees (1984), and Gerhard (1992,1994).

2. Characteristic Length and Time Scales

The radius of the event horizon of a nonrotating hole of mass M_\bullet is

$$r_S = \frac{2GM_\bullet}{c^2} \approx 9.6 \times 10^{-6} \text{pc} \left(\frac{M_\bullet}{10^8 M_\odot} \right). \quad (2)$$

The dynamical influence of a SBH extends far beyond r_S however. In a stellar nucleus with 1D velocity dispersion σ , the SBH’s “influence radius” is customarily defined as

$$r_h = \frac{GM_\bullet}{\sigma^2} \approx 11 \text{ pc} \left(\frac{M_\bullet}{10^8 M_\odot} \right) \left(\frac{\sigma}{200 \text{ km s}^{-1}} \right)^{-2}. \quad (3)$$

In a singular isothermal sphere (SIS) nucleus, $\rho = \sigma^2/2\pi Gr^2$, the velocity dispersion is constant with radius in the absence of the SBH, and the stellar mass within r_h is $2M_\bullet$. This is often taken as an alternate definition of r_h : the influence radius is the radius containing a stellar mass equal to $2M_\bullet$, or

$$M_\star(r \leq r_h) = 2M_\bullet. \quad (4)$$

The second definition of r_h is generally to be preferred since σ is a function of radius near the SBH, and unless otherwise stated, this is the definition that will be adopted below. In the Milky Way, $r_h \approx 3 \text{ pc}$ according to either definition.

The tidal disruption radius r_t is the distance from the SBH where tidal forces can pull a star apart. Strictly, r_h depends on the structure of the star and on the shape of its orbit, but it is of order

$$r_t \approx r_\star \left(\frac{M_\bullet}{m_\star} \right)^{1/3} \approx 1.0 \times 10^{-5} \text{pc} \left(\frac{M_\bullet}{10^8 M_\odot} \right)^{1/3} \quad (5)$$

where the latter expression assumes stars of Solar mass and radius. In terms of the radius of the event horizon,

$$\frac{r_t}{r_S} \approx \left(\frac{M_\bullet}{10^8 M_\odot} \right)^{-2/3} \quad (6)$$

so that SBHs more massive than $\sim 10^8 M_\odot$ “swallow stars whole.”

The relaxation time is defined as the time for (mostly distant) gravitational encounters between stars to establish a locally Maxwellian velocity distribution. Assuming a homogenous isotropic distribution of equal-mass stars, the relaxation time is approximately

$$\begin{aligned} T_r &\approx \frac{0.34\sigma^3}{G^2 \rho m_\star \ln \Lambda} \\ &\approx 0.95 \times 10^{10} \text{yr} \left(\frac{\sigma}{200 \text{ km s}^{-1}} \right)^3 \left(\frac{\rho}{10^6 M_\odot \text{pc}^{-3}} \right)^{-1} \left(\frac{m_\star}{M_\odot} \right)^{-1} \left(\frac{\ln \Lambda}{15} \right)^{-1} \end{aligned} \quad (7a) \quad (7b)$$

(Spitzer 1987). The Coulomb logarithm, $\ln \Lambda$, is a “fudge factor” that accounts approximately for the divergent total perturbing force in an infinite homogeneous medium. Within the SBH’s sphere of influence, N -body experiments (Preto et al. 2004) suggest that

$$\ln \Lambda \approx \ln(r_h \sigma^2 / 2Gm_\star) \approx \ln(M_\bullet / 2m_\star) \approx \ln(N_\bullet / 2) \quad (8)$$

with $N_\bullet \equiv M_\bullet / m_\star$ the number of stars whose mass makes up M_\bullet . For $m_\star = M_\odot$ and $M_\bullet = (0.1, 1, 10) \times 10^8 M_\odot$, $\ln \Lambda \approx (15, 18, 20)$. In the gravitational field of a SBH, i.e. at $r \lesssim r_h$, encounters lead to a steady-state distribution of orbital energies in a time $\sim T_r$, as discussed in §5.

Figure 1 shows estimates of T_r , measured at $r = r_h$, in a sample of early-type galaxies and bulges. The relaxation time at r_h is almost always in excess of 10^{10} yr, although there is a clear trend with luminosity, suggesting that $T_r(r_h)$ drops below 10^{10} yr for spheroids fainter than absolute magnitude $M_V \approx -18$, roughly the luminosity of the Milky Way bulge. Furthermore, in the handful of Local Group galaxies for which the SBH influence radius is well resolved, T_r continues to decrease inside of r_h : in the case of the Milky Way, to $\sim 6 \times 10^9$ yr at $0.2r_h$ and $\sim 3.5 \times 10^9$ yr at $\sim 0.1r_h$. At radii $r \ll r_h$ where $\sigma^2 \propto r^{-1}$, the relaxation time varies as $T_r \sim r^{\gamma-3/2}$ if $\rho \sim r^{-\gamma}$. Several Local Group galaxies are known to have $\gamma \approx 1.5$ at $r \lesssim r_h$ (Lauer et al. 1998) implying that T_r is approximately constant into the SBH in these galaxies. Relaxation times in the nuclei of brighter galaxies are probably always longer than a Hubble time, and the stellar distribution at $r \lesssim r_h$ in these galaxies should still reflect the details of their formation.

In what follows, *collisional nuclei* are defined as those which have $T_r \lesssim 10^{10}$ yr at $r < r_h$, while *collisionless nuclei* have $T_r \gtrsim 10^{10}$ yr.

A number of other physical processes have time scales that are related to T_r . The core-collapse time T_{cc} is $\sim 10^2 T_r$; in a time of order T_{cc} , a nucleus *lacking* a SBH develops a high-density core and a power-law envelope, $\rho \sim r^{-2.2}$. The core collapse time is interestingly short at the centers of M33 and NGC205: both have $T_r \lesssim 10^8$ yr (Hernquist et al. 1991, Valluri et al. 2005) and both lack dynamical signatures of a SBH. However core collapse is probably unimportant in galaxies with SBHs, both because T_r is $\gtrsim 10^9$ yr, and because the collapse would be inhibited by the presence of the hole. Another relaxation-driven mechanism is diffusion of stars into the tidal disruption sphere of the SBH. The rate is approximately $\dot{N} \approx N / [\ln(2/\theta_{lc})] T_r$, where $\theta_{lc} \approx \sqrt{r_t/r_h}$ is the angular size subtended by the sphere $r = r_t$ as seen from $r = r_h$ and N is the number of stars within r_h (Frank & Rees 1976, Lightman & Shapiro 1977).

Physical collisions between stars take place in a time T_{coll} where

$$T_{coll} = [16\sqrt{\pi}n\sigma r_\star^2(1+\Theta)]^{-1} \quad (9a)$$

$$\approx 1.1 \times 10^{11} \text{yr} \left(\frac{n}{10^6 \text{pc}^{-3}} \right)^{-1} \left(\frac{\sigma}{200 \text{km s}^{-1}} \right)^{-1} \left(\frac{r_\star}{R_\odot} \right)^{-2} \left(\frac{1+\Theta}{3} \right)^{-1} \quad (9b)$$

and Θ is the Safronov number:

$$\Theta = \frac{Gm_\star}{2\sigma^2 r_\star} \quad (10a)$$

$$\approx 2.38 \left(\frac{m_\star}{M_\odot} \right) \left(\frac{\sigma}{200 \text{ km s}^{-1}} \right)^{-2} \left(\frac{r_\star}{R_\odot} \right)^{-1}. \quad (10b)$$

The ratio of the collision time to the relaxation time is

$$\frac{T_{coll}}{T_r} \approx 0.8 \ln \Lambda \frac{\Theta^2}{1 + \Theta} \approx 0.3 \left(\frac{r}{0.01 \text{ pc}} \right)^4; \quad (11)$$

the right-hand expression assumes Solar-type stars around the Milky Way SBH, and shows that even in the very dense environment of the Galactic center, physical collisions are significant only at very small radii, $r \lesssim 0.02 \text{ pc} \approx 10^{-2} r_h$ for Solar-type stars. Stellar collisions may be responsible for the depletion of luminous, late-type giant stars at the Galactic center (Phinney 1989, Alexander 1999, Alexander 2003) or for the formation of the so-called S-stars (Morris 1993, Genzel et al. 2003). There is little evidence that stellar collisions have affected the stellar populations at the centers of any of the other Local Group galaxies however (e.g. Lauer et al. 1998). From the point of view of nuclear dynamics, stellar collisions are probably always of minor importance (e.g. Freitag & Benz 2002) and they will not be discussed further in this article.

The spheroids that host SBHs are believed to have formed via mergers, and in many cases, the merging galaxies would have contained pre-existing SBHs. The result is a binary SBH (Begelman et al. 1980). A number of additional length and time scales are associated with the binaries. Let M_1 and M_2 be the masses respectively of the larger and smaller of the two SBHs, with $q = M_2/M_1 \leq 1$ the mass ratio, $M_{12} = M_1 + M_2$ the total mass, and $\mu = M_1 M_2 / M_{12}$ the reduced mass. Two SBHs form a gravitationally-bound pair when their separation falls below the influence radius defined by the larger hole. Approximating the relative orbit as Keplerian, i.e. ignoring the force perturbations from stars, the binary's binding energy is

$$|E| = \frac{GM_1 M_2}{2a} = \frac{G\mu M_{12}}{2a} \quad (12)$$

with a the semi-major axis, and the orbital period is

$$P = 2\pi \left(\frac{a^3}{GM_{12}} \right)^{1/2} = 9.36 \times 10^3 \text{ yr} \left(\frac{M_{12}}{10^8 M_\odot} \right)^{-1/2} \left(\frac{a}{1 \text{ pc}} \right)^{3/2}. \quad (13)$$

The relative velocity of the two SBHs, assuming a circular orbit, is

$$V_{bin} = \sqrt{\frac{GM_{12}}{a}} = 658 \text{ km s}^{-1} \left(\frac{M_{12}}{10^8 M_\odot} \right)^{1/2} \left(\frac{a}{1 \text{ pc}} \right)^{-1/2}. \quad (14)$$

A massive binary is called “hard” when its binding energy per unit mass, $|E|/M_{12} = G\mu/2a$, exceeds $\sim \sigma^2$. (The motivation for this definition is given in §7.) A standard definition for the semi-major axis of a hard binary is

$$a_h = \frac{G\mu}{4\sigma^2} \approx 2.7 \text{ pc} (1 + q)^{-1} \left(\frac{M_2}{10^8 M_\odot} \right) \left(\frac{\sigma}{200 \text{ km s}^{-1}} \right)^{-2}. \quad (15)$$

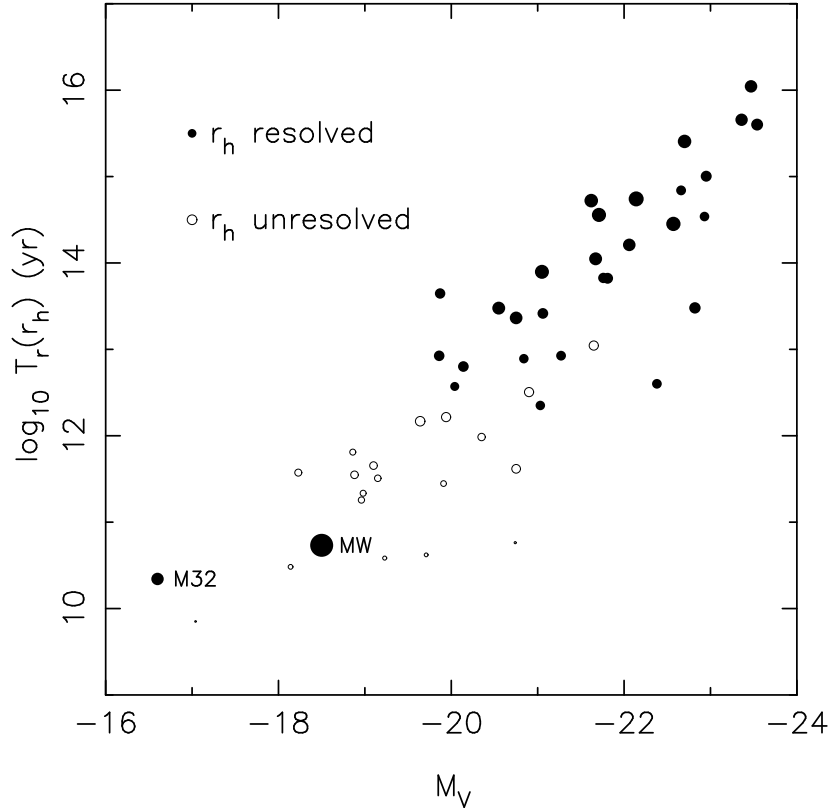


Figure 1. Estimates of the relaxation time T_r (Eq. 7b) at the SBH’s influence radius r_h (Eq. 4), in the sample of early-type galaxies modelled by Wang & Merritt (2004). SBH masses were computed from the $M_\bullet - \sigma$ relation, except in the case of the Milky Way, for which $M_\bullet = 3.7 \times 10^6 M_\odot$ was assumed (Ghez et al. 2005). The stellar mass was set equal to $0.7 M_\odot$ when computing T_r . Horizontal axis is absolute visual magnitude of the galaxy or, in the case of the Milky Way, the stellar bulge. The size of the symbols is proportional to $\log_{10}(\theta_{r_h}/\theta_{obs})$, where θ_{r_h} is the angular size of the black hole’s influence radius and θ_{obs} is the observational resolution. Filled symbols have $\theta_{r_h} > \theta_{obs}$ (r_h resolved) and open circles have $\theta_{r_h} < \theta_{obs}$ (r_h unresolved). Values of $T_r(r_h)$ in the unresolved galaxies should be considered approximate. In the Milky Way, the stellar density profile is resolved at $r \ll r_h$ and T_r is found to drop below its value at r_h , to $\sim 4 \times 10^9$ yr at $\sim 0.1 r_h \approx 0.3$ pc. Time scales for physical collisions between stars are longer than T_r (Eq. 11). (From Merritt & Szell 2005)

Defining r_h as GM_{12}/σ^2 then implies

$$a_h = \frac{\mu}{4M_{12}} r_h = \frac{1}{4} \frac{q}{(1+q)^2} r_h. \quad (16)$$

For an equal-mass binary, $a_h \approx 0.06 r_h$, and for a more typical mass ratio of $q = 0.1$, $a_h \approx 0.02 r_h$.

If the binary’s semi-major axis is small enough that its subsequent evolution is dominated by emission of gravitational radiation, then $\dot{a} \propto -a^{-3}$ and coalescence takes place in a time t_{gr} , where (Peters 1964)

$$t_{gr} = \frac{5}{256 F(e)} \frac{c^5}{G^3} \frac{a^4}{\mu M_{12}^2},$$

$$F(e) = (1 - e^2)^{7/2} \left(1 + \frac{73}{24}e^2 + \frac{37}{96}e^4 \right). \quad (17)$$

This can be written

$$\begin{aligned} t_{gr} &= \frac{5}{16^4 F(e)} \frac{G \mu^3 c^5}{\sigma^8 M_{12}^2} \left(\frac{a}{a_h} \right)^4 \\ &\approx \frac{3.07 \times 10^8 \text{ yr}}{F(e)} \frac{q^3}{(1+q)^6} \left(\frac{M_{12}}{10^8 M_\odot} \right) \left(\frac{\sigma}{200 \text{ km s}^{-1}} \right)^{-8} \left(\frac{a}{10^{-2} a_h} \right)^4 \end{aligned} \quad (18)$$

with e the orbital eccentricity. Separations much less than a_h are required in order for emission of gravitational waves to induce coalescence in 10^{10} yr.

Many of these expressions can be simplified by making use of the empirical correlations between SBH mass and galaxy properties. The tightest of these is the $M - \sigma$ relation, which has two extant forms, based either on the velocity dispersion σ_c measured in an aperture centered on the nucleus (but large compared with r_h) (Ferrarese & Merritt 2000) or on the global rms stellar velocity (Gebhardt et al. 2000). The first form is the more relevant here since σ as used above is defined near the center of a galaxy; the alternative form (Gebhardt et al. 2000) defines σ as a mean value along a slit that extends over the entire half-light radius of the galaxy and can be strongly influenced by rotation, inclination and other factors extraneous to nuclear dynamics. (The Gebhardt et al. form of the relation also exhibits substantially more scatter.) In terms of σ_c , the best current determination of the $M - \sigma$ relation is

$$\left(\frac{M_\bullet}{10^8 M_\odot} \right) = (1.66 \pm 0.24) \left(\frac{\sigma_c}{200 \text{ km s}^{-1}} \right)^\alpha \quad (19)$$

with $\alpha = 4.86 \pm 0.43$ (Ferrarese & Ford 2005). The intrinsic scatter in this relation is consistent with zero (Merritt & Ferrarese 2001*c*, Ferrarese & Ford 2005), although the number of galaxies with well-determined SBH masses is still very small, of order a dozen or less (Valluri et al. 2004). The relations between M_\bullet and the mass or luminosity of the host spheroid (elliptical galaxy or spiral galaxy bulge) appear to be less tight; the mean ratio of M_\bullet to M_{gal} is $\sim 1.3 \times 10^{-3}$ (Merritt & Ferrarese 2001*a*, Marconi & Hunt 2003).

Using Equation 19, one can write

$$r_h \approx 18 \text{ pc} \left(\frac{\sigma_c}{200 \text{ km s}^{-1}} \right)^{2.86} \quad (20a)$$

$$\approx 13 \text{ pc} \left(\frac{M_\bullet}{10^8 M_\odot} \right)^{0.59} \quad (20b)$$

and

$$a_h \approx 4.5 \text{ pc} \frac{q}{(1+q)^2} \left(\frac{\sigma_c}{200 \text{ km s}^{-1}} \right)^{2.86} \quad (21a)$$

$$\approx 3.2 \text{ pc} \frac{q}{(1+q)^2} \left(\frac{M_\bullet}{10^8 M_\odot} \right)^{0.59}. \quad (21b)$$

Setting $M = M_{12}$, $F(e) = 1$ in Equation (18) gives

$$t_{gr} \approx 5.0 \times 10^8 \text{ yr} \frac{q^3}{(1+q)^6} \left(\frac{\sigma_c}{200 \text{ km s}^{-1}} \right)^{-3.14} \left(\frac{a}{10^{-2} a_h} \right)^4$$

$$\approx 7.1 \times 10^8 \text{yr} \frac{q^3}{(1+q)^6} \left(\frac{M_{12}}{10^8 M_\odot} \right)^{-0.65} \left(\frac{a}{10^{-2} a_h} \right)^4. \quad (22)$$

3. Structural Properties of Galaxies and Nuclei

Knowledge of the distribution of mass and light near the centers of galaxies is limited by the $\sim 0.1''$ angular resolution of the Hubble Space Telescope (although ground-based adaptive optics are starting to improve on this, e.g. Melbourne et al. 2005, Davidge et al. 2005). The corresponding linear scale is $\sim 5 \text{ pc}(D/10\text{Mpc})$; at the distance of the Virgo cluster ($D \approx 16 \text{ Mpc}$), resolving r_h is only possible in galaxies with $M_\bullet \gtrsim 10^8 M_\odot$ (Eq. 20b). While a great deal is known about the morphology of bright ($M_B \lesssim -20$) galaxies on scales $r < r_h$, the central structure of fainter spheroids is poorly understood, and what little we know comes almost entirely from Local Group galaxies (including the bulge of the Milky Way). Not surprisingly, parametric functions that were developed to fit the luminosity profiles of distant galaxies often fail to describe the well-resolved centers of Local Group galaxies. In this section, an attempt is made to synthesize recent work on the light distributions in both bright (distant) and fainter (mostly nearby) galaxies.

Among the various functional forms that have been proposed to fit galaxy luminosity profiles, the most generally successful have been those based on Sérsic's (1968) law,

$$\ln I(R) = \ln I_e - b(n_S) \left[(R/R_e)^{1/n_S} - 1 \right]. \quad (23)$$

The constant b is normally chosen such that R_e is the projected radius containing one-half of the total light. The shape of the profile is then determined by n_S ; $n_S = 4$ is the de Vaucouleurs (1948) law, which is a good representation of bright elliptical galaxies, while $n_S = 1$ is the exponential law, which approximates the luminosity profiles of dwarf galaxies (Binggeli et al. 1984). Deviations from the best-fitting Sérsic law are typically 0.05 mag rms and, at least in the case of galaxies outside the Local Group, the fits are often good over the full observed range, typically two to three decades in radius (Graham & Guzmán 2003, Graham et al. 2003, Trujillo et al. 2004). An alternative way to write Equation (23) is

$$\frac{d \ln I}{d \ln R} = -\frac{b}{n_S} \left(\frac{R}{R_e} \right)^{1/n_S}, \quad (24)$$

i.e. the logarithmic slope varies as a power of the projected radius, falling to zero at the center. While there is no consensus on why the Sérsic law is such a good representation of galactic spheroids, a possible hint comes from the dark-matter halos produced in N -body simulations of hierarchical structure formation, which have density profiles that are also well described by Equation (24) (Navarro et al. 2004, Merritt, Navarro, Ludlow & Jenkins 2005, Graham et al. 2005). This functional form may be characteristic of systems that form via chaotic, collisionless relaxation.

The Sérsic index n_S correlates reasonably well with galaxy absolute magnitude (Graham & Guzmán 2003), and less well with other structural parameters like R_e (Caon

et al. 1993, Graham & Guzmán 2003). In a recent comprehensive study (Ferrarese et al. 2006), the Advanced Camera for Surveys on the Hubble Space Telescope was used to measure luminosity profiles of 100 early-type galaxies in the Virgo cluster. The best-fitting relations $n_S(M_B)$ and $R_e(M_B)$ were found to be

$$\log n_S \approx \log(3.89) - 0.10(M_B + 20), \quad (25)$$

$$\log R_e \approx \log(17.8) - 0.055(M_B + 20) \quad (26)$$

where R_e is in units of kpc.

In galaxies resolved on scales of order a few r_h or better, systematic deviations from the Sérsic law often appear near the center. These deviations are of two kinds. Galaxies fainter than $M_B \approx -20$ are generally observed to have *higher* surface brightnesses at small radii than predicted by Sérsic’s law. These galaxies are sometimes called “power-law” galaxies since $I(R)$ can be reasonably well approximated as a power law at $R \lesssim R_e$. Galaxies brighter than $M_B \approx -20$ generally exhibit central *deficits* in the intensity, inside of a “break” radius R_b that is of order a few times r_h . These are sometimes called “core” galaxies.

The surface brightness surpluses at small radii are most clearly defined in Local Group galaxies like the Milky Way, M31 and M32. Each of these galaxies exhibits an approximately power-law dependence of I on R into the innermost resolved radius, $I \sim R^{-\Gamma}$, implying a spatial density $\rho \sim r^{-\gamma}$, $\gamma \approx \Gamma + 1$ (Figure 2). In the bulge of the Milky Way, the stellar density has been derived from number counts that extend down to ~ 0.005 pc $\approx 10^{-3}r_h$; the result is

$$\rho(r) \approx 1.8 \times 10^5 M_\odot \text{pc}^{-3} \left(\frac{r}{0.38 \text{pc}} \right)^{-\alpha} \quad (27)$$

with $\alpha \approx 2.0$ at $r \geq 0.38$ pc and $\alpha \approx 1.4$ at $r < 0.38$ pc (Genzel et al. 2003, Schödel et al. 2006). M31 and M32 have central density profiles very similar to that of the Milky Way, both in slope and normalization (Lauer et al. 1998), although $I(R)$ in both galaxies can not be measured on scales much smaller than r_h . Deviations from a Sérsic law in M32 appear inside of $R \approx 10'' \approx 40$ pc $\approx 20r_h$ (Tonry 1984, Graham 2002), which suggests that the central surplus can not be ascribed solely to the dynamical influence of the SBH.

Inner light surpluses are also seen in galaxies beyond the Local Group (e.g. Côté et al. 2006 and references therein), although in most cases the central regions are not well enough resolved that it is possible to determine the functional form of the deviation. At the innermost resolved radii, most galaxies in this class have $-2.5 \lesssim d \log \rho / d \log r \lesssim -1.5$ (Gebhardt et al. 1996, Ferrarese et al. 2006). A reasonable ansatz is that the inner, unresolved density profiles in these galaxies are similar to the power laws observed at the centers of Local Group galaxies. However there is evidence that the central surpluses in spheroids fainter than $M_B \approx -18$ can be modelled as distinct nuclei, i.e. as components that rise suddenly above the best-fitting Sérsic law at some radius, then level out into a constant-density core. Such a profile is definitely seen in NGC205 (Valluri et al. 2005); the upward inflection appears at $R \approx 3''$ and the core

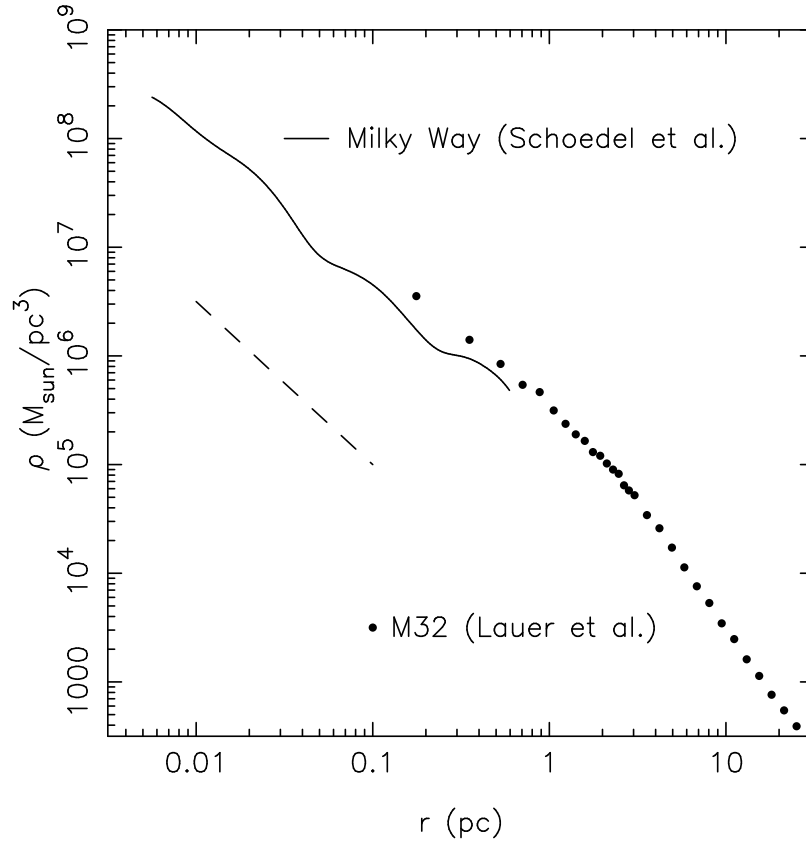


Figure 2. Mass density profiles near the centers of the Milky Way and M32 (Schödel et al. 2006, Lauer et al. 1998). Dashed line is $\rho \propto r^{-1.5}$. Both galaxies contain SBHs with masses $\sim 3 \times 10^6 M_\odot$ and with influence radii $r_h \approx 3$ pc.

radius is $\sim 0.1''$. Distinct nuclei are ubiquitous in spheroids with $M_B \approx -17$, gradually disappearing in spheroids fainter than $M_B \approx -12$ (van den Bergh 1986).

There is no compelling explanation for the power-law density profiles observed at the centers of galaxies like the Milky Way and M32. The scale-free nature of a power law suggests a gravitational origin, but no obvious dynamical mechanism suggests itself. In the region dominated by the gravitational force from the SBH, $r \lesssim 0.2r_h$ say, processes like adiabatic contraction (Young 1980) and collisional relaxation (Bahcall & Wolf 1976) can produce power-law profiles, but these mechanisms are ineffective at $r \gtrsim r_h$.

Very recently, a possible connection has been found between the central luminosity excesses in low-luminosity galaxies and the SBHs in brighter galaxies (Ferrarese et al. 2006, Wehner & Harris 2006). If the “nucleus” is defined as the interior light or mass in excess of the best-fitting Sérsic profile, then the ratio of “nuclear” mass to total galaxy mass is found to be roughly equal to the ratio M_\bullet/M_{gal} in galaxies with SBHs, or $\sim 10^{-3}$ (Fig. 3). This has led to the suggestion that galaxies always form a “central massive object” (CMO): either a SBH, or a compact stellar nucleus.

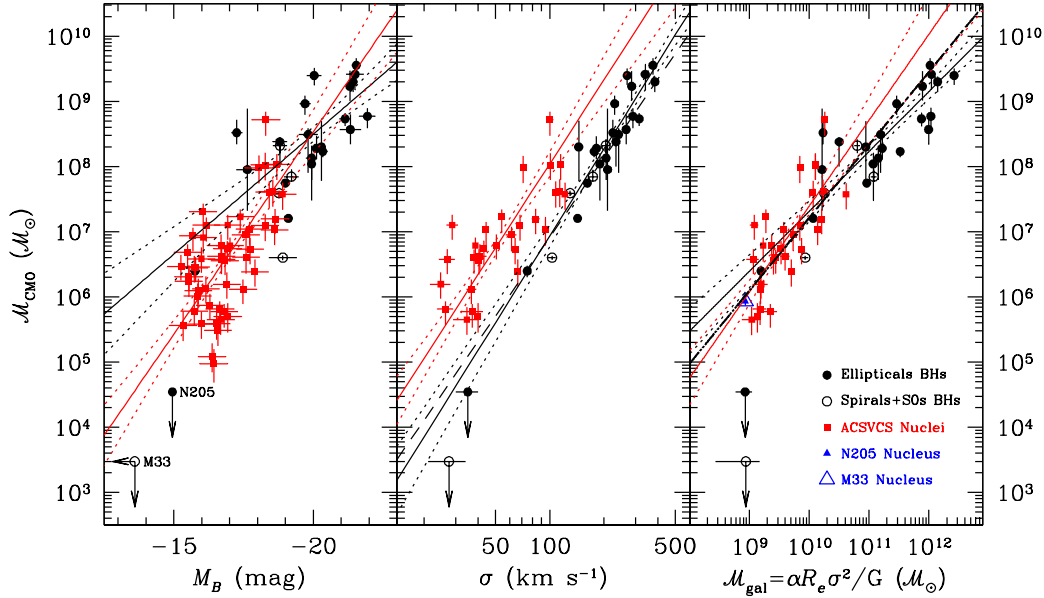


Figure 3. (*Left Panel*) Mass of the “central massive object” (CMO) plotted against absolute blue magnitude of the host galaxy (or bulge for spiral galaxies). Stellar nuclei (defined as an excess with respect to the best-fitting Sérsic profile) are shown as red squares. SBHs in elliptical and spiral galaxies are shown as filled and open circles respectively. Upper limits on the SBH mass are shown for NGC205 and M33. (*Middle Panel*) CMO mass as a function of velocity dispersion of the host galaxy. (*Right Panel*) CMO mass plotted against galaxy mass. The solid red and black lines show the best-fit relations fit to the nuclei and to the SBH samples respectively, with 1σ confidence levels on the slope shown by the dotted lines. In the middle panel, the dashed line is the $M_{\bullet} - \sigma$ relation. In the right panel, the dashed line is the fit obtained for the combined nuclei+SBH sample. (Adapted from Ferrarese et al. 2006.)

A possible objection to this appealing picture is that it fails to describe some of the best-resolved galaxies, e.g. M31, M32 and the Milky Way, all of which contain SBHs, as well as “nuclei,” i.e. central excesses with respect to the best-fitting Sérsic law (e.g. Graham 2002). It is possible that the “nuclei” in some of the unresolved galaxies in Figure 3 are similar to the power-law cusps observed in the well-resolved Local Group galaxies, rather than distinct, compact cores like in NGC 205.

At the other extreme of luminosity, bright elliptical galaxies generally show central *deficits* in $I(R)$, or “cores.” The cores extend outward to a break radius R_b of order a few times r_h . The profiles at $R \lesssim R_b$ are well described as power laws but with small slopes, $\Gamma \lesssim 0.3$, and furthermore the profiles often show a distinct inflection, or change of slope, at R_b (Lauer et al. 1995, Trujillo et al. 2004, Ferrarese et al. 2006). Such cores are apparent in elliptical galaxies brighter than $M_V \approx -19.5$, but this number may be resolution-dependent since fainter galaxies are mostly unresolved on scales of r_h .

One model, discussed in detail below, attributes the cores to the dynamical influence

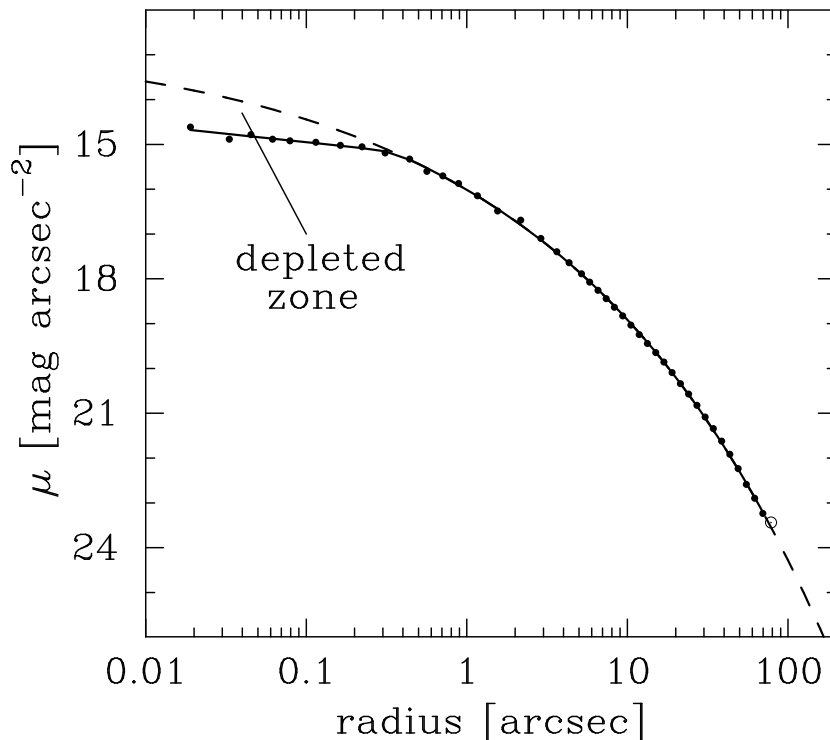


Figure 4. Surface brightness profile in the R band of NGC 3348, a “core” galaxy. The dashed line is the best-fitting Sérsic model; the observed profile (points, and solid line) falls below this inside of a break radius $r_b \approx 0''.35$ (From Graham 2004)

of binary SBHs. If this model is correct, the “mass deficit” – the amount of mass that was removed in creating the core – is a measure of the time-integrated effect of the binary on the nucleus. The mass deficit is defined (Milosavljević et al. 2002) as the difference in integrated mass between the deprojected density profile $\rho(r)$ and an inward extrapolation of the outer, deprojected profile $\rho_{fit}(r)$:

$$M_{def} \equiv 4\pi \int_0^{r_b} [\rho_{fit}(r) - \rho(r)] r^2 dr. \quad (28)$$

Here, r_b is the (spatial) radius where the luminosity profile departs from the fitted profile. Figure 4 illustrates the computation of M_{def} in NGC 3348. Note that the pre-existing profile was assumed to be a Sérsic law; under this assumption, the mass deficit is found to be roughly equal to M_\bullet , the mass currently in the SBH (Graham 2004). This is consistent with the mass displaced by an infalling SBH (§7).

The idea that the cores of bright elliptical galaxies are created during mergers provides a nice solution to a long-standing puzzle: why dwarf and giant elliptical galaxies appear to occupy two distinct families in terms of their central properties (Jerjen & Binggeli 1997, Graham & Guzmán 2003). Dwarf ellipticals define a continuous sequence spanning ten magnitudes, such that the central surface brightness increases linearly with absolute magnitude. In galaxies brighter than $M_B \approx -20.5$, the central surface brightness *declines* with increasing luminosity, leading Kormendy (1985) to suggest that

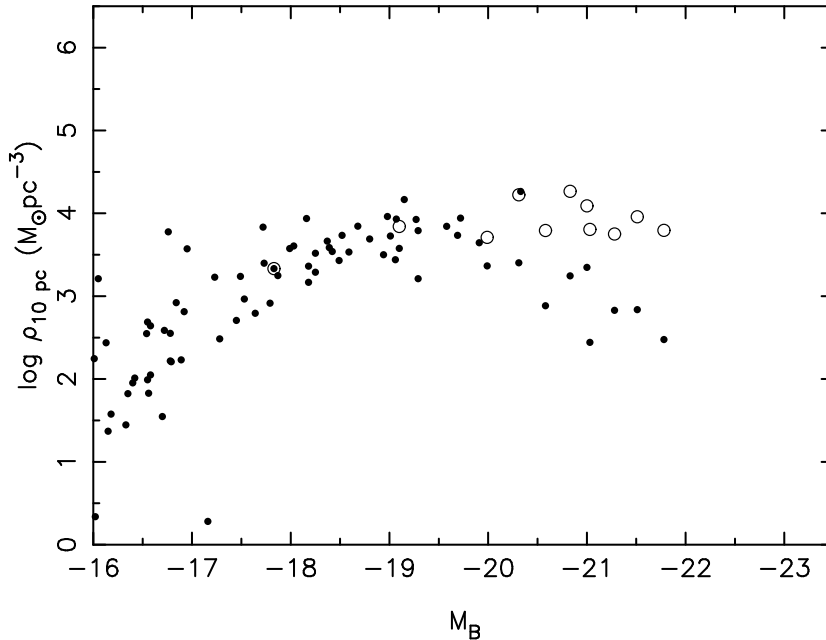


Figure 5. Filled circles show the density at $r = 10$ pc in a sample of early-type galaxies in Virgo (Ferrarese et al. 2006); M_B is the absolute blue magnitude. After increasing monotonically with luminosity over ~ 10 magnitudes, the central density begins to decline at $M_B \approx -20$, roughly the magnitude at which galaxies begin to exhibit central depletions, or “cores.” Open circles show the density computed via an inward extrapolation of a Sérsic profile fit to the large-radius data, as in Fig. 4. The open circles presumably represent more closely the density before a binary SBH “carved out” a core; this density follows the trend of increasing density with galaxy luminosity exhibited by the fainter galaxies. This argument, first made by Jerjen & Binggeli (1997) and Graham & Guzmán (2003), plausibly explains why the centers of dwarf and giant galaxies appear at first sight to define two distinct “families” (Kormendy 1985).

“dwarf elliptical galaxies are very different from the sequence of giant ellipticals.” But $M_B \approx -20.5$ is also roughly where cores appear, and if the cores are “removed” as in Figure 4 by fitting a smooth profile to the surface brightness data at $R > R_b$, one finds that bright ellipticals smoothly continue the sequence defined by dwarf ellipticals of central density increasing with luminosity. Figure 5 illustrates this for a sample of early-type galaxies in Virgo. Even after this adjustment, the central densities of the “core” galaxies in Figure 5 should probably be interpreted as lower limits, since the pre-binary-SBH nuclei might have had central excesses like those observed in many fainter galaxies.

Our current understanding of nuclear cusps and cores presents an interesting contrast to the earlier view, in which cores were seen as generic (e.g. Tremaine 1997) and the presence of power-law inner profiles was attributed to some secondary process like adiabatic contraction driven by growth of the SBH (e.g. van der Marel 1999a). Nowadays, power-law profiles are deemed “natural” and special explanations are sought for cores. Preconceptions aside, the existence of a core begs the question: What

determines the core radius? A reasonable answer in the case of galactic nuclei, as discussed in §7, is that the size of the core is determined by the radius at formation of the binary SBH that preceded the current, single SBH. (A similar explanation appears to work for cores of globular clusters; see Merritt, Piatek, Zwart & Hemsendorf 2004.) No comparably compelling explanation currently exists either for the inner power-law profiles or the compact nuclei observed in fainter elliptical galaxies, although it is intriguing that the latter appear to be present only in galaxies that lack a SBH.

4. Collisionless Equilibria

Collisionless nuclei have relaxation times greater than the age of the universe (§2), so the distribution of stars around the SBH still reflects to some extent the details of the nuclear formation process, including possibly the effects of binary SBHs (§7). While little can be said *ab initio* about the expected form of $\rho(\mathbf{r})$, a collisionless steady state must satisfy the coupled equations

$$\rho(\mathbf{r}) = \int \int \int f(E, I_2, I_3) d^3v, \quad (29a)$$

$$\nabla^2 \Phi = 4\pi G \rho(\mathbf{r}). \quad (29b)$$

Here f is the number density of stars in phase space; $\Phi(\mathbf{r})$ is the gravitational potential, which includes contributions both from the SBH and from the stars; $E = v^2/2 + \Phi(\mathbf{r})$ is the orbital energy per unit mass; and I_2 and I_3 are additional isolating integrals of the motion in Φ , if they exist. For instance, in an axisymmetric nucleus, $I_2 = J_z$, the angular momentum about the symmetry axis. Jeans's theorem states that a steady-state f must be expressible in terms of the isolating integrals of the motion in the potential Φ , or equivalently that f must be independent of phase on every invariant torus.

A useful way to think about the self-consistency problem is to view each set of integral values (E, I_2, I_3) as defining a single, time-averaged orbital density; the total density $\rho(\mathbf{r})$ must then be representable as a superposition of orbits with non-negative weights (Schwarzschild 1979, Vandervoort 1984). Roughly speaking, self-consistency requires that there exist at least as many distinct orbit families as there are dimensions in ρ ; for instance, a triaxial mass distribution requires three isolating integrals (Schwarzschild 1981). This condition places almost no restrictions on the form of ρ in spherical or axisymmetric geometries but can be an important constraint in non-axisymmetric nuclei (see Merritt 1999 for a review).

4.1. Spherical Nuclei

The most general form of f that preserves spherical symmetry is $f = f(E, L^2)$ with $\mathbf{L} = \mathbf{r} \times \mathbf{v}$ the angular momentum per unit mass. If the velocity distribution is assumed to be isotropic, $f = f(E)$, f is determined uniquely by ρ and Φ via Equation (29a). For example, if the stellar density follows a power law near the SBH, $\rho(r) = \rho_0(r/r_0)^{-\gamma}$, and

assuming that $r \ll r_h$ so that the contribution to Φ from the stars can be ignored, then

$$f(E) = \frac{3-\gamma}{8} \sqrt{\frac{2}{\pi^5}} \frac{\Gamma(\gamma+1)}{\Gamma(\gamma-\frac{1}{2})} \frac{M_\bullet}{m_\star} \frac{\phi_0^{3/2}}{(GM_\bullet)^3} \left(\frac{|E|}{\phi_0}\right)^{\gamma-3/2}, \quad \gamma > 1/2. \quad (30)$$

Here m_\star is the stellar mass, $\phi_0 = GM_\bullet/r_h$, and r_h is the radius containing a mass in stars equal to twice M_\bullet (§2).

For $\gamma \leq 1/2$, Equation (30) states that $f(E)$ is undefined; the reason is that the low- L orbits at each E force the density to increase faster than $r^{-1/2}$ toward the center. Achieving a steady state in this case requires a depopulation of the eccentric orbits, i.e. a velocity ellipsoid that is biased toward circular orbits. The amplitude of the anisotropy required can be estimated by repeating the derivation above after setting $f = f(E, L^2) = KL^{-2\beta}|E|^q$, which imposes a constant degree of anisotropy, $\sigma_t^2/\sigma_r^2 = 1 - \beta$; here σ_t and σ_r are the velocity dispersions perpendicular and parallel to the radius vector. The result is

$$f(E, L^2) = \frac{3-\gamma}{2^{3-\beta}} \sqrt{\frac{2}{\pi^5}} \frac{\Gamma(\gamma+1-2\beta)}{\Gamma(1-\beta)\Gamma(\gamma-\frac{1}{2}-\beta)} \frac{M_\bullet}{m_\star} \frac{\phi_0^{3/2}}{(GM_\bullet)^3} \left(\frac{L^2}{L_0^2}\right)^{-\beta} \left(\frac{|E|}{\phi_0}\right)^{\gamma-3/2-\beta} \quad (31)$$

where $L_0^2 = GM_\bullet r_h$. In this more general case, a non-negative f implies $\beta < \gamma - 1/2$, i.e. $\sigma_t^2/\sigma_r^2 > 3/2 - \gamma$.

This result is relevant to the “core” galaxies (§3), some of which have essentially flat or even centrally-decreasing densities within r_h (e.g. Lauer et al. 2002). The velocity distribution of stars near the SBHs in these galaxies must be biased toward circular orbits. The effect has probably been seen in M87 (Figure 6; Merritt & Oh 1997, Cappellari & McDermid 2005). An example of a formation mechanism that produces an anisotropic core is ejection of stars on radial orbits by a binary SBH (§7).

Even in spherical nuclei without cores, Jeans’s theorem permits large anisotropies, both toward circular orbits ($\sigma_t > \sigma_r$) and radial orbits ($\sigma_r > \sigma_t$) (Merritt 1985, Dejonghe 1989). Circularly-biased velocity distributions are generically stable on dynamical time scales (Barnes et al. 1986, Dejonghe & Merritt 1988); very radial velocity distributions, like that of a proposed, SBH-free model for the nucleus of M87 (Binney & Mamon 1982, Newton & Binney 1984), are unstable to nonspherical modes that convert the nucleus into a triaxial spheroid (Merritt 1987). However it is hard to see how strong radial anisotropies would develop in the first place. A moderate radial anisotropy has been claimed for stars within ~ 0.1 pc of the Milky Way SBH based on proper motion measurements (Schödel et al. 2003).

Figure 6 illustrates an important point about anisotropic models for galactic nuclei. In general, one expects a *degeneracy* in the inferred gravitational potential as a result of the nonuniqueness of f . For any choice of $\Phi(r)$, there are many 2D functions $f(E, L^2)$ that can precisely reproduce the 1D function $\rho(r)$. The same turns out to be true if additional moments of the velocity distribution function are measured, e.g. the line-of-sight velocity dispersion: there will generally exist a range of functions $\Phi(r)$ such that a non-negative $f(E, L^2)$ can be found which reproduces a finite set of observed moments exactly. In practice, the range of allowed Φ ’s is often extremely wide (e.g. Dejonghe

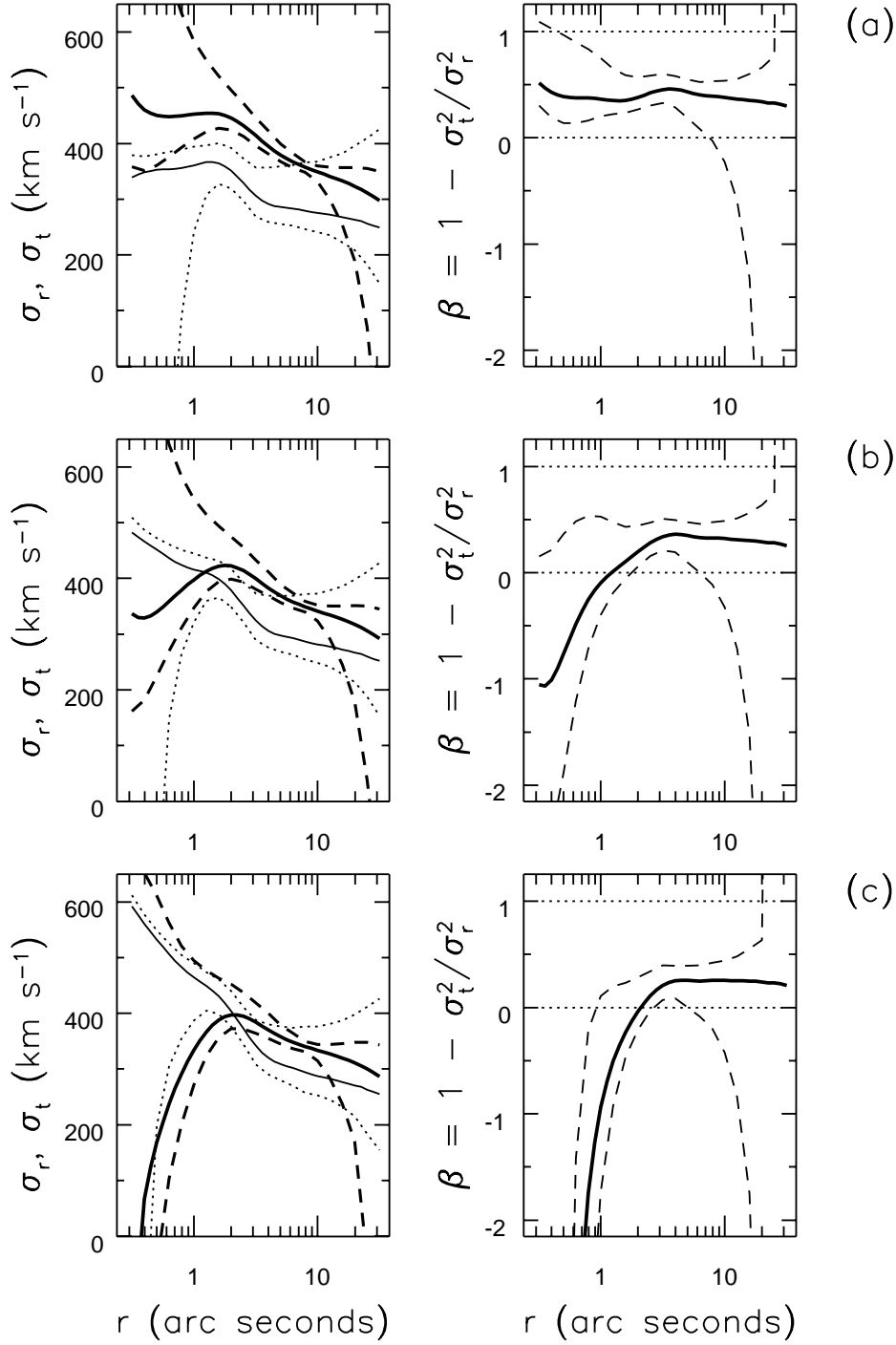


Figure 6. Velocity dispersions and velocity anisotropy in a spherical model of the center of M87, a “core” galaxy, under three different assumptions about the mass of the SBH: (a) $M_\bullet = 1.0 \times 10^9 M_\odot$, $r_h \approx 0.3''$; (b) $M_\bullet = 2.4 \times 10^9 M_\odot$, $r_h \approx 0.8''$; (c) $M_\bullet = 3.8 \times 10^9 M_\odot$, $r_h \approx 1.3''$. The individual components σ_r, σ_t of the velocity dispersion tensor were derived from the observed run of line-of-sight velocity dispersion with radius, under the assumption that the mass-to-light ratio of the stars is constant. Models with $M_\bullet \gtrsim 1 \times 10^9 M_\odot$ are characterized by tangential anisotropy, $\sigma_t > \sigma_r$, at $r \lesssim r_h$, a consequence of the very flat stellar density profile and the presence of a central mass. The best current estimate of M_\bullet is $3.6 \pm 1 \times 10^9 M_\odot$ (Macchetto et al. 1997). (From Merritt & Oh (1997).)

& Merritt 1992, Merritt 1993). This means that one can not expect to infer a unique value for M_\bullet , the mass of the SBH, in spherical nuclei unless substantially more data are available than the low-order velocity moments; for instance, each of the three models illustrated in Figure 6 makes identical predictions about the observed velocity dispersion profile. A similar indeterminacy afflicts axisymmetric models, as discussed below.

Anisotropy in the stellar velocity distribution at $r < r_h$ has consequences for the rate of interaction of stars with the SBH (§7). It also complicates inferences, based on the observed kinematics, about the mass of the SBH, as discussed in more detail below.

4.2. Axisymmetric Nuclei

Axisymmetric nuclei have a density $\rho = \rho(\varpi, z)$ where z is parallel to the symmetry axis and $\varpi^2 = x^2 + y^2$. The axisymmetric analog of an isotropic spherical model is a so-called “two-integral” model, $f = f(E, L_z)$ with L_z the component of the angular momentum about the symmetry axis. In two-integral models, the functional form of f is determined uniquely once $\rho(\varpi, z)$ and $\Phi(\varpi, z)$ are specified; the only freedom that remains is the choice of which sign to attach to L_z for each orbit, i.e. the degree of streaming about the symmetry axis (Lynden-Bell 1962, Dejonghe 1986, Hunter & Qian 1993). Since f depends on v_ϖ and v_z through the symmetric combination $v_r^2 + v_\varpi^2$, the velocity distribution at every position is forced to be the same with respect to ϖ and z , e.g. $\sigma_\varpi = \sigma_z$ (sometimes called “isotropy”). As the flattening of the mass distribution increases, the tensor virial theorem demands that σ_z decrease, and so σ_ϖ falls as well, i.e. the velocity distribution becomes more biased toward circular motions; in the disk limit, two-integral models contain only circular orbits.

Two-integral models are consistent with virtually every oblate-spheroidal mass distribution, i.e. the f inferred from ρ and Φ is nonnegative at every (E, L_z) . However prolate mass models tend to require negative f ’s unless they are nearly spherical (Batsleer & Dejonghe 1993, Dejonghe 1986) or have unrealistic isodensity contours (Jiang & Moss 2002), implying that prolate or barlike nuclei are dependent on a third integral.

The ease with which two-integral models can be constructed has made them popular for modelling the central parts of galaxies (e.g. Binney et al. 1990, Kuijken 1995, Verolme et al. 2002), and the same approach is sometimes used when estimating the mass of the SBH from kinematical data (e.g. van der Marel et al. 1994, Dehnen 1995, Magorrian et al. 1998). However it is dangerous to base estimates of M_\bullet on two-integral modelling, since one has no freedom to adjust f once the galaxy mass model has been specified; the kinematical data are not used at all aside from determining the fraction of orbits that rotate in the two directions about the symmetry axis. The best-fit M_\bullet is determined by the choice mandated for f (van der Marel 1999b). Indeed most of the putative SBH detections based on two-integral models (e.g. Magorrian et al. 1998) are now believed to be spurious since they were based on data that failed to resolve the SBH’s sphere of influence, sometimes by as much as two orders of magnitude (Merritt & Ferrarese 2001b).

Numerical integrations reveal that the majority of orbits in realistic axisymmetric potentials are regular, i.e. they respect a third isolating integral I_3 (e.g. Richstone 1982, Evans 1994). The main family of regular orbits are the tubes, which fill a torus-shaped region having the same symmetries as the potential. Varying I_3 at fixed E and L_z is roughly equivalent to varying the extent of the orbit in the z direction. Since the self-consistency problem (29a, 29b) generally has a solution for the restricted form $f = f(E, L_z)$, allowing the additional freedom of a third integral typically results in a large degeneracy of solutions, just as in the spherical geometry with $f = f(E, L)$. This freedom is exploited by modellers to construct self-consistent models which reproduce not only $\rho(\varpi, z)$, but also whatever additional kinematical information is available, e.g. the rotation curve near SBH (van der Marel et al. 1998, Bower et al. 2001, Gebhardt et al. 2003, Verolme et al. 2002, Valluri et al. 2005).

Originally it was hoped that kinematical information could eliminate the degeneracy inherent in three-integral modelling and permit well-constrained estimates of M_\bullet in nearby galaxies. Instead, it was found that in many galaxies, variations in the assumed value of M_\bullet could be compensated for by variations in $f(E, L_z, I_3)$ without changing the predicted line-of-sight kinematics at all; indeed models with $M_\bullet = 0$ often provide fits to the nuclear kinematics that are of precisely the same quality as models with a putative “best-fit” value of M_\bullet (e.g. in NGC 4342, Cretton & van den Bosch 1999; in NGC 3379, Gebhardt et al. 2000). This degeneracy is similar to that which characterizes the spherical geometry (Figure 6): the extra dimensionality in the data (1D→2D) is matched (crudely speaking) by the extra freedom in f ($f(E, L^2) \rightarrow f(E, L_z, I_3)$). The degeneracy is illustrated in Figure 7 for the galaxy M32, one of the best observed and best resolved of the SBH candidate galaxies; each of the models whose properties are illustrated there is an equally good fit to the kinematical data even though the assumed value of M_\bullet varies from 1.4 to $4.8 \times 10^6 M_\odot$ (Valluri et al. 2004).

While M32 is currently the only galaxy for which such comprehensive modelling has been carried out, it is likely that M_\bullet as derived from stellar kinematics in other galaxies is comparably degenerate, if not more so, since many of these galaxies were observed at lower effective resolutions than M32. Indeed a conservative, but justifiable, view is that no best-fit value of M_\bullet has been derived from stellar kinematics in *any* galaxy aside from the Milky Way. Even in the case of the Milky Way, it is instructive to recall that until about 2004, stellar-kinematical estimates of M_\bullet varied by roughly a factor of two, from $\sim 1.8 \times 10^6 M_\odot$ (Chakrabarty & Saha 2001) to $\sim 3.3 \times 10^6 M_\odot$ (Genzel et al. 2000), in spite of the availability of velocity data that were resolved into a distance of $\sim 10^{-3} r_h$ from the SBH. It was only after the orbits of individual stars, some with pericenter distances smaller than $10^{-4} r_h$, had been traced that the degeneracy was removed; the best current determination is $M_\bullet = 3.7 \pm 0.2 \times 10^6 M_\odot$ (Ghez et al. 2005). No external galaxy has stellar kinematical data of quality remotely comparable with that of the Galactic center, even *ca* 2000, and so a factor of four degeneracy in M_\bullet in a galaxy like M32 (the nearest external galaxy, which is resolved on a scale of $\sim 0.1 r_h$) is not surprising.

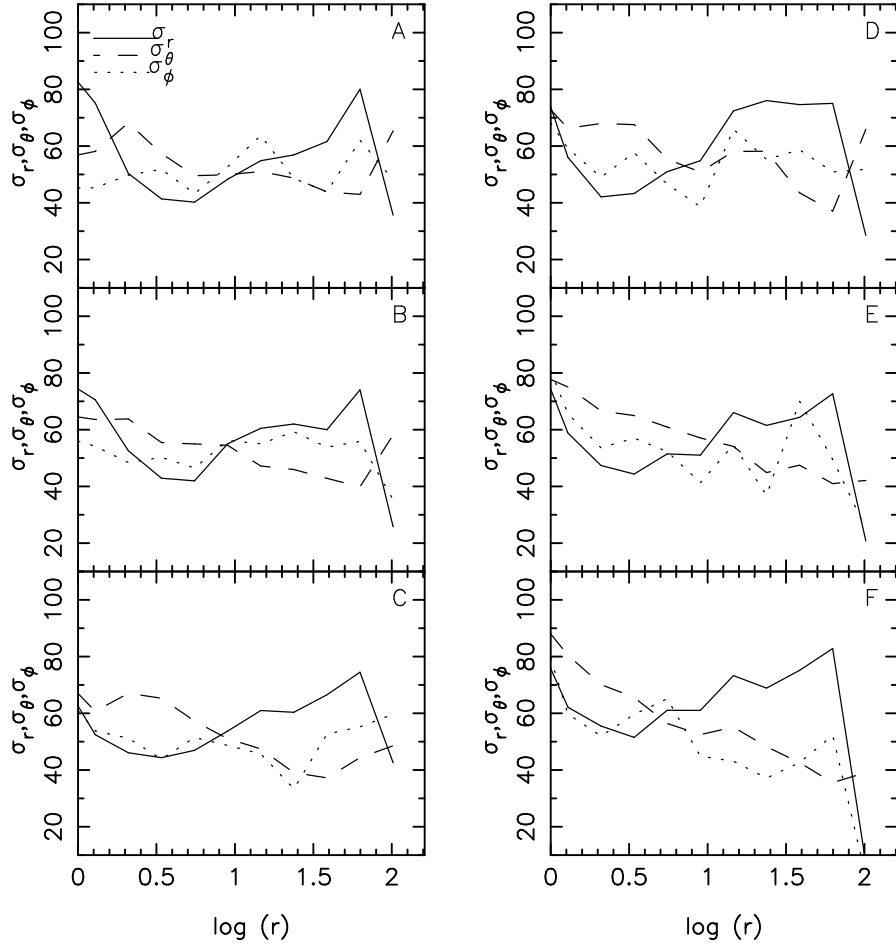


Figure 7. Internal kinematics of six, three-integral axisymmetric models of the galaxy M32. Each panel shows the three velocity dispersions $\sigma_r, \sigma_\phi, \sigma_\theta$ versus distance along the major axis in seconds of arc ($1'' \approx 3$ pc). The assumed value of M_\bullet increases from $1.4 \times 10^6 M_\odot$ (Model A; $r_h \approx 0.4''$) to $4.8 \times 10^6 M_\odot$ (Model F; $r_h \approx 1''$). Each of these models provides an equally good fit to the HST/FOS and ground-based kinematical data for M32. Models with small M_\bullet have radially-biased velocity ellipsoids ($\sigma_r > \sigma_\phi, \sigma_\theta$) at $r \lesssim r_h$, while models with large M_\bullet have tangentially-biased velocities; in other words, the indeterminacy in M_\bullet implies an indeterminacy also in the nuclear kinematics (Valluri et al. 2004).

It is common practice to “remove” the degeneracy in spherical or axisymmetric modelling by imposing ad hoc regularization on the solutions, e.g. “maximum entropy” (Richstone & Tremaine 1988, Gebhardt et al. 2003). The regularization constraint has the effect of singling out a single solution (M_\bullet, f) as “most probable,” even (or especially) in cases where the data are of insufficient quality to select a best-fit model.

The indeterminacy in stellar-dynamical estimates of M_\bullet is currently the biggest impediment to refining our understanding of SBH demographics, and it also severely limits the inferences that can be drawn about the stellar kinematics of nuclei (e.g. Figs. 6, 7). In collisional nuclei like that of M32, the indeterminacy might be reduced

by requiring the stellar distribution function to be collisionally relaxed in the sense defined below (§5). However the majority of galaxies with claimed SBH detections have collisionless nuclei, and the indeterminacy in stellar-dynamical estimates of M_\bullet in these galaxies will probably persist for the foreseeable future.

4.3. Nonaxisymmetric Nuclei

The degeneracy inherent in axisymmetric models becomes even more marked in triaxial models, and this fact, plus the complexity of dealing with an additional degree of freedom, has kept most galaxy modellers from venturing beyond the axisymmetric paradigm. But there are compelling reasons for considering non-axisymmetric models of galactic nuclei. Imaging of the centers of galaxies reveals a wealth of features in the stellar distribution on scales $r \approx r_h$ that are not consistent with axisymmetry, including bars, bars-within-bars and nuclear spirals (e.g. Shaw et al. 1995, Peng et al. 2002, Erwin & Sparke 2002). Even if these features are transient, they may be present for a significant part of a galaxy’s lifetime. Since orbits in non-axisymmetric potentials do not conserve any component of the angular momentum, “centrophilic” orbits like the boxes (Schwarzschild 1979) are allowed, which can pass arbitrarily close to the center after a finite time. This can imply chaos in the motion (Gerhard & Binney 1985), as well as much greater rates of interaction of stars with the SBH (Norman & Silk 1983).

Triaxiality is usually defined via the index T where

$$T \equiv \frac{a^2 - b^2}{a^2 - c^2} \quad (32)$$

and (a, b, c) are the scale lengths of the long (x), intermediate (y), and short (z) axes respectively. Oblate spheroids have $T = 0$, prolate spheroids have $T = 1$, and $T = 1/2$ is the “maximally triaxial” case.

In a triaxial nucleus containing a SBH, the character of the orbits depends on the distance from the center. (1) In the region near the SBH, $r \lesssim r_h$, the motion is nearly Keplerian and the forces from the stars constitute a perturbation, causing orbits to precess typically without destroying their integrability (Sridhar & Touma 1999, Sambhus & Sridhar 2000). Nearly-circular orbits are converted into tubes similar to the tube orbits in axisymmetric potentials. Nearly-radial orbits are converted into “pyramids,” Keplerian ellipses with one focus lying near the SBH and which precess in x and y (Figure 8; Poon & Merritt 2001). A symmetric pair of pyramid orbits oriented above and below the $x - y$ plane looks similar to a classical box orbit (Schwarzschild 1979), although with the opposite orientation, i.e. along the short axis of the figure, making it less useful for reconstructing the stellar density. A number of other, minor orbit families associated with resonances can be identified (Figure 8). (2) At intermediate radii, the SBH acts as a scattering center, rendering almost all of the boxlike orbits chaotic (Gerhard & Binney 1985). This “zone of chaos” extends outward from a few times r_h to a radius where the enclosed stellar mass is roughly 10^2 times the mass of the SBH (Valluri & Merritt 1998, Papaphilippou & Laskar 1998, Poon & Merritt 2001, Kalapotharakos

et al. 2004, Kalapotharakos & Voglis 2005). Integrable tube orbits continue to exist at these energies, as do resonant families like the 2 : 1 “banana” orbits that avoid the center (Miralda-Escude & Schwarzschild 1989). (3) At still larger energies, the phase space is a complex mixture of chaotic and regular orbits, including resonant boxlike orbits that remain stable by avoiding the center (Merritt & Valluri 1999).

Little is apparently known about the influence of figure rotation on the structure of orbits in triaxial black-hole nuclei. One study (Valluri 1999) found that figure rotation tends to increase the degree of orbital chaos, apparently because the Coriolis forces broaden orbits that would otherwise be thin, driving them into the destabilizing center.

The importance of these various orbit families is a function of how useful they are for solving the triaxial self-consistency problem. Following M. Schwarzschild’s (1979, 1993) pioneering work, it was generally assumed that triaxial nuclei would need to be supported by the regular (nonchaotic) orbit families like the pyramids and bananas (Kuijken 1993, Syer & Zhao 1998, Zhao et al. 1999, Jalali & de Zeeuw 2002). The first full self-consistency studies of triaxial nuclei (Poon & Merritt 2002, Poon & Merritt 2004) revealed that this was only partly correct. When only regular orbits were included in the orbital libraries, solutions were found in the nearly oblate and “maximally” triaxial geometries; the dominant orbits were the tubes circulating around the short axis, and the pyramid orbits. These models had power-law ($\rho \propto r^{-1}, r^{-2}$) radial density profiles and extended outward to $\sim 5r_h$. But when chaotic orbits were also included, at least 40%, and as much as 75%, of the mass was found to be assigned to these orbits. N -body integrations of these self-consistent models confirmed their stability, at least for several crossing times. Highly prolate models could not be constructed, with or without chaotic orbits.

This work showed for the first time that chaotic orbits could be major components of galactic nuclei. In retrospect, this need not have been surprising. Chaotic orbits fill a volume defined by an equipotential surface. Far from the center of a galaxy, the equipotential surfaces are nearly spherical, and so chaotic orbits at large energies are not very useful for reconstructing an elongated triaxial figure. Near the center of a galaxy with a power-law density profile, however, equipotentials are only slightly rounder than equidensities (Figure 9). Add to this the fact that many of the regular orbit families in triaxial nuclei tend to be oriented counter to the figure (Poon & Merritt 2001), and it follows that self-consistent solutions (if they exist) will draw heavily from the chaotic orbits.

Jeans’s theorem in its usual form (e.g. Equation 29a; Binney & Tremaine 1987) seems to exclude chaotic orbits. However a little thought confirms that chaotic orbits are perfectly acceptable components of steady-state galaxies, as long as they are populated with a uniform phase-space density throughout the accessible part of phase space (Kandrup 1998); indeed chaos is considered almost a *requirement* for defining a steady state in statistical mechanics (e.g. Sinai 1963). In triaxial black-hole nuclei, the time scale for achieving a uniform population of chaotic phase space – the “chaotic mixing” time – would be very short, of order a few crossing times (Merritt & Valluri 1996, Valluri

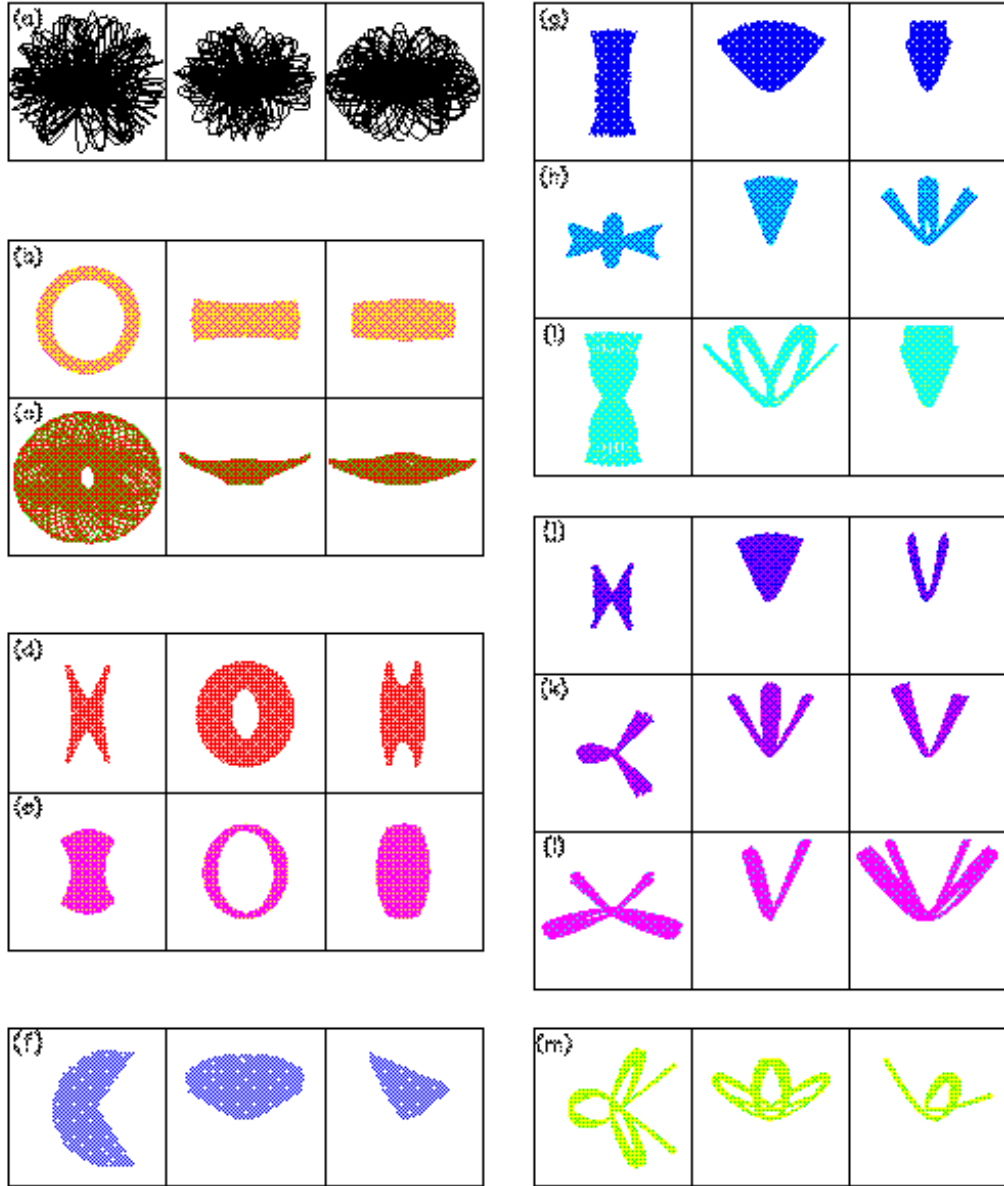


Figure 8. Major families of orbits in triaxial black-hole nuclei. Each set of three frames shows, from left to right, projections onto the (x, y) , (y, z) and (x, z) planes. (a) Stochastic orbit. (b) Short-axis tube orbit. (c) Saucer orbit, a resonant short-axis tube. (d) Inner long-axis tube orbit. (e) Outer long-axis tube orbit. (f) $(1, -2, 1)$ resonant orbit. (g) Pyramid orbit. (h) $(3, 0, -4)$ resonant pyramid orbit. (i) $(0, 6, -5)$ resonant pyramid orbit. (j) Banana orbit. (k) $2 : 3 : 4$ resonant banana orbit. (l) $3 : 4 : 6$ resonant banana orbit. (m) $6 : 7 : 8$ resonant orbit. (From Poon & Merritt (2001).)

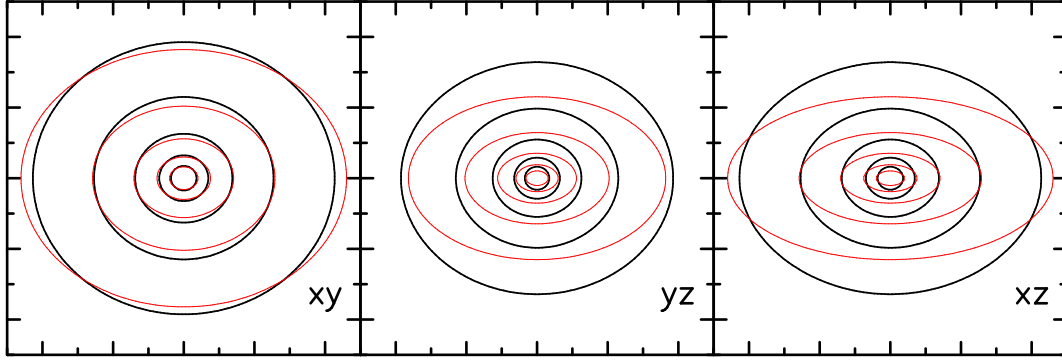


Figure 9. Principal-plane cuts through the equipotential (black/thick) and equidensity (red/thin) surfaces of a triaxial nucleus containing a SBH. The density falls off as $r^{-3/2}$ and the density axis ratios are $c/a = 0.5$, $b/a = 0.7$. The plots extend to ~ 5 times the SBH’s influence radius r_h in each direction. The equipotential surfaces are only moderately rounder than the equidensity surfaces. Chaotic orbits, which fill equipotential surfaces, can therefore be useful building blocks in the triaxial self-consistency problem.

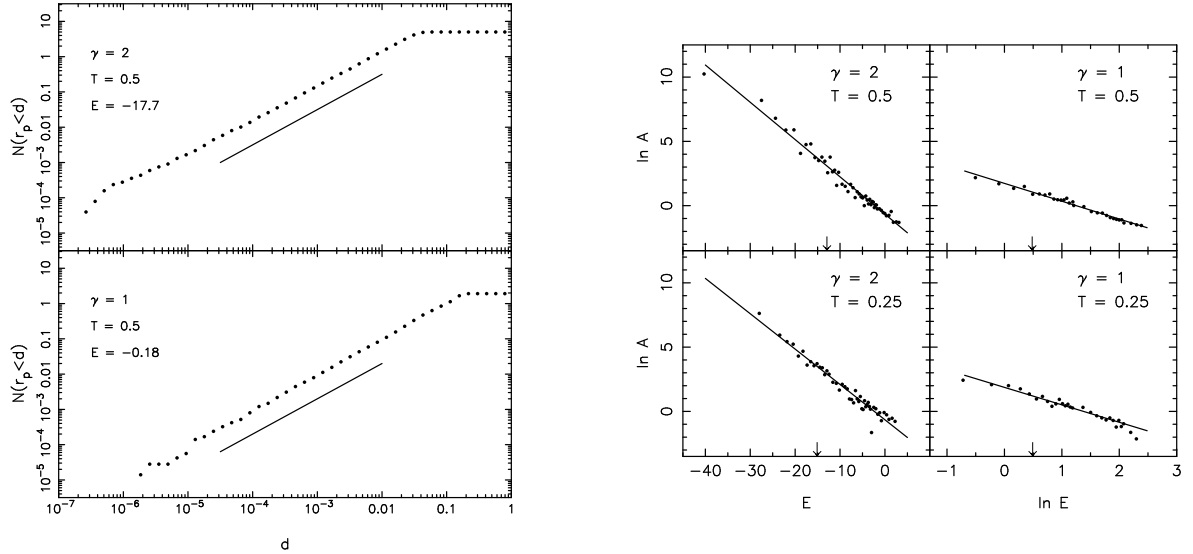


Figure 10. *Left panel:* Distribution of close approaches of a chaotic orbit to the central SBH in two triaxial nucleus models. Vertical axis shows the cumulative number of approaches having pericenter distances less than d ; the SBH’s tidal disruption radius is of order 10^{-7} in these units. The radial density profile is $\rho \propto r^{-\gamma}$ with $\gamma = 2$ (top panel) and $\gamma = 1$ (bottom panel). Both orbits have energies $\sim E_h \equiv \Phi(r_h)$. The solid lines have unit slope. *Right panel:* The function $A(E)$ (Equation 33) that describes the cumulative rate of pericenter passages in four triaxial nucleus models. The triaxiality index is $T \equiv (a^2 - b^2)/(a^2 - c^2)$; $T = 0.25$ is a nearly-oblate model and $T = 0.5$ is a “maximally triaxial” model. Points are from integrations of chaotic orbits; lines show fits; arrows indicate E_h . (From Merritt & Poon 2004)

& Merritt 2000, Kandrup & Sideris 2002, Kandrup & Siopis 2003).

Chaotic orbits have well-defined statistical properties. Let $N_E(r_p < d)$ be the

number of pericenter passages per unit time for a chaotic orbit of energy E , such that the distance from the SBH at pericenter r_p is less than d . Numerical integrations show (e.g. Figure 10) that

$$N_E(r_p < d) \approx A(E) \times d, \quad (33)$$

i.e. the number of close encounters with the SBH is an approximately linear function of the encounter distance. The function $A(E)$, in a singular isothermal sphere ($\rho \propto r^{-2}$) nucleus, is roughly

$$A(E) \approx \frac{\sigma^5}{G^2 M_\bullet^2} e^{-(E-E_h)/\sigma^2} \quad (34)$$

and in a triaxial nucleus with $\rho \propto r^{-1}$,

$$A(E) \approx \sqrt{\frac{GM_\bullet}{r_h^5}} \left(\frac{E}{E_h} \right)^{-1.4} \quad (35)$$

with $E_h \equiv \Phi(r_h)$ (Merritt & Poon 2004). These relations, together with estimates of the fraction of chaotic orbits at each energy (e.g. from the self-consistent solutions), can be used to estimate the total rate at which stars are “scattered” by the triaxial potential into the SBH, or into its tidal disruption sphere (§6). Here we emphasize that this mechanism of feeding stars to the SBH is collisionless, i.e. independent of gravitational encounters.

Poon & Merritt’s (2004) study is still the only attempt to solve the self-consistency problem for triaxial, black-hole nuclei on scales $r \lesssim r_h$. There is however a large body of work addressing the *large-scale* effects of central mass concentrations on triaxial spheroids or bars (e.g. Norman et al. 1985, Hasan et al. 1993, Dubinski 1994, Merritt & Quinlan 1998, Holley-Bockelmann et al. 2002, Kalapotharakos et al. 2004, Kalapotharakos & Voglis 2005, Athanassoula et al. 2005). These studies generally proceed by first constructing an N -body model for the bar or triaxial spheroid, then a compact mass is inserted or grown at the center and the model is integrated forward. Typically the model isophotes evolve toward rounder and/or more axisymmetric shapes on scales $\gtrsim r_h$; the evolution can be very striking when the mass of the central object exceeds $\sim 1\%$ of the total galaxy mass (compared with $\sim 0.1\%$ for real SBHs) and when the figure is elongated. When the mass of the SBH is smaller, $M_\bullet \lesssim 10^{-3} M_{gal}$, evolution is often still observed but the final shape can still be non-axisymmetric. The sudden evolution for large M_\bullet is likely due to conversion of the box orbits to chaotic orbits and the ensuing chaotic mixing. It is currently unclear whether Nature would select stable triaxial configurations for galactic nuclei like those constructed by Poon & Merritt (2004), or whether the presence of a SBH would mitigate against such equilibria, as it seems to do on larger scales.

Statler et al. (2004) used the measured streaming velocities of stars in NGC 4365 to model its intrinsic shape; they concluded that the galaxy was strongly triaxial, $T \approx 0.45$, and fairly elongated, $c/a \approx 0.6$. This result implies that SBH’s of mass $M_\bullet \approx 10^{-3} M_{gal}$ do not impose large-scale axisymmetry in galaxies. The velocity data on which this

conclusion was based were only resolved on scales $r \gtrsim 10r_h$ however and so do not constrain the triaxiality of the nucleus.

Due to the near-Keplerian nature of the potential at $r < r_h$, orbits like the pyramids are not centered on the SBH. Sridhar & Touma (1999) noted that off-center orbits can persist even in nuclei where the SBH itself is offset from the center of the stellar spheroid; furthermore they identified one family of loop orbits for which the offset was in the same direction as that of the spheroid. Salow & Statler (2001) and Sambhus & Sridhar (2002) used this result to construct self-consistent, planar, lopsided models for the nucleus of M31, and Jacobs & Sellwood (2001) showed via N -body simulations that the lopsided models could be relatively long-lived.

4.4. The “Adiabatic Growth” Model

It is tempting to try to derive the distribution of stars around a SBH from first principles (Peebles 1972a). For instance, if the stellar velocity distribution is assumed to be Maxwellian, $f(v) \propto e^{-v^2/2\sigma^2}$, with constant σ , then Jeans’s theorem implies $f(E) \propto e^{-E} \propto e^{-[v^2/2+\Phi(r)]/\sigma^2}$ and Equation (29a) gives for the stellar density near the SBH

$$\rho(r) \propto \int_0^{\sqrt{2GM_\bullet/r}} e^{-[v^2/2+\Phi(r)]/\sigma^2} v^2 dv \propto e^{GM_\bullet/\sigma^2 r}, \quad r \ll GM_\bullet/\sigma^2. \quad (36)$$

This expression implies an exponentially divergent stellar mass within r . It has other unphysical features as well: for instance, the fact that the velocity dispersion σ is constant implies that typical kinetic energies near the SBH are much smaller than binding energies, hence most stars must be near their apocenters.

A slightly more sophisticated approach is to start with an “isothermal” nucleus, $f \propto e^{-E}$, *without* a central mass, then increase the value of M_\bullet from zero and ask what happens to f and ρ . The initial model has a constant-density core; as the black hole grows, stars are pulled in and the density increases. In the limit that the rate of change of M_\bullet is slow compared with orbital periods, this “adiabatic growth” model yields for the final stellar distribution at $r \ll r_h$

$$f(E) = \text{const.}, \quad \rho(r) \propto \left(\frac{r}{r_h}\right)^{-3/2} \quad (37)$$

(Peebles 1972b, Young 1980). This model and variations (nonspherical or rotating nuclei, etc.) has been very widely investigated (see Merritt 2004 for a comprehensive review).

At first sight, Equation (37) is very promising: as Figure 2 shows, the stellar densities near the centers of the Local Group galaxies M32 and the Milky Way increase as $\rho \sim r^{-3/2}$ at $r \lesssim r_h$. But there is a consensus that the adiabatic growth model is probably *not* relevant to the structure of galaxy cores, for the following reasons.

- Both galaxies in Figure 2 have collisional nuclei, i.e. the relaxation time at $r < r_h$ is shorter than the age of the galaxy. The nuclear density profiles in these galaxies must have been strongly modified by energy exchange between stars (§5).

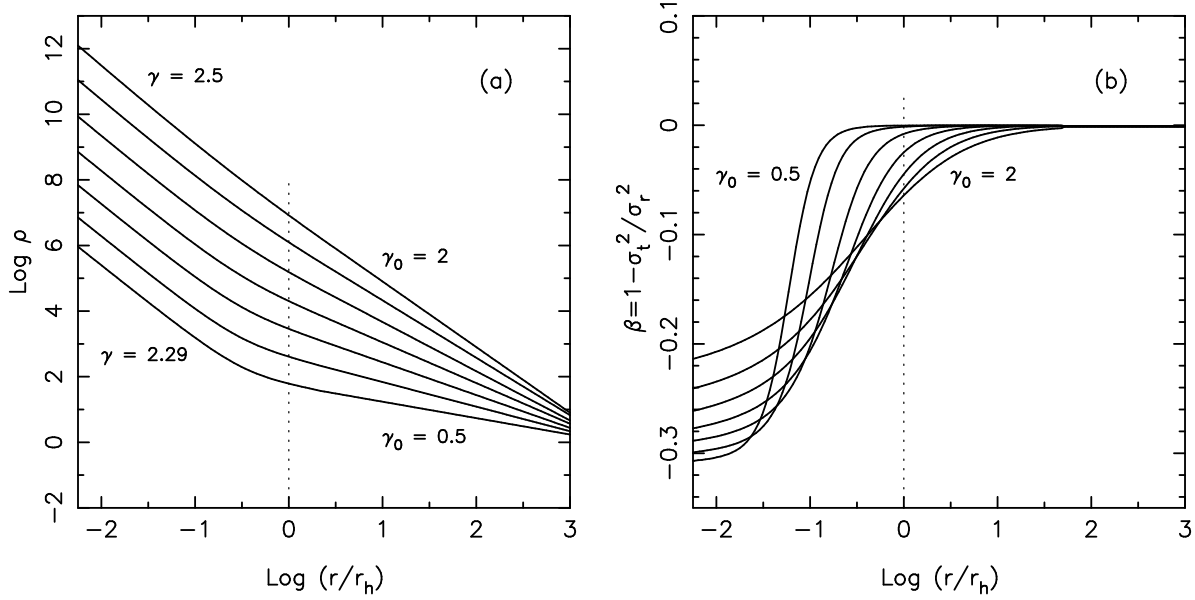


Figure 11. Influence of the adiabatic growth of a black hole on its nuclear environment in a spherical, isotropic galaxy. (a) Density profiles after growth of the black hole. Initial profiles were power laws, $\rho_i \propto r^{-\gamma_0}$, with γ_0 increasing upwards in steps of 0.25. The radial scale is normalized to r_h as defined in the initial galaxy (Eq. 4). The slope of the final profile at $r < r_h$ is almost independent of the initial slope. (b) Velocity anisotropies after growth of the black hole. A slight bias toward circular motions appears at $r < r_h$.

- The postulates of the adiabatic growth model – that the SBH grew in mass at a fixed location via spherically-symmetric accretion – are extremely unlikely; almost all models for growth of SBHs invoke strong departures from spherical symmetry in order to remove angular momentum from the infalling gas (e.g. Shlosman et al. 1990).
- Density profiles in the Milky Way, M32 and many other galaxies are steep power laws, $\rho \sim r^{-2}$, at $r \gtrsim r_h$. If a SBH grows at the center of a galaxy with a pre-existing power-law cusp, the profile at $r \lesssim r_h$ is an even steeper power law: an initial profile $\rho \propto r^{-\gamma_0}$ becomes $\rho \propto r^{-\gamma}$, $\gamma = 2 + (4 - \gamma_0)^{-1} > 2$ (Figure 11). Such steep profiles are not observed (although they might be present, but unresolved, in some galaxies).
- The adiabatic growth model can not explain the flat inner density profiles of the “core” galaxies (§3) without ad-hoc assumptions (e.g. van der Marel 1999b). The existence of the cores is now generally attributed to ejection of stars by a binary SBH following a galaxy merger (§7); this process would likely have taken place at some point during the formation of virtually every spheroid, destroying an adiabatic cusp even if it had been present.

Recently there has been a revival of interest in the adiabatic growth model in the context of the *dark matter* distribution at the center of the Milky Way and other galaxies

(Gondolo & Silk 1999). Some of the objections just raised to the adiabatic growth model for stellar nuclei do not apply to dark matter (Bertone & Merritt 2005).

5. Collisional Equilibria

Most galaxies with well-determined SBH masses have central relaxation times much longer than 10^{10} yr (Figure 1): their nuclei are “collisionless.” In a collisionless nucleus, the distribution of stars near the SBH will reflect the details of the nuclear formation process, and many steady-state configurations are possible, as discussed in §4. But Figure 1 reveals a clear trend of $T_r(r_h)$ with luminosity, such that galactic spheroids fainter than $M_V \approx -18$ have relaxation times at r_h shorter than 10^{10} yr. The Milky Way nucleus has $T_r(r_h) \approx 5 \times 10^{10}$ yr but the steep density profile implies shorter relaxation times at smaller radii: $\sim 6 \times 10^9$ yr at $0.2r_h$ (0.6 pc) and $\sim 3.5 \times 10^9$ yr at $0.1r_h$ (0.3 pc) (assuming Solar-mass stars). The nucleus of the Milky Way is therefore “collisional” in the sense defined in §2. Three other Local Group galaxies, M32, M33 and NGC 205, also have collisional nuclei (Lauer et al. 1998, Hernquist et al. 1991, Valluri et al. 2005) although M32 is the only one of these to exhibit dynamical evidence for a SBH (Merritt et al. 2001, Valluri et al. 2005).

Beyond the Local Group, essentially all of the galaxies for which the SBH’s influence radius is spatially resolved are “core” galaxies (§3) with low nuclear densities and long relaxation times. Still, it is reasonable to suppose that collisional nuclei are present in at least some galaxies with spheroid luminosities below the value at which the cores appear, $M_V \approx -20$. Furthermore the nuclei of the “core” galaxies may have been much denser before the cores were created by binary SBHs (§7).

In a collisional nucleus, an approximately steady-state distribution of stars is set up around the SBH in a time $\sim T_r(r_h)$. In the case of a single stellar mass, the steady-state density is $\rho \propto r^{-7/4}$; if there is a mass spectrum, the heavier stars will concentrate to the center (“mass segregation”). “Core collapse,” the runaway increase in density that occurs in isolated stellar systems after $\sim 10^2 T_r$, does not occur in nuclei containing SBHs, because the time required is too long and because the presence of the SBH inhibits the runaway (Marchant & Shapiro 1980).

Continued loss of stars to the SBH implies that no precisely steady-state equilibrium can exist; for instance, the nucleus will slowly expand due to the effective heat input as stars are destroyed (Shapiro 1977). This and related effects are discussed in more detail in §6.

5.1. The Bahcall-Wolf Solution

Gravitational encounters drive the local velocity distribution toward a Maxwellian, but a Maxwellian velocity distribution implies an exponentially divergent mass near the SBH (Equation 36). The existence of a region close to the hole where stars are captured or destroyed prevents the nucleus from reaching thermal equilibrium. The density must

drop to zero on orbits that intersect the SBH's event horizon at $r = r_S$, or that pass within the tidal disruption sphere at r_t ; the latter radius is most relevant since galaxies with collisional nuclei probably always have $M_\bullet \lesssim 10^8 M_\odot$ (§2). Ignoring for the moment a possible dependence of the stellar phase space density on orbital angular momentum L , and assuming spherical symmetry, the evolution of f can be approximated via the isotropic orbit-averaged Fokker Planck equation,

$$4\pi^2 p(E) \frac{\partial f}{\partial t} = -\frac{\partial F_E}{\partial E}, \quad (38a)$$

$$F_E(E, t) = -D_{EE} \frac{\partial f}{\partial E} - D_E f \quad (38b)$$

(Spitzer 1987). Here $p(E)$ is a phase-space volume element, $p(E) = 2^{-3/2} \pi G^3 M_\bullet^3 |E|^{-5/2}$ near the SBH, F_E is the flux of stars in energy space, and D_E and D_{EE} are diffusion coefficients that describe the effects of small-angle scattering:

$$\begin{aligned} D_{EE}(E) &= 64\pi^4 G^2 m^2 \ln \Lambda \left[q(E) \int_{-\infty}^E dE' f(E') + \int_E^0 dE' q(E') f(E') \right], \\ D_E(E) &= -64\pi^4 G^2 m^2 \ln \Lambda \int_E^0 dE' p(E') f(E') \end{aligned} \quad (39)$$

with $\ln \Lambda \approx \ln(M_\bullet/m)$ the Coulomb logarithm and $q(E) = (2^{1/2} \pi / 6) G^3 M_\bullet^3 |E|^{-3/2}$. The boundary conditions are $f(E_t) = 0$ and $f(0) = f_0$; $E_t = GM_\bullet/r_t$ is the energy at which stars are lost to the SBH and f_0 is the phase space density at $E = 0$. (The inner boundary condition is only approximate since the condition for a star to pass inside r_t is angular-momentum dependent, as discussed in more detail below. The outer boundary condition is also approximate since a non-zero f at large radii implies a population of stars whose contribution to the potential has been ignored.)

Bahcall & Wolf (1976) first presented numerical solutions to Equations (38a, 38b). They found that a steady state is reached after roughly one relaxation time at r_h . If $|E_t| \gg GM_\bullet/r_h$, i.e. if the disruption radius r_t is much smaller than r_h (which is the case in real nuclei), the steady-state solution is close to a power law,

$$f(E) = f_0 |E|^{1/4}, \quad \rho(r) = \rho_0 r^{-7/4}, \quad |E| \ll |E_t|, \quad r_t \ll r. \quad (40)$$

Equation (40) is a “zero-flux” solution, i.e. it implies $F_E = 0$. (An “isothermal” distribution, $f \sim e^{E/\sigma_0^2}$, also implies zero flux but is unphysical for the reasons discussed above.)

Figure 12 illustrates the evolution of $f(E, t)$ in the case of a cluster that extends beyond the SBH's influence radius. The Bahcall-Wolf cusp rises above the pre-existing density inside a radius $\sim 0.2r_h$.

In the numerical solutions, the steady-state flux is found to be small but non-zero, of order

$$F(E) \approx \frac{n(r_t) r_t^3}{T_r(r_t)} \propto r_t. \quad (41)$$

In other words, the flux is determined by the rate at which stars can diffuse into the disruption sphere at r_t . This flux is “small” in the sense that the one-way flux of

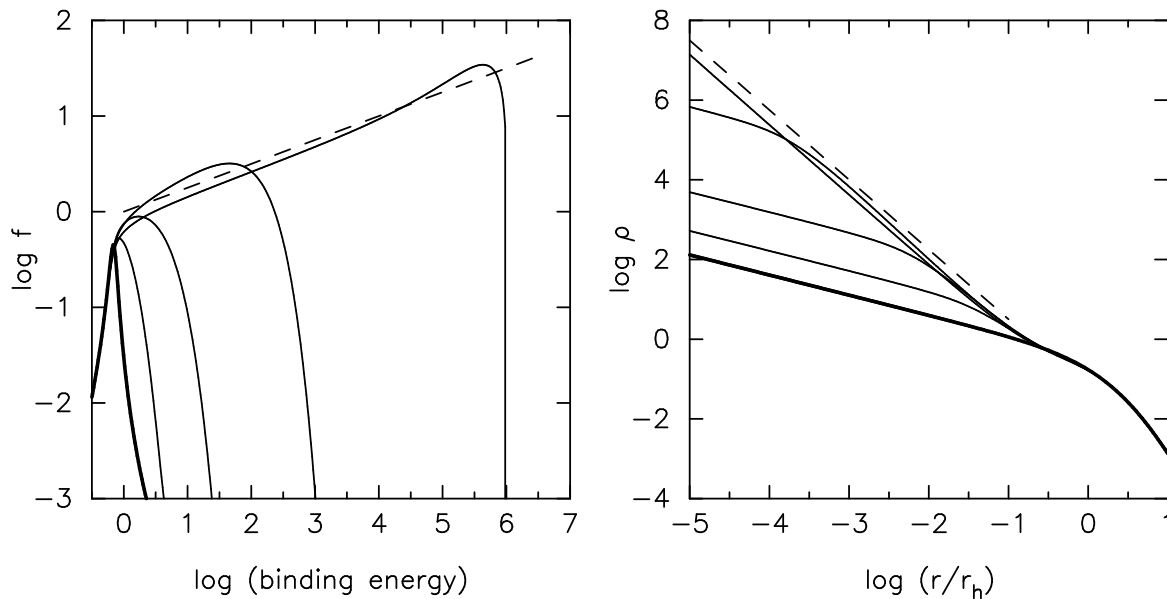


Figure 12. Evolution of the stellar distribution around a SBH due to energy exchange between stars. These curves were computed from the isotropic, orbit-averaged Fokker-Planck equation (Equations 38a, 38b) with boundary condition $f = 0$ at $\log |E| = 6$. Left panel: phase-space density f ; right panel: configuration-space density ρ . The initial distribution (shown in bold) had $\rho \propto r^{-0.5}$ near the SBH; thin curves show f and ρ at times of (0.2, 0.4, 0.6, 1.0) in units of the relaxation time at the SBH’s initial influence radius r_h . Dashed lines show the “zero-flux” solution $f \propto |E|^{1/4}$, $\rho \propto r^{-7/4}$. The steady-state density is well approximated by the zero-flux solution at $r \lesssim 0.2r_h$.

stars in or out through a surface at $r_t \ll r \lesssim r_h$ is much greater; except near r_t , the inward and outward fluxes almost cancel. Thus, the steady-state flux is limited by the “bottleneck” at $r = r_t$. As r_t is reduced, the flux approaches zero and the numerical solution approaches the power-law form of Equation (40).

At the center of the Milky Way, the flux implied by the Bahcall-Wolf solution would only be of order $\sim 10^{-12}$ stars yr^{-1} . Frank & Rees (1976) pointed out that the actual loss rate to a black hole would be dominated by changes in angular momentum, not energy, implying a much higher flux. (This is discussed in more detail in §6.) Bahcall & Wolf (1977) included these loss-cone effects heuristically, by finding steady-state solutions of the modified equation

$$4\pi^2 p(E) \frac{\partial f}{\partial t} = -\frac{\partial F_E}{\partial E} - \rho_{lc}(E, t) \quad (42)$$

where the term ρ_{lc} is an approximate representation of the true loss rate into the SBH (Lightman & Shapiro 1977). They found that the addition of the loss term had only a small effect on the steady-state form of $f(E)$ and $\rho(r)$ even though it substantially increased the implied loss rate.

Solutions of the full, anisotropic Fokker-Planck equation, including a careful treatment of loss cone dynamics as well as physical collisions between stars, were first presented by Cohn & Kulsrud (1978). (The parameters in this study were chosen

to mimic the distribution of stars around a black hole in a globular cluster.) The logarithmic derivative of the steady-state density was found to be $d \ln \rho / d \ln r \approx -1.65$ for r in the range $10^{-3} < r/r_h < 10^{-1}$, compared with the Bahcall-Wolf value of -1.75 . The velocity anisotropy was found to be close to zero for $r \gtrsim 10^{-3} r_h$. The Bahcall-Wolf solution has been verified in a number of other studies based on fluid (Amaro-Seoane et al. 2004) or Monte-Carlo (Marchant & Shapiro 1980, Duncan & Shapiro 1983, Freitag & Benz 2002) approximations to the Fokker-Planck equation.

Most recently, advances in computer hardware (e.g. Makino et al. 2003) and software (e.g. Mikkola & Aarseth 1990, Mikkola & Aarseth 1993) have made it possible to test the Bahcall-Wolf solution via direct N -body integrations, avoiding the approximations of the Fokker-Planck formalism (Preto et al. 2004, Baumgardt et al. 2004a, Merritt & Szell 2005). Figure 13 shows a set of N -body simulations of collisional cusp growth compared with the predictions of the isotropic Fokker-Planck equation. In these simulations, there was no loss of stars and so a true “zero-flux” equilibrium was established.

The Milky Way is probably the only galaxy in which a Bahcall-Wolf cusp could currently be detected: its central relaxation time is shorter than 10^{10} yr and its nuclear density profile is resolved on scales $\ll r_h$. Figure 2 suggests that the bright stars have $\rho \sim r^{-1.5}$ at $10^{-3} \lesssim r/r_h \lesssim 10^{-1}$. This is slightly shallower than the Bahcall-Wolf “zero-flux” prediction but probably consistent given the uncertainties in the observed profile (Schödel et al. 2006). The presence of a mass spectrum also implies a smaller slope (§5.2). In addition, the time required to reach a steady state at the Galactic center may be $\gtrsim 10^{10}$ yr (Merritt & Szell 2005).

5.2. Multi-Mass Equilibria

Galaxies contain stars with a range of masses. The initial mass function, i.e. the distribution of masses at the time of formation, is believed to be roughly a power-law, $n(m) \propto m^{-\alpha}$, $\alpha \approx 2$ (Salpeter 1955, Miller & Scalo 1979), but the mass function changes with time as stars lose mass and as new stars are formed. Mass functions near the centers of galaxies are difficult to constrain observationally; this is true even at the Galactic center due to crowding and obscuration. Evolutionary models assuming a constant rate of star formation (e.g. Alexander 2005) suggest that $\sim 75\%$ of the mass after 10 Gyr would be in the form of “live” stars with $\langle m \rangle \approx 0.5 M_\odot$, $\sim 20\%$ in white dwarves with $0.6 M_\odot \leq m \leq 1.1 M_\odot$, and a few percent in neutron stars ($m = 1.4 M_\odot$) and black holes ($m \approx 10 M_\odot$). At the center of the Milky Way there is also known to be a population of more massive stars, $3 M_\odot \lesssim m \lesssim 15 M_\odot$, inside $\sim 10^{-2} r_h$, which probably could not have formed *in situ* due to tidal stresses from the SBH (Ghez et al. 2003, Eisenhauer et al. 2005).

Exchange of energy between stars with different masses tends to establish local equipartition of kinetic energy, leading to spatial segregation (Spitzer & Shull 1975): the more massive stars congregate closer to the center.

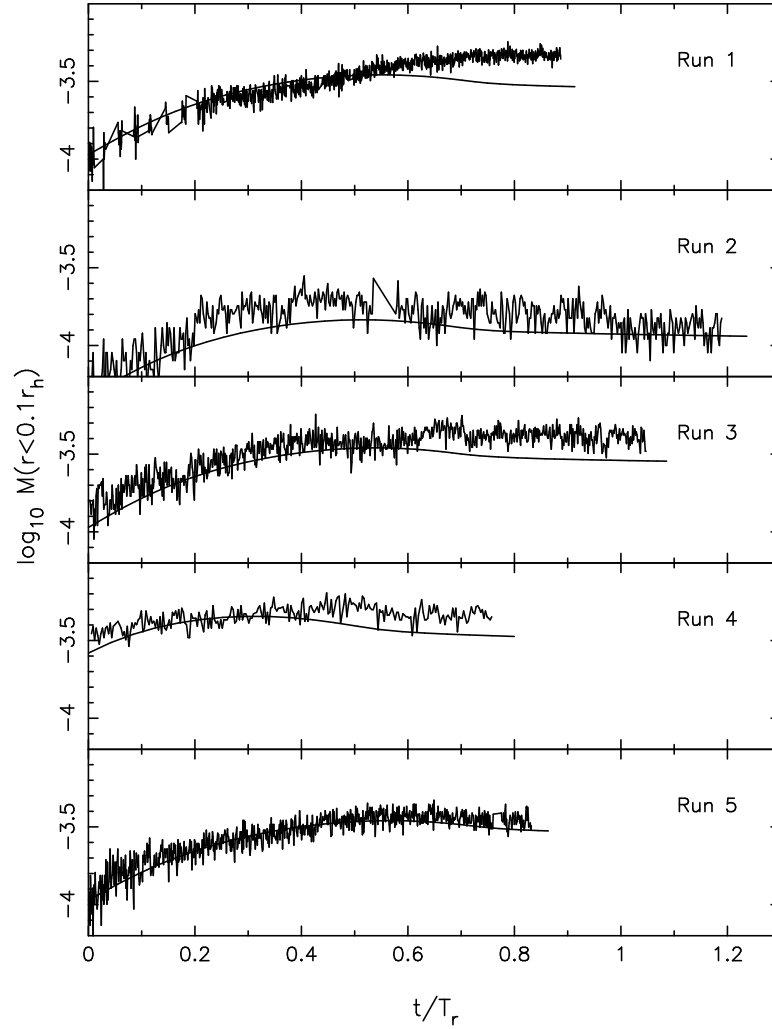


Figure 13. Evolution of the mass in stars within a distance $0.1r_h$ from a massive body (“black hole”) in a set of N -body simulations with different initial conditions and different particle numbers. A chain-regularization algorithm was used to handle close encounters between stars and the black hole. Smooth curves are solutions to the Fokker-Planck equation (38a,38b). (From Preto et al. 2004)

The mass-segregation time scale can be estimated by considering two mass groups m_1 and m_2 . Assuming Maxwellian velocity distributions, the mean rate of change of kinetic energy for stars of mass m_1 due to encounters with stars of mass m_2 is

$$\frac{d\epsilon_1}{dt} = \frac{8(6\pi)^{1/2} G^2 m_1 \rho_2 \ln \Lambda}{(v_{1,rms}^2 + v_{2,rms}^2)^{3/2}} (\epsilon_2 - \epsilon_1) \quad (43)$$

where $\epsilon_i = \frac{1}{2} m_i v_{i,rms}^2$; the same expression with indices interchanged gives $d\epsilon_2/dt$ (Spitzer 1987). Suppose that $m_2 \ll m_1$ and assume $v_{1,rms} \approx v_{2,rms}$, appropriate shortly after the nucleus forms. Then

$$T_1 \equiv \left| \frac{1}{\epsilon_1} \frac{d\epsilon_1}{dt} \right|^{-1} = \frac{0.0814 v_{rms}^3}{G^2 m_1 \rho_2 \ln \Lambda}, \quad T_2 \equiv \left| \frac{1}{\epsilon_2} \frac{d\epsilon_2}{dt} \right|^{-1} = \frac{\rho_2}{\rho_1} T_1. \quad (44)$$

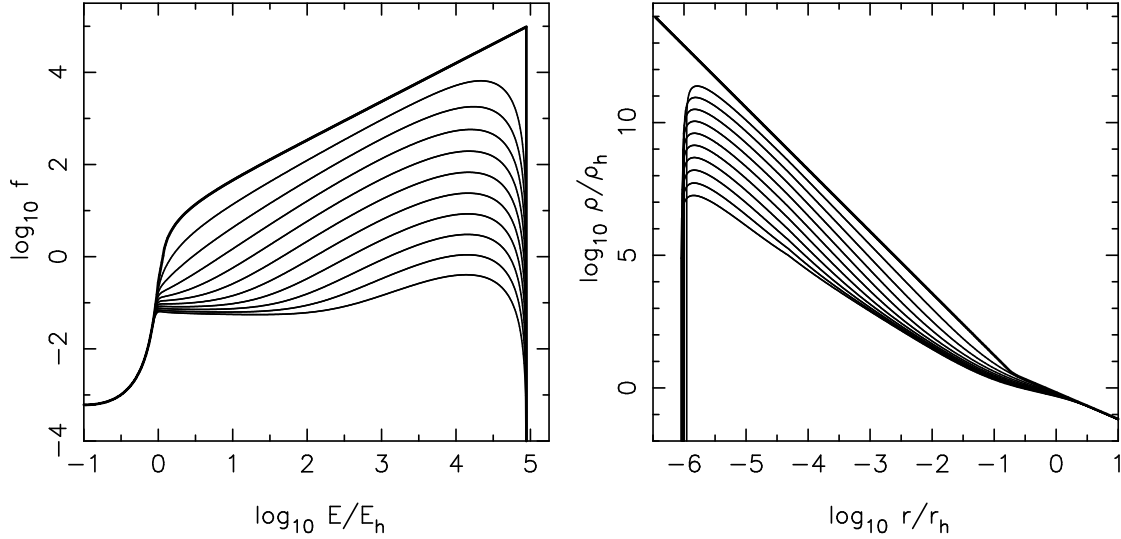


Figure 14. Evolution of a population of low-mass objects due to heating from a dominant, high-mass population and to scattering into the SBH. $f(E, t)$ and $\rho(r, t)$ are the phase-space and configuration-space densities respectively of the low-mass population. Times shown are 2, 4, ..., 20 in units of the time T_2 defined in Eq. 44. The space density evolves from $\rho \sim r^{-2.3}$ to $\sim r^{-1.5}$. (Adapted from Merritt 2004)

Consider first the case that the heavier stars dominate the total density and have a relaxation time $T_{r,1}$. Then $T_2 \approx T_{r,1}$ and the light stars reach equipartition on the same time scale that the heavy stars establish a collisional steady-state. On the other hand, if the light stars dominate, with relaxation time $T_{r,2}$, then $T_1 \approx (m_2/m_1)T_{r,2}$, and the heavy stars lose energy to the light stars very rapidly compared with $T_{r,2}$. The first case describes a nucleus containing stars and particle dark matter, while the latter describes a nucleus containing stars and a population of massive remnants. In either case, the time for the sub-dominant component to reach equipartition with the dominant component is of order T_r for the dominant component or less.

The single-mass Fokker-Planck equation can be generalized to the multi-mass case by defining $f(E, m, t)dm$ as the number density of stars in phase space with masses in the range m to $m + dm$. Then (e.g. Merritt 1983)

$$4\pi^2 p(E) \frac{\partial f}{\partial t} = -\frac{\partial F_E}{\partial E},$$

$$F_E(E, m, t) = -D_{EE} \frac{\partial f}{\partial E} - m D_E f, \quad (45)$$

with diffusion coefficients

$$D_{EE}(E) = 64\pi^4 G^2 \ln \Lambda \left[q(E) \int_{-\infty}^E dE' h(E') + \int_E^0 dE' q(E') h(E') \right],$$

$$D_E(E) = -64\pi^4 G^2 \ln \Lambda \int_E^0 dE' p(E') g(E') \quad (46)$$

and g and h are moments over mass of f :

$$g(E, t) = \int_0^\infty f(E, m, t) m \, dm,$$

$$h(E, t) = \int_0^\infty f(E, m, t) m^2 dm. \quad (47)$$

Considering again the case of a nucleus containing stars with just two masses, $m_1 \gg m_2$, the evolution equation for the lighter component may be found by taking the first moment over mass of Equation (45), restricting the integral to the mass range which characterizes the lighter stars. The result is

$$4\pi^2 p(E) \frac{\partial g_2}{\partial t} = \frac{\partial}{\partial E} \left(D_{EE} \frac{\partial g_2}{\partial E} \right), \quad (48a)$$

$$D_{EE}(E) = 64\pi^4 G^2 \ln \Lambda \left[q(E) \int_{-\infty}^E dE' h_1(E') + \int_E^0 dE' q(E') h_1(E') \right] \quad (48b)$$

with g_2 the phase-space mass density of the lighter stars. (These equations apply also to the more general case of a distribution of light-star masses; g_2 is then the total mass density of the lighter population.) The steady-state solution is obtained by setting $\partial g_2 / \partial E = 0$, yielding a density profile for the light component $\rho_2 \propto r^{-3/2}$ (cf. Equation 30), *independent* of the f that describes the heavier stars. Figure 14 illustrates the evolution toward this state. If the heavier objects dominate the density, then their steady-state density is $\rho \propto r^{-7/4}$; in other words, the lighter component is less centrally concentrated than the heavier component. Note however the difference in density slopes is fairly small even in this extreme case.

Bahcall & Wolf (1977) solved the coupled Fokker-Planck equations for systems containing stars of two masses around a SBH. They assumed that the two populations had similar densities at $r \gtrsim r_h$. The heavier component was found to always attain a steady-state density with slope close to the single-mass value $-7/4$, while the lighter component was less centrally condensed, with index

$$-\frac{d \ln \rho_2}{d \ln r} \approx \left(\frac{m_2}{4m_1} + \frac{3}{2} \right). \quad (49)$$

This expression gives the expected results $\rho_2 \propto r^{-7/4}$ when $m_2 = m_1$ and $\rho_2 \propto r^{-3/2}$ when $m_2 \ll m_1$.

Murphy et al. (1991) incorporated realistic mass spectra into their time-dependent solutions of the isotropic Fokker-Planck equation; they also included physical collisions as well as mass loss from stars. Murphy et al. found that the more massive component always attained a power-law slope close to $-7/4$, the least massive component had a slope near $-3/2$, and intermediate mass groups scaled approximately as Equation (49). Baumgardt et al. (2004b, 2005) carried out N -body simulations of star clusters containing a massive black hole and a range of stellar masses; they observed mass segregation but did not compare their results in detail with the Bahcall-Wolf formula. Baumgardt et al. found that the density profile of the “bright stars” in their simulations (i.e. the particles representing giants) was very flat after a relaxation time, with no hint of a power-law cusp. This puzzling result appears not to have been satisfactorily explained. Most recently, Freitag et al. (2006) presented Monte-Carlo models of the evolution of the Galactic center star cluster including a Kroupa et al. (1993) mass function. The heaviest mass group in their simulations consisted of the $\sim 10M_\odot$ stellar

black holes; in models designed to mimic the Galactic center cluster, they found that the black holes segregated to the center in ~ 5 Gyr, after which loss of stars into the SBH drove a general expansion (§6.5). The stellar black holes were found to dominate the mass density within ~ 0.2 pc $\approx 0.1r_h$ of the center. The density profile of the black holes was found to be “compatible” (modulo noise) with the Bahcall-Wolf single mass form, $d \log \rho / d \log r = -7/4$, while the main-sequence stars near the center had $-d \log \rho / d \log r \approx 1.3 - 1.4$. Freitag et al.’s simulations were targeted toward nuclei with SBHs in the mass range $10^5 M_\odot \leq M_\bullet \leq 10^7 M_\odot$, even though there is no firm evidence for SBHs with masses below $\sim 10^{6.5} M_\odot$, since these would be the SBHs of most interest to gravitational-wave physicists. Their results suggest that mass segregation is likely to be of marginal importance in the majority of nuclei with confirmed SBHs due to the long relaxation times (§2).

5.3. Cusp Regeneration

As discussed below (§7), binary SBHs formed during galaxy mergers are efficient at destroying dense nuclei. Essentially all stellar spheroids are believed to have experienced such events in the past, and evidence for the “scouring” effect of binary SBHs is seen in the flat, central density profiles or “mass deficits” of bright elliptical galaxies (Figure 4). An important question is whether the existence of dense cusps at the centers of galaxies like the Milky Way and M32 implies that no binary SBH was ever present, or whether a collisional cusp could have spontaneously regenerated after being destroyed. Merritt & Szell (2005) used N -body integrations to simulate cusp destruction by a binary SBH, then combined the two “black holes” into one and continued the integrations until a Bahcall-Wolf cusp had formed around the single massive particle. Figure 15 shows the results of one such integration for mass ratio $q = 0.5$ and initial density profile $\rho \sim r^{-1.5}$. Cusp regeneration was found to require roughly one relaxation time as measured at the SBH’s influence radius r_h ; for reasonable mass ratios ($M_2/M_1 \lesssim 0.5$), the binary hardly affects the density at this radius (Fig. 15). Growth of the cusp is preceded by a stage in which the stellar velocity dispersion evolves toward isotropy and away from the tangentially-anisotropic state induced by the binary. When scaled to the Galactic center, these experiments suggest that a dense cusp could have been regenerated in 10^{10} yr, although evolution toward the steady-state profile might still be occurring.

As discussed above (§3), “mass deficits,” or cores, are observed to disappear in galaxies fainter than $M_V \approx -19.5$. This might be due in part to cusp regeneration in these galaxies, although central relaxation times are almost always too long for this explanation to be convincing (Fig. 1). An alternative explanation is suggested by Figure 1: galaxies fainter than $M_V \approx -19.5$ are mostly unresolved on scales of r_h , which is also approximately the size of a core created by a binary SBH. The lack of mass deficits in galaxies with $M_V \gtrsim -19.5$ probably just reflects a failure to resolve the cores in these galaxies.

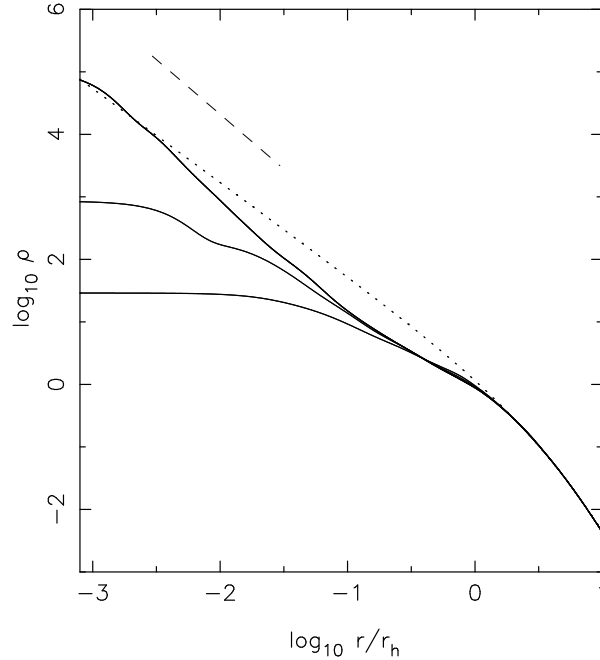


Figure 15. Regeneration of a Bahcall-Wolf cusp around a black hole after destruction by a massive binary. Dotted line is the initial density profile of an N -body model containing a massive central particle (the “black hole”) of mass 0.01, in units where the total galaxy mass is one. Lower solid line shows the density after infall of a second “black hole” of mass 0.005 has destroyed the cusp. Upper solid lines show the evolving density after the two black hole particles were combined into one, simulating coalescence. The final time would be roughly 10^{10} yr if scaled to the Galactic center. The dashed line has logarithmic slope of $-7/4$. (Adapted from Merritt & Szell 2005.)

6. Loss-Cone Dynamics

As discussed in §5.1, the existence of a region $r \leq r_t$ close to the SBH where stars are captured or destroyed can have a significant influence on the steady-state distribution of stars even at radii $\gg r_t$, since it precludes the formation of an “isothermal” distribution of velocities. Loss of stars is also important because of its observational consequences: tidally disrupted stars are expected to produce X- and UV radiation with luminosities of $\sim 10^{44}$ erg s $^{-1}$, potentially outshining their host galaxies for a period of days or weeks (Rees 1990, Kobayashi et al. 2004, Khokhlov & Melia 1996, Kochanek 1994). A handful of X-ray flaring events have been observed that have the expected signature (Komossa 2002, Komossa et al. 2004, Halpern et al. 2004), and the number of detections is crudely consistent with theoretical estimates of the event rate (Donley et al. 2002, Wang & Merritt 2004). Tidal flaring events may dominate the X-ray luminosity function of AGN at $L_X \lesssim 10^{44}$ erg s $^{-1}$ (Milosavljević et al. 2006).

Compact objects (neutron stars or stellar-mass black holes) can remain intact at much smaller distances from the SBH; these objects would emit gravitational waves at potentially observable amplitudes before spiralling in, and may dominate the event

rate for low-frequency gravitational wave interferometers like LISA (Sigurdsson & Rees 1997, Gair et al. 2004, Hopman & Alexander 2006). (The other major categories of low-frequency gravitational wave events are compact, stellar binaries and binary SBHs; the latter are discussed in §7.)

A central SBH acts like a sink, removing stars on “loss-cone” orbits, i.e. orbits that intersect the capture or disruption sphere $r = r_t$. In a spherical galaxy, this removal is complete after just one galaxy crossing time, and continued supply of stars to the SBH requires some mechanism for loss-cone repopulation. The most widely discussed mechanism is gravitational encounters, which drive a diffusion in energy (E) and angular momentum (L). The latter dominates the loss rate (Frank & Rees 1976, Lightman & Shapiro 1977). Roughly speaking, many of the stars within the SBH’s influence radius will be deflected into r_t in one relaxation time, i.e. the loss rate is roughly $(M_\bullet/m_\star)T_r(r_h)^{-1}$. In a collisional nucleus (§2) with $M_\bullet \approx 10^6 M_\odot$, this is $\sim 10^6/(10^{10} \text{ yr}) \approx 10^{-4} \text{ yr}^{-1}$.

Classical loss cone theory (Bahcall & Wolf 1976, Lightman & Shapiro 1977, Ipser 1978, Cohn & Kulsrud 1978) was directed toward understanding the observable consequences of massive black holes at the centers of globular clusters. Globular clusters are many relaxation times old, and this assumption was built into the theory, by requiring the stellar phase space density f near the black hole to have reached an approximately steady state under the influence of gravitational encounters. One consequence of the much longer ($\gtrsim 10^{10} \text{ yr}$) relaxation times in galactic nuclei is that the stellar density profile near the SBH need not have the collisionally-relaxed, Bahcall-Wolf form (§5.1). Another is that nuclei can be strongly nonspherical or non-axisymmetric, which permits the existence of centrophilic (box or chaotic) orbits (§4.3); stars on centrophilic orbits can easily dominate the loss rate. In addition, depending on the details of the nuclear formation process, the stellar phase-space density in a galactic nucleus can depart strongly from its steady-state form near the loss cone, even in a precisely spherical galaxy. For instance, if the current SBH was preceded by a binary SBH, stars on orbits with pericenter distances $\sim a_h \gg r_t$ will have been ejected by the binary, and until these orbits are repopulated (on a time scale $\sim T_r$), the loss rate to the SBH can be much smaller than in the steady state. Other initial conditions, e.g. an “adiabatic” cusp around the SBH (§4.4), could result in higher loss rates than predicted by the steady-state theory.

6.1. Classical Loss-Cone Theory

Stars are swallowed or tidally disrupted after coming within a certain distance of the hole. The tidal disruption radius is

$$r_t = \left(\eta^2 \frac{M_\bullet}{m_\star} \right)^{1/3} r_\star. \quad (50)$$

Here m_\star and r_\star are the stellar mass and radius, and η is a form factor of order unity; $\eta = 0.844$ for an $n = 3$ polytrope. Tidal disruption occurs outside of the hole’s

event horizon for a solar-type star when $M_\bullet \gtrsim 10^8 M_\odot$. In what follows, r_t will be used indiscriminately to denote the radius of capture or disruption, and stars will be assumed to vanish instantaneously when $r < r_t$. Galaxies with the highest feeding rates are expected to be those with the smallest SBHs, $M_\bullet \lesssim 10^7 M_\odot$, and in these galaxies $r_t > r_s$.

In a spherical galaxy, an orbit that just grazes the tidal disruption sphere has angular momentum

$$L_{lc}^2 = 2r_t^2 [E - \Phi(r_t)] \approx 2GM_\bullet r_t; \quad (51)$$

the latter expression assumes $|E| \ll GM_\bullet/r_t$, i.e. that stars are on nearly-radial orbits with apocenters much larger than r_t .

An upper limit to the consumption rate in a spherical galaxy comes from assuming that stars are instantaneously replaced on their original orbits after being consumed by the hole. In this “full loss cone” model, stars are consumed at a constant rate

$$\dot{N}^{\text{FLC}} \approx \int \frac{N_{lc}(E)}{P(E)} dE = \int F(E)^{\text{FLC}} dE \quad (52)$$

where $P(E)$ is the period of a nearly-radial orbit of energy E and $N_{lc}(E)dE$ is the number of stars at energies E to $E + dE$ on orbits with $L \leq L_{lc}$. In a spherical galaxy,

$$N(E, L)dEdL = 8\pi^2 L f(E, L) P(E, L) dEdL \quad (53)$$

(Spitzer 1987) and

$$\dot{N}^{\text{FLC}} \approx 4\pi^2 \int f(E) L_{lc}^2(E) dE \approx 8\pi^2 r_t^2 \int f(E) (E - \Phi_t) dE \quad (54)$$

where $\Phi_t \equiv \Phi(r_t)$ and the stellar velocity distribution has been assumed to be isotropic. Using Equation (30) for $f(E)$ near the SBH in a power-law ($\rho \propto r^{-\gamma}$) nucleus, this expression can be evaluated:

$$\dot{N}^{\text{FLC}} \approx (3 - \gamma) \sqrt{\frac{2}{\pi}} \frac{\Gamma(\gamma + 1)}{\Gamma(\gamma + 3/2)} \left(\frac{M_\bullet}{m_\star}\right) \left(\frac{r_t}{r_h}\right)^{3/2-\gamma} \left(\frac{GM_\bullet}{r_h^3}\right)^{1/2}. \quad (55)$$

For $\gamma = 3/2$, which is close to the value observed near the Milky Way SBH (Fig. 2, the time T_\bullet required to consume $N_\bullet = M_\bullet/m_\star$ stars is independent of r_t :

$$T_\bullet \approx \frac{2\sqrt{2}}{9} \left(\frac{GM_\bullet}{r_h^3}\right)^{-1/2} \approx 0.3 \frac{r_h}{\sigma}, \quad (56)$$

i.e. the hole consumes its mass in stars in roughly one crossing time at r_h .

Early discussions of SBH feeding (e.g. Hills 1975, Ozernoy 1976, Shields & Wheeler 1978) sometimes assumed a full loss cone; for instance, in the “black tide” model for quasar fueling (Young et al. 1977, Young 1977), gas from tidally disrupted stars radiates as it spirals into the SBH, and the the hole shines as a quasar until its mass reaches $\sim 10^8 M_\odot$ at which point stars are swallowed whole and the quasar fades. A number of recent studies (Zhao et al. 2002, Miralda-Escudé & Kollmeier 2005, Holley-Bockelmann et al. 2005, Holley-Bockelmann & Sigurdsson 2006) have revived the full loss cone idea in the context of single or binary SBHs. At least in spherical or axisymmetric

galaxies, feeding rates as large as (55) would only persist for single orbital periods, long enough for stars on loss-cone orbits to be consumed; presumably these orbits would have been depleted already during the chaotic events associated with SBH formation. Various justifications have been invoked for assuming that \dot{N} remains of order \dot{N}^{FLC} for much longer times; perhaps the most plausible is that the nucleus is strongly non-axisymmetric and contains centrophilic orbits (§6.4). Under the full-loss-cone assumption, feeding rates are high enough that the mass accumulated in 10 Gyr can be sufficient to reproduce observed SBH masses (Zhao et al. 2002), although presumably only a fraction of the mass liberated when $r_t > r_S$ would find its way into the hole.

A more common assumption is that loss cone orbits were depleted at some early time, and that continued supply of stars to the SBH is limited by the rate at which these orbits can be re-populated. The most widely discussed mechanism for orbital repopulation is two-body relaxation. Consider again a spherical galaxy. Star-star encounters induce changes in orbital energy and angular momentum. The former were considered above (§5) and shown to imply very low consumption rates. Much larger rates are implied by changes in orbital angular momentum (Frank & Rees 1976, Lightman & Shapiro 1977, Young 1977). In a time $T_r(E)$, the two-body relaxation time for orbits of energy E , the typical change in L^2 is of order $\sim L_c^2(E) \approx G^2 M_\bullet^2 / (2|E|)$, the squared angular momentum of a circular orbit. In a single orbital period $P \ll T_r$, the rms angular momentum change is roughly

$$(\delta L)^2 \approx (P/T_r) L_c^2. \quad (57)$$

Near the hole, orbital periods are short, and a star will complete many orbits before being deflected in. Far from the hole, on the other hand, orbital periods are long enough that a star can be deflected in and out of the loss cone in a single orbital period. For stars in this outer (“pinhole”) region, consumption by the hole has almost no effect on the orbital population, and the feeding rate is equal to the full loss cone rate defined above. The energy separating the inner, diffusive region from the outer, full-loss-cone region is E_{crit} , defined as the energy such that

$$\delta L \approx L_{lc}. \quad (58)$$

A more quantitative definition of E_{crit} is in terms of the orbit-averaged quantity $q(E)$: $q(E_{crit}) = 1$, where

$$q(E) \equiv \frac{1}{R_{lc}(E)} \oint \frac{dr}{v_r} \lim_{R \rightarrow 0} \frac{\langle (\Delta R)^2 \rangle}{2R} = \frac{P(E) \bar{\mu}(E)}{R_{lc}(E)}, \quad (59)$$

here $R \equiv L^2/L_c(E)^2$, a dimensionless angular momentum variable, and $\langle (\Delta R)^2 \rangle$ is defined in the usual way as the sum, over a unit interval of time, of $(\Delta R)^2$ due to encounters. As the second expression in Equation (59) shows, $q(E)$ is the ratio of the orbital period to the orbit-averaged time $(\bar{\mu}/R_{lc})^{-1}$ for angular momentum to change by L_{lc} , with $\bar{\mu}(E)$ the orbit-averaged diffusion coefficient. In terms of q , the “diffusive” loss cone regime has $q(E) < 1$ and the “pinhole” regime has $q(E) > 1$.

Typically, the total consumption rate is dominated by stars with $q(E) \lesssim 1$, i.e. by stars that diffuse gradually into the loss cone. For $q \ll 1$, there is almost no

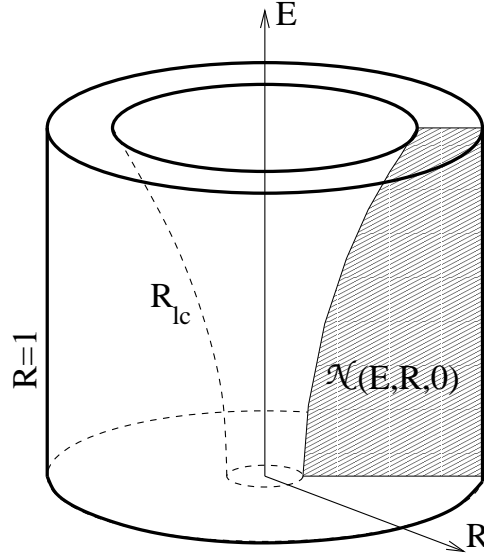


Figure 16. Schematic representation of the loss cone.

dependence of density on orbital phase since changes in L take much longer than an orbital period. In this regime, it is appropriate to describe the diffusion in terms of the Fokker-Planck equation (Lightman & Shapiro 1977). Ignoring changes in E , the Fokker-Planck equation describing diffusion in angular momentum is

$$\frac{\partial N}{\partial t} = \frac{1}{2} \frac{\partial}{\partial R} \left[\langle (\Delta R)^2 \rangle \frac{\partial N}{\partial R} \right] \quad (60)$$

where the dependence of N on E is understood. Taking the limit $R \rightarrow 0$ and averaging over one orbital period, this becomes

$$\frac{\partial N}{\partial t} = \bar{\mu} \frac{\partial}{\partial R} \left(R \frac{\partial N}{\partial R} \right) \quad (61)$$

where $\bar{\mu}(E)$ is the orbit-averaged diffusion coefficient defined above. Equation (61) has the same form as the heat conduction equation in cylindrical coordinates, as can be seen by changing variables to $j = R^{1/2}$:

$$\frac{\partial N}{\partial t} = \frac{\bar{\mu}}{4j} \frac{\partial}{\partial j} \left(j \frac{\partial N}{\partial j} \right); \quad (62)$$

j plays the role of a radial variable and $\bar{\mu}/4$ is the diffusivity. Figure 16 illustrates the geometry. The loss cone is sometimes called a “loss cylinder” by virtue of this analogy with the heat conduction problem.

The steady-state solution to Equation (61) is

$$N(R; E) = \frac{\ln(R/R_{lc})}{\ln(1/R_{lc}) - 1} \bar{N}(E) \quad (63)$$

where

$$\bar{N}(E) = \int_{R_{lc}}^1 N(E, R) dR \quad (64)$$

or, in terms of the phase space density f ,

$$f(R; E) = \frac{\ln(R/R_{lc})}{\ln(1/R_{lc}) - 1} \bar{f}(E). \quad (65)$$

The phase space density tends logarithmically to zero at the loss cone boundary $R = R_{lc}$. The implied (number) flux of stars into the loss cone is

$$F(E)dE = \frac{4\pi^2 P(E) L_c^2(E) \bar{\mu}(E) \bar{f}(E)}{\ln(1/R_{lc}) - 1} dE \quad (66a)$$

$$\approx \frac{\bar{N}(E) \bar{\mu}(E)}{\ln(1/R_{lc})} dE \quad (66b)$$

where the latter expression assumes $L_{lc} \ll L_c$ and $P(E, R) \approx P(E)$. This is lower than the full-loss-cone feeding rate by a factor $\sim q/\ln(1/R_{lc}) \approx q/\ln(GM_\bullet/4|E|r_t)$. Equation (66b) implies that a large fraction of the stars in the diffusive regime will migrate into the hole in one relaxation time; the consumption rate depends only logarithmically on the “size” r_t of the tidal disruption sphere (Frank & Rees 1976, Lightman & Shapiro 1977). In the 1D (energy-dependent) problem, the consumption rate is much smaller, scaling as r_t^{-1} (§5).

This analysis breaks down where $q \gtrsim 1$, since changes in L over one orbital period are of order L , and the separation of time scales that is implicit in the orbit-averaged treatment does not apply. Cohn & Kulsrud (1978) developed an approximate scheme to deal with this situation. In the presence of relaxation, some stars will enter and exit the loss cone $R \leq R_{lc}$ in one orbital period, thus evading disruption. Cohn & Kulsrud (1978) wrote the r -dependent Fokker-Planck equation for stars near the loss cone and computed how the density changes *along* orbits due to the competing effects of capture at $r < r_t$ and relaxation-driven repopulation at $r > r_t$. They found that the L -dependence of the steady-state phase-space density near the loss could be approximated by replacing R_{lc} in Equation (65) by R_0 , where

$$R_0(E) = R_{lc}(E) \times \begin{cases} \exp(-q), & q(E) > 1 \\ \exp(-0.186q - 0.824\sqrt{q}), & q(E) < 1 \end{cases}. \quad (67)$$

Near the hole, $q \ll 1$ and $R_0 \approx R_{lc}$: relaxation effects are small and the phase-space density falls to zero just at the loss-cone boundary. Far from the hole, relaxation dominates, and f only falls to zero for orbits with $L \ll L_{lc}$. Cohn & Kulsrud (1978) then computed the flux by assuming that Equations (65) and (66b) still applied, even in the “pinhole” regime where the diffusion approximation breaks down; this assumption gives the reasonable result that the flux approaches the full loss cone value far from the hole.

Cohn & Kulsrud (1978) included this “boundary layer” prescription into a fully time-dependent calculation of the evolution of $f(E, R, t)$ for stars around a black hole. They were primarily interested in the case of a $\sim 10^3 M_\odot$ black hole in a globular cluster, and so their solution was required to match on to a constant-density (isothermal) core at large radii. The contribution of the stars to the gravitational potential was

ignored. Cohn & Kulsrud (1978) also assumed that the star cluster was many relaxation times old, and so they evolved their time-dependent equations until a steady state was reached. The stellar density profile evolved approximately to the Bahcall-Wolf form, $\rho \sim r^{-7/4}$, near the hole and the feeding rate attained a constant value. This value was substantially larger than had been found by earlier authors who adopted more approximate descriptions of the loss-cone boundary, by factors ranging from ~ 2 (Shapiro & Marchant 1978) to ~ 15 (Lightman & Shapiro 1977), showing the sensitive dependence of the feeding rate on the assumed form of f near the loss cone.

6.2. Application to Galactic Nuclei

Loss cone theory as developed in the classic papers of Frank & Rees (1976), Lightman & Shapiro (1977) and Cohn & Kulsrud (1978) can be used to estimate feeding rates for SBHs in galactic nuclei. A number of possible complications arise however:

- Much of the total consumption occurs from orbits that extend beyond $\sim r_h$, hence the contribution of the stars to the gravitational potential can not be ignored.
- Galactic nuclei are often much less than one relaxation time old (§2). This means that the stellar density near the SBH need not have the Bahcall-Wolf (1976) steady-state form. In the most luminous galaxies, the nuclear density profile is in fact known to be much flatter than $\rho \sim r^{-7/4}$ at $r \lesssim r_h$ (§3).
- The dependence of f on L near the loss cone boundary can also be very different from its steady-state form, regardless of the form of $\rho(r)$. For instance, if the current SBH was preceded by a massive binary, almost all low-angular-momentum stars will have been ejected by the binary.
- Galactic nuclei need not be spherical or even axisymmetric. In a triaxial nucleus containing centrophilic orbits, the mass in stars on orbits that intersect the SBH's capture sphere can be enormous, much greater than M_\bullet , so that the loss cone is never fully depleted. Even in a spherical nucleus, the velocity distribution can be anisotropic (§4).
- Galactic nuclei sometimes undergo catastrophic changes, due to galaxy mergers, infall of star clusters or black holes, star formation, etc. all of which can substantially affect the feeding rate on both the short and long terms.

Starting with Murphy et al. (1991), a standard approach has been to consider only the first two of these complications when computing feeding rates of SBHs in galactic nuclei, i.e. to allow the density profile around the SBH to have whatever form is implied by the observations (which however often do not resolve r_h) and to include the contribution of the stars to the gravitational potential when computing the angular-momentum diffusion coefficient (e.g. Murphy et al. 1991, Syer & Ulmer 1999, Magorrian & Tremaine 1999, Wang & Merritt 2004). The energy dependence of the stellar distribution function is then fixed by $\rho(r)$ and by the assumed (or measured) value of M_\bullet ; the L -dependence of f near the loss cone is taken from the steady-state theory.

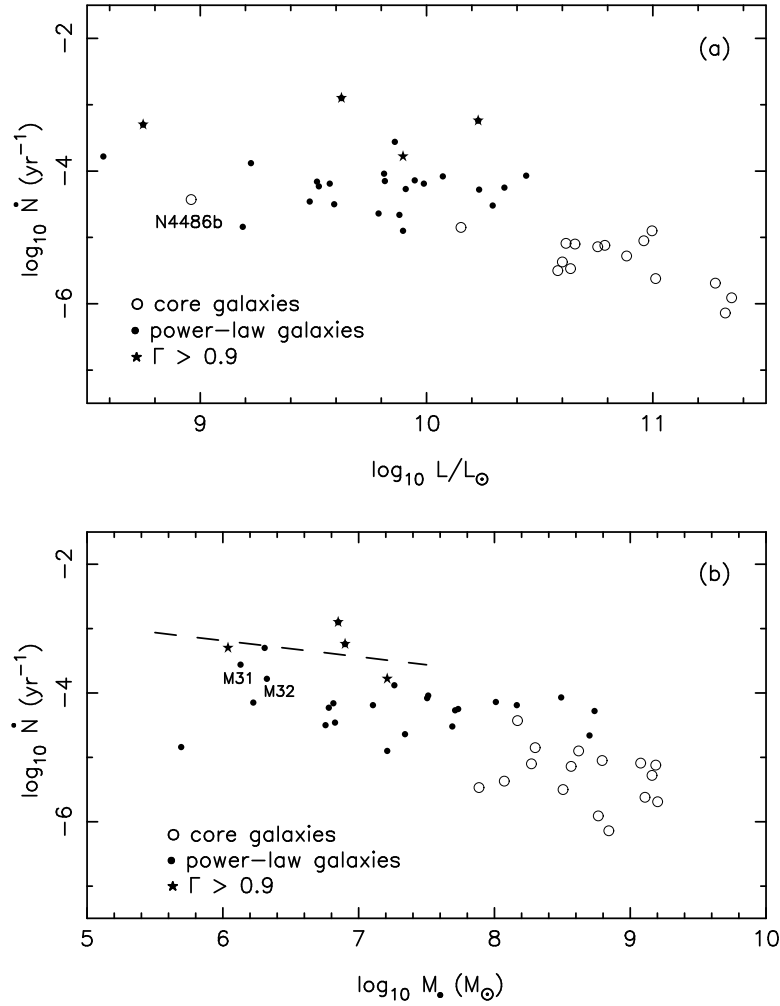


Figure 17. Consumption rate as a function of galaxy luminosity (a) and SBH mass (b) for a sample of elliptical galaxies. Plotted is the rate at which stars (assumed to have the mass and radius of the Sun) are scattered into a radius r_t (Eq. 50); note that for the most massive SBHs plotted here, $r_t \lesssim r_S$ and stars would not be tidally disrupted before falling into the hole. The dashed line in (b) is the relation defined by the singular isothermal sphere, Eq. 69; it is a good fit to the galaxies plotted with stars, which have central density profiles with $\rho \sim r^{-2}$ at $r \gtrsim r_h$. (From Wang & Merritt 2004.)

Figure 17 shows tidal disruption rates computed in this way for a sample of early-type galaxies (Wang & Merritt 2004). There is a weak net dependence of \dot{N} on M_{\bullet} , in the sense that nuclei with smaller SBHs tend to have higher feeding rates. In the smallest galaxies with well-determined SBH masses, e.g. M32, \dot{N} is predicted to exceed 10^{-4} yr^{-1} . A similar rate would be predicted for the Milky Way, which is almost an exact copy of M32 in terms of its central density profile and SBH mass. It follows that, at the Galactic center, the most recent tidal disruption event should have occurred just a few thousand years ago.

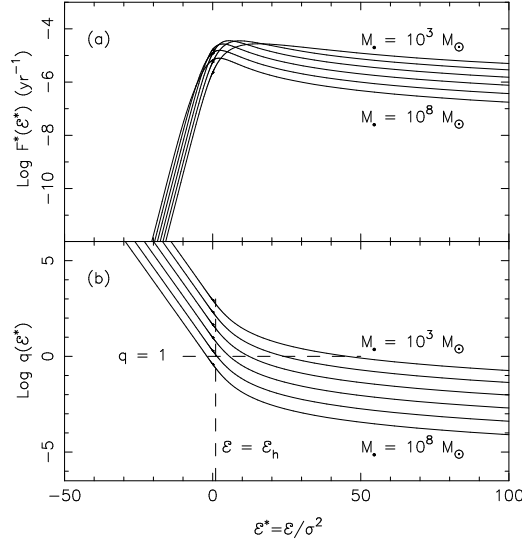


Figure 18. Energy-dependent loss cone flux $F(E)$ (Eq. 66b) and $q(E)$ (Eq. 59) for a SBH in a singular isothermal sphere nucleus, $\rho \propto r^{-2}$. The $M_\bullet - \sigma$ relation was used to relate σ to M_\bullet . (From Wang & Merritt 2004.)

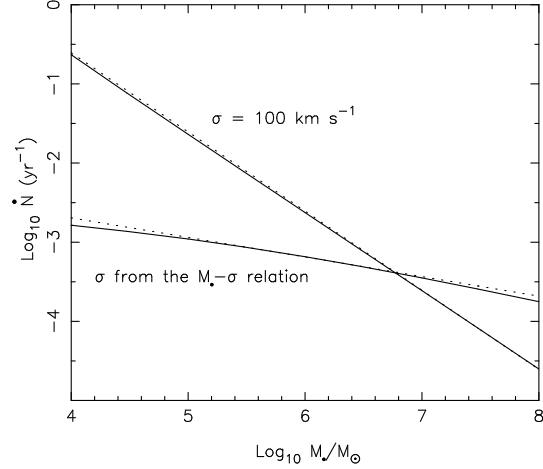


Figure 19. Consumption rate as a function of M_\bullet in singular isothermal sphere nuclei, for two assumptions about $\sigma(M_\bullet)$. (From Wang & Merritt 2004.)

The galaxies in Figure 17 with the highest feeding rates have density profiles $\rho \sim r^{-2}$ at $r \gtrsim r_h$. In the case of the Milky Way bulge, which is the only spheroid in this category near enough to be well resolved on scales $\ll r_h$, we know that $\rho(r)$ flattens from $\sim r^{-2}$ to $\sim r^{-1.5}$ at $r < r_h$ (Genzel et al. 2003). However much of the loss cone flux comes from stars with apocenters $\gtrsim r_h$, and so it is reasonable to approximate $\rho(r)$ as a singular isothermal sphere (SIS), $\rho \propto r^{-2}$, in these low-luminosity galaxies. Figures 18 and 19 show the predicted loss rates in SIS nuclei. The total \dot{N} depends on the two parameters $(M_\bullet/m_\star, r_h/r_t)$; adopting (50) for r_t , the second of these parameters can be written

$$\frac{r_h}{r_t} = \frac{2\Theta}{\eta^{2/3}} \left(\frac{M_\bullet}{m_\star} \right)^{2/3} \quad (68a)$$

$$= 21.5 \left(\frac{M_\bullet}{m_\star} \right)^{2/3} \left(\frac{\sigma}{100 \text{ km s}^{-1}} \right)^{-2} \left(\frac{m_\star}{M_\odot} \right) \left(\frac{r_\star}{R_\odot} \right)^{-1} \quad (68b)$$

with $\Theta = Gm_\star/2\sigma^2 r_\star$ the Safronov number; η in (50) has been set to 0.844. In Figure 19, two different assumptions have been made about the relation between M_\bullet and σ : constant σ , and the $M_\bullet - \sigma$ relation. The stellar mass and radius were set equal

to the Solar values. In both cases, the results are well fit by the simple expression

$$\dot{N} \approx 7.1 \times 10^{-4} \text{yr}^{-1} \left(\frac{\sigma}{70 \text{ km s}^{-1}} \right)^{7/2} \left(\frac{M_{\bullet}}{10^6 M_{\odot}} \right)^{-1}. \quad (69)$$

The normalization constant in equation (69) was chosen to reproduce \dot{N} exactly for $\sigma = 70 \text{ km s}^{-1}$, $M_{\bullet} = 10^6 M_{\odot}$; the consumption rate scales as $m_{\star}^{-1/3} r_{\star}^{1/4}$ for non-Solar stars. Equation (69), combined with the $M_{\bullet} - \sigma$ relation, implies $\dot{N} \sim M_{\bullet}^{-0.25}$. Equation 69 is consistent with the rates computed directly from the observed luminosity profiles in the fainter galaxies (Fig. 17).

Tidal disruption rates as high as $\sim 10^{-4} \text{ yr}^{-1}$ in nuclei with $M_{\bullet} \approx 10^6 M_{\odot}$ imply a liberated mass of $\sim M_{\bullet}$ after 10 Gyr. This is not necessarily a problem since only a fraction of the gas removed from stars is expected to find its way into the hole (Rees 1990). Nevertheless, the high values of \dot{N} in low-luminosity galaxies suggest that matter tidally liberated from stars might contribute substantially to SBH masses in these galaxies.

The faintest systems in which there is solid kinematical evidence for SBHs are M32 and the bulge of the Milky Way ($L \approx 10^9 L_{\odot}$, $M_{\bullet} \approx 10^{6.5} M_{\odot}$). However there is strong circumstantial evidence for massive black holes in fainter systems (e.g. Filippenko & Ho 2003) and for intermediate mass black holes (IMBHs) in starburst galaxies and star clusters (e.g. van der Marel 2004). If nuclear black holes are common in the so-called dE (dwarf elliptical) galaxies and in the bulges of late-type spiral galaxies, these systems would dominate the total tidal flaring rate, due both to their large numbers and to their high individual event rates. A simple calculation (Wang & Merritt 2004) suggests that the tidal flaring rate due to dwarf galaxies in the Virgo cluster alone would be of the order of 10^{-1} yr^{-1} . Nondetection of flares after a few years of monitoring would argue against the existence of IMBHs in dwarf galaxies.

6.3. Time-Dependent Loss Cone Dynamics

The majority of galaxies with detected SBHs have collisionless nuclei (§2). In these galaxies, the assumption that the stellar phase space density has reached an approximate steady state under the influence of gravitational encounters breaks down. One consequence is that the stellar density near the SBH need not have the Bahcall-Wolf $r^{-7/4}$ form. As discussed above, it is straightforward to modify the classical loss-cone treatment for arbitrary $\rho(r)$. But the fact that galactic nuclei are not collisionally relaxed also has implications for the more detailed form of the phase space density near the loss cone boundary. For instance, in a nucleus that once contained a binary SBH, stars on orbits such that $L \lesssim L_{bin} = (2GM_{12}a_h)^{1/2}$ will have been ejected, where M_{12} is the binary mass and $a_h \approx G\mu/4\sigma^2$ is the “hard” binary separation (Eq. 15). Since $a_h \gg r_t$, there will be a gap in angular momentum space around the single SBH that subsequently forms, corresponding to stars with $L \lesssim L_{bin}$ that were ejected by the binary. Before the single SBH can begin to consume stars at the steady-state rate computed above, this gap needs to be refilled. At the other extreme, one can imagine a nucleus that formed

in such a way that the gradients in f near the loss cone boundary are much greater than their steady state values, implying larger feeding rates.

Equation (61) implies a characteristic time to set up a steady-state distribution in angular momentum near the loss cone:

$$t_L \approx \frac{R}{\bar{\mu}} \approx \frac{L^2}{L_c^2} T_r. \quad (70)$$

Setting $L^2 \approx 2GM_\bullet a_h$ – the appropriate value for a loss cone that was emptied by a binary SBH – and $L_c^2 \approx GM_\bullet r_h$, appropriate for stars at a distance $\sim r_h$ from the hole,

$$\frac{t_L}{T_r(r_h)} \approx \frac{a_h}{r_h} \approx \frac{M_2}{M_1} \quad (71)$$

with $M_2/M_1 \leq 1$ the mass ratio of the binary that created the gap. Since $T_r(r_h)$ can be much greater than 10^{10} yr in the bright elliptical galaxies that show evidence of cusp destruction (Fig. 1), even large mass ratio binaries can open up phase-space gaps that would not be refilled in a galaxy’s lifetime, implying much lower rates of SBH feeding than in the steady-state theory.

Figure 20 illustrates this for a particular giant elliptical galaxy, NGC 4168, assuming a binary mass ratio $M_2/M_1 = 0.1$ (Merritt & Wang 2005). Equation (61) was integrated forward assuming an initially sharp phase-space cutoff at $L = L_{lc}$. Stars with energies near $\Phi(r_h)$ are the first to be scattered into the hole; the total flux reaches 1%, 10%, 50% and 90% of its steady state value in a time of 4.5, 9.8, 17 and 97 Gyr. Figure 21 shows the results of a similar calculation for each of the “core” galaxies from Figure 18; the time for the total flux to reach 1/2 of its steady-state value is roughly

$$\frac{t_{1/2}}{10^{11}\text{yr}} \approx \frac{q}{(1+q)^2} \frac{M_\bullet}{10^8 M_\odot} \quad (72)$$

with $q \leq 1$ the mass ratio of the pre-existing binary. While highly idealized, calculations like these demonstrate how different the feeding rates in collisionless nuclei can be from the predictions of steady-state theory. Hopefully, more progress on this important problem can be expected in the near future.

6.4. Nonaxisymmetric Nuclei

A qualitatively different kind of SBH feeding can occur in nonaxisymmetric (triaxial or barlike) nuclei. Orbits in nonaxisymmetric potentials do not conserve any component of the angular momentum and certain orbits, the so-called centrophilic orbits, have “filled centers”: they pass arbitrarily close to the potential center after a sufficiently long time (Norman & Silk 1983, Gerhard & Binney 1985). In the presence of a massive central object like a SBH, centrophilic orbits tend to be unstable (chaotic) (e.g. Merritt & Valluri 1999) and this fact was long taken to imply that triaxiality could not be maintained in galaxies containing SBHs. However as discussed in §4, recent work suggests that nuclei can remain stably triaxial even when most of their stars are on chaotic orbits. Even if long-lived triaxial equilibria are not possible, the high frequency of

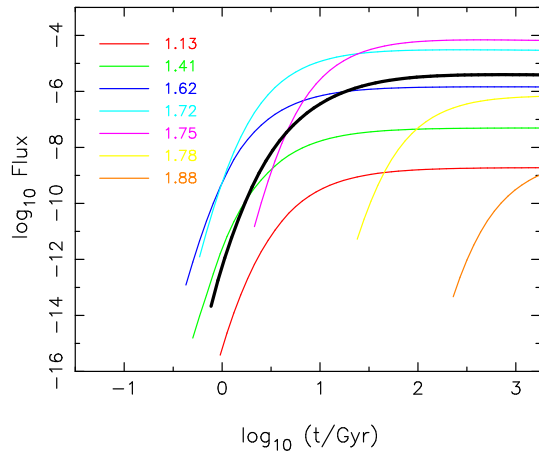


Figure 20. Dependence of the loss-cone flux on energy and time in the galaxy NGC 4168 assuming a binary mass ratio of $q = 0.1$. Curves are labelled by their binding energy; the value of the gravitational potential at $r = r_h$ in this galaxy is 1.76. Thick black curve is the total flux, in units of stars per year. (From Merritt & Wang 2005.)

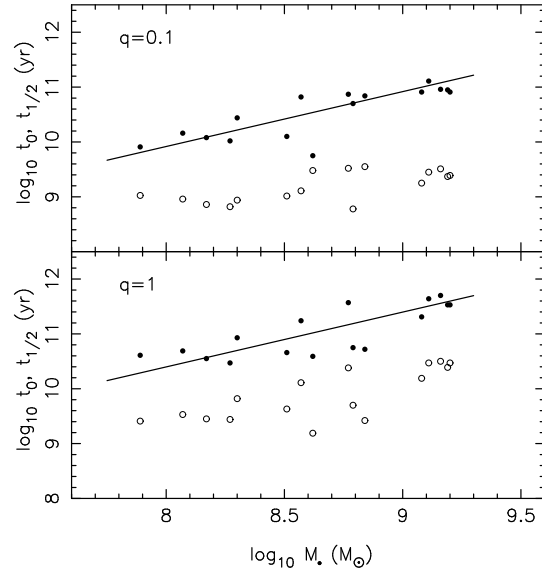


Figure 21. Two characteristic times associated with loss-cone refilling in a sample of elliptical galaxies, assuming that a phase-space gap was created by a binary SBH with mass ratio q . t_0 is the elapsed time before the first star is scattered into the single, coalesced hole and $t_{1/2}$ is the time for the loss-cone flux to reach 1/2 of its steady-state value. Solid lines are the approximate fitting function, Eq. 72. (From Merritt & Wang 2005.)

barlike distortions observed at the centers of galaxies suggests that transient departures from axisymmetry are common.

The mass associated with stars on centrophilic orbits in triaxial galaxies can easily be $\gg M_\bullet$, greatly exceeding than the mass on loss-cone orbits in the spherical or axisymmetric geometries. A lower limit on the feeding rate in the triaxial geometry comes from ignoring collisional loss cone refilling and simply counting the rate at which stars on centrophilic orbits pass within a distance r_t from the center as they move along their orbits. For a single orbit, this rate is $\sim A(E)r_t$ (§4.3) where the function $A(E)$ can be determined by numerical integrations (Merritt & Poon 2004, Holley-Bockelmann & Sigurdsson 2006). If $N_c(E)dE$ is the number of stars on centrophilic orbits in the energy range E to $E + dE$, then the loss rate to the SBH (ignoring orbital depletion) is

$$\dot{N} \approx r_t \int A(E) N_c(E) dE. \quad (73)$$

In a SIS ($\rho \sim r^{-2}$) nucleus, if the fraction $f_c(E)$ of chaotic orbits at energy E is initially independent of E , the accumulated mass after time t is

$$\Delta M \approx 1 \times 10^8 M_\odot f_c \left(\frac{r_t}{r_s} \right)^{1/2} \left(\frac{\sigma}{200 \text{ kms}^{-1}} \right)^{5/2} \left(\frac{M_\bullet}{10^8 M_\odot} \right)^{1/2} \left(\frac{t}{10^{10} \text{ yr}} \right)^{1/2} \quad (74)$$

(Merritt & Poon 2004); the $t^{1/2}$ dependence reflects the reduction in the feeding rate as centrophilic orbits are depleted. Even for modest values of f_c (~ 0.1), this collisionless mechanism can supply stars to the SBH at higher rates than collisional loss-cone repopulation, particularly in galaxies with $M_\bullet \gtrsim 10^7 M_\odot$ in which relaxation times are very long. Indeed after 10^{10} yr, Equation (74) predicts an accumulated mass

$$\frac{M_\bullet}{10^8 M_\odot} \approx f_c \left(\frac{\sigma}{200 \text{ km s}^{-1}} \right)^5. \quad (75)$$

This is remarkably similar in form to the $M_\bullet - \sigma$ relation, and even the normalization is of the right order if $f_c \approx 1$.

Hills pointed out already in 1975 that full-loss-cone feeding rates in spherical galaxies could grow $\sim 10^8 M_\odot$ holes in 10^{10} yr, and Zhao et al. (2002) noted that the accumulated mass would satisfy a relation like (75) between M_\bullet and σ . Although there are many problems with this simple idea – for instance, when $M_\bullet \lesssim 10^8 M_\odot$, most of the mass liberated from tidally disrupted stars would be lost from the nucleus – the idea that supply rates can plausibly approach the (spherical) full-loss-cone rate in a triaxial nucleus appears to be quite solid. An important next step will be to extend the Poon & Merritt (2004) self-consistency studies of triaxial black-hole nuclei to full galaxy models, using both orbital-superposition and N -body techniques to ensure that the models are long-lived.

6.5. Black-Hole-Driven Expansion

Steady-state solutions like the ones described above can only be approximate descriptions of nuclei, since the supply of stars in a galaxy is finite, and destruction of stars by the SBH will eventually cause the stellar density to drop. In the equilibrium models of Bahcall & Wolf (1976), Cohn & Kulsrud (1978) and others, this effect is absent since the stellar distribution function is fixed far from the hole, enforcing an inward flux of stars precisely large enough to replace the stars being destroyed or consumed by the hole. In reality, the relaxation time beyond a certain radius would be so long that the encounter-driven flux of stars could not compensate for losses near the hole, forcing the density to drop. Expansion occurs for two reasons: (1) Stars are physically destroyed, reducing their numbers. (2) Disrupted stars are those most tightly bound to the hole, on loss-cone orbits, and to achieve such an orbit a star must have given up energy to other stars. In effect, the black hole acts as a heat source (Shapiro 1977, Dokuchaev 1989), in much the same way that hard binary stars inject energy into a post-core-collapse globular cluster and cause it to re-expand (Hénon 1961, Hénon 1965).

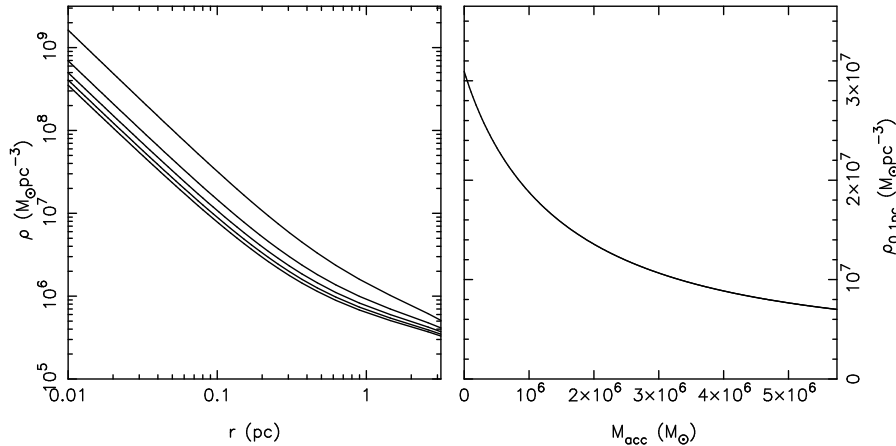


Figure 22. Black-hole-driven expansion of a nucleus, as computed via the Fokker-Planck equation. In this calculation, the total gravitational potential (galaxy + black hole) was assumed fixed; this is a good approximation since the potential in the region of changing density is dominated by the hole, and at large radii the evolution times are very long. Stars were assumed to vanish instantaneously after being scattered into the tidal destruction sphere. The left panel shows density profiles at constant time intervals after a Bahcall-Wolf cusp has been established; the density normalization was fixed by requiring the final (lowest) curve to have roughly the same density as the nucleus of M32 at 0.1 pc, and the other parameters in the model (e.g. black hole mass) also mimic M32; the final influence radius is $r_h \approx 3$ pc. The right panel shows the evolution of the density at 0.1 pc as a function of M_{acc} , the accumulated mass in tidally-disrupted stars. As scaled to M32, the final time is roughly 2×10^{10} yr. This plot suggests that the densities of collisional nuclei like those of M32 and the Milky Way were once higher, by factors of \sim a few, than at present.

A very simple model that produces self-similar expansion of a black-hole nucleus can be constructed by simply changing the outer boundary condition in the Bahcall-Wolf (1976) problem (§5.1) from $f(0) = f_0$ to $f(0) = 0$. Equations (38a,38b) then describe the evolution of a finite cluster of stars as they diffuse to lower energies and are consumed by the hole. One finds that the evolution after \sim one relaxation time can be described as $\rho(r, t) = \rho_c(t)\rho^*(r)$, with $\rho^*(r)$ slightly steeper than the $\rho \sim r^{-7/4}$ Bahcall-Wolf form; the normalization drops off as $\rho_c \propto t^{-1}$ at late times (Merritt, unpublished). Figure 22 shows the results of a slightly more realistic calculation in a model designed to mimic M32. After reaching approximately the Bahcall-Wolf steady-state form, the density drops in amplitude with roughly fixed slope for $r \lesssim r_h$. This example suggests that the nuclei of galaxies like M32 or the Milky Way might have been \sim a few times denser in the past than they are now, with correspondingly higher rates of stellar tidal disruption and stellar collisions.

Expansion due to a central black hole has been observed in a handful of studies

based on fluid (Amaro-Seoane et al. 2004), Monte-Carlo (Shapiro & Marchant 1978, Marchant & Shapiro 1980, Freitag et al. 2006), Fokker-Planck (Murphy et al. 1991), and N -body (Baumgardt et al. 2004*a*, Baumgardt et al. 2004*b*) algorithms. All of these studies allowed stars to be lost into or destroyed by the black hole; however most adopted parameters more suited to globular clusters than to nuclei, e.g. a constant-density core. Murphy et al. (1991) applied the isotropic, multi-mass Fokker-Planck equation to the evolution of nuclei containing SBHs, including an approximate loss term in the form of equation (42) to model the scattering of low-angular-momentum stars into the hole. Most of their models had what would now be considered unphysically high densities and the evolution was dominated by physical collisions between stars. However in two models with lower densities, they reported observing significant expansion over 10^{10} yr; these models had initial central relaxation times of $T_r \lesssim 10^9$ yr when scaled to real galaxies, similar to the relaxation times near the centers of M32 and the Milky Way. The $\rho \sim r^{-7/4}$ form of the density profile near the SBH was observed to be approximately conserved during the expansion. Freitag et al. (2006) carried out Monte-Carlo evolutionary calculations of a suite of models containing a mass spectrum, some of which were designed to mimic the Galactic center star cluster. After the stellar-mass black holes in their models had segregated to the center, they observed a strong, roughly self-similar expansion. Baumgardt et al. (2004*a*) followed core collapse in N -body models with and without a massive central particle; “tidal destruction” was modelled by simply removing stars that came within a certain distance of the massive particle. When the “black hole” was present, the cluster expanded almost from the start and in an approximately self-similar way.

These important studies notwithstanding, there is a crucial need for more work on this problem. Establishing the self-similarity of the expansion in the Fokker-Planck or fluid descriptions would be a good start; such studies (e.g. Lynden-Bell & Inagaki 1983, Heggie 1985, Heggie & Stevenson 1988) were an important complement to numerical simulations in understanding the post-core-collapse evolution of star clusters.

6.6. Constraining the Consumption Rate

Calculations of SBH feeding rates in real galaxies are subject to many uncertainties, particularly in collisionless nuclei, due to the wide range of possible geometries (§6.4) and initial conditions (§6.3). Additional uncertainties include the form of the nuclear density profile at $r \ll r_h$ and, of course, the mass of the SBH. Plots like Figure 18, which was based on spherical, steady-state loss cone theory, should probably be seen as little more than order-of-magnitude estimates of the true tidal flaring rate. In such an uncertain situation, it makes sense to look for observational evidence of tidal disruptions as a constraint on the theory. The *ROSAT* All-Sky Survey detected soft X-ray outbursts from a number of galaxies with no previous history of nuclear activity. Roughly half a dozen of these events had the properties of a tidal disruption flare (Komossa 2002 and references therein), and follow-up optical spectroscopy of the candidate galaxies

confirmed that at least two were subsequently inactive (Gezari et al. 2003). The mean event rate inferred from these outbursts is roughly consistent with theoretical predictions (Donley et al. 2002). Some fraction of the X-ray luminosity function of active galaxies (Hasinger et al. 2005) must also be due to stellar tidal disruptions. Convolving Equation 69 for the disruption rate with the SBH mass function, and assuming that individual tidal disruption events have a $L_X \propto t^{-5/3}$ time dependence as predicted in “fallback” models (Li et al. 2002), one concludes (Milosavljević et al. 2006) that tidal disruptions can account for the majority of X-ray selected AGN with soft X-ray luminosities below $\sim 10^{43} - 10^{44}$ erg s $^{-1}$. Nearer to home, it might be possible to search for “afterglows” of the most recent tidal disruption event at the Galactic center, which could plausibly have occurred as little as $\sim 10^3$ yr ago. Possible examples of such signatures include X-ray fluorescence of giant molecular clouds (Sunyaev & Churazov 1998) and changes in the surface properties of irradiated stars (Jimenez et al. 2006).

7. Dynamics of Binary Black Holes

Galaxies are believed to grow through the agglomeration of smaller galaxies and proto-galactic fragments. If more than one of the fragments contained a SBH, the two SBHs will form a bound system in the merger product (Begelman et al. 1980). This scenario has received considerable attention since the ultimate coalescence of a binary SBH would generate an observable outburst of gravitational waves (Thorne & Braginskii 1976) and possibly electromagnetic radiation as well (Milosavljević & Phinney 2005). Binary SBHs are also increasingly invoked to explain the properties of active galaxies, including AGN variability (Valtaoja et al. 2000, Xie 2003), the bending and precession of radio jets (Roos et al. 1993, Romero et al. 2000), *X*- and *Z*-shaped radio lobes (Merritt & Ekers 2002, Gopal-Krishna et al. 2003), and the correlation of radio loudness with galaxy morphology (Wilson & Colbert 1995, Balmaverde & Capetti 2006).

Komossa et al. (2003) reviews the observational evidence for binary SBHs. A handful of galaxies exhibit two active nuclei with separations as small as ~ 1 kpc (Komossa 2003, Ballo et al. 2004, Hudson et al. 2006), much greater however than the parsec-scale separations that characterize true binaries. Very recently (Rodriguez et al. 2006), VLBA observations of an elliptical galaxy at $z = 0.055$ with two compact central radio sources were used to infer the presence of the first, true binary SBH; the projected separation is only ~ 7 pc and the inferred total mass is $\sim 1.5 \times 10^8 M_\odot$.

A binary SBH with $a \approx a_h$ (Equation 15) contains a fraction $\sim (M_1 + M_2)/M_{gal} \approx 10^{-3}$ of the total gravitational energy of its host galaxy, and such a large binding energy implies a significant change in the distribution of stars, gas or dark matter at the center of the galaxy when the binary forms. If stars are the dominant component, formation of the binary results in a low-density core, with a displaced mass of order the mass of the binary. As discussed in §3 and §7.3, luminous elliptical galaxies always contain such cores, with masses and sizes that are roughly consistent with predictions of the binary

SBH model (Merritt 2006). Other dynamical effects associated with binary SBHs include high-velocity ejection of stars via the gravitational slingshot (Hills 1988), chaos induced in stellar orbits by the time-dependent potential of the binary (Kandrup et al. 2003), and the “gravitational rocket” effect, the kick imparted to a coalescing binary due to anisotropic emission of gravitational waves (Favata et al. 2004, Baker et al. 2006), which can displace a coalesced SBH from its central location and potentially eject it into intergalactic space. These mechanisms all go in the direction of “heating” the nucleus, and collectively, they set the initial conditions for evolution of the nucleus after the two SBHs coalesce.

Binary SBHs may fail to coalesce in some galaxies because their evolution stalls at a separation much greater than required for the efficient emission of gravitational waves (Valtonen 1996). In a galaxy where this occurs, the binary may be present when a third SBH (or a second binary) falls in, resulting in a complicated interaction between the multiple SBHs (Mikkola & Valtonen 1990), and possibly ejection of one or more from the nucleus or even from the galaxy. Such events can not be too frequent or the tight correlations observed between SBH mass and galaxy properties would be violated. Furthermore the total mass density in SBHs in the local universe is consistent with that inferred from high-redshift AGN (Merritt & Ferrarese 2001a, Yu & Tremaine 2002), implying that only a small fraction of SBHs could have been ejected from galaxies in the intervening period.

In what follows, the focus will be on the interaction of binary and multiple SBHs with (point-mass) stars in galactic nuclei and on the implications for nuclear dynamics. Merritt & Milosavljević (2005) present a more general review of the astrophysics of massive black hole binaries.

7.1. Early evolution of binary SBHs and the generation of mass deficits

In galaxy mergers in the local universe, typical mass ratios are believed to be large, of order 10 : 1 (e.g. Sesana et al. 2004). To a good approximation, the initial approach of the two SBHs can therefore be modelled by assuming that the galaxy hosting the smaller SBH spirals inward under the influence of dynamical friction from the fixed distribution of stars in the larger galaxy. Modelling both galaxies as singular isothermal spheres ($\rho \sim r^{-2}$) and assuming that the smaller galaxy spirals in on a circular orbit, its tidally-truncated mass is $\sim \sigma_g^3 r / 2G\sigma$, with σ and σ_g the velocity dispersions of large and small galaxies respectively (Merritt 1984). Chandrasekhar’s (1943) formula then gives for the orbital decay rate and infall time

$$\frac{dr}{dt} = -0.30 \frac{Gm_2}{\sigma_1 r} \ln \Lambda, \quad t_{infall} \approx 3.3 \frac{r_0 \sigma^2}{\sigma_g^3} \quad (76)$$

where $\ln \Lambda$ has been set to 2. Using Equation (19) to relate σ and σ_g to the respective SBH masses M_1 and M_2 , this becomes

$$t_{infall} \approx 3.3 \frac{r_0}{\sigma} \left(\frac{M_1}{M_2} \right)^{0.62}, \quad (77)$$

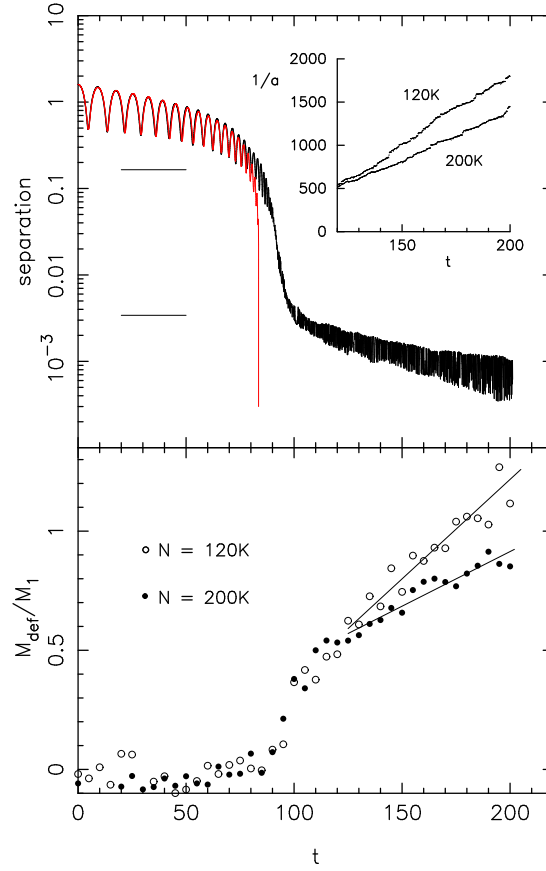


Figure 23. *Upper panel:* Thick (black) line shows the N -body evolution of a massive binary with $M_2/M_1 = 0.1$; the initial galaxy model had a $\rho \sim r^{-1}$ density cusp. Thin (red) line is the evolution predicted by the Chandrasekhar’s dynamical friction formula assuming a fixed galaxy. Horizontal lines indicate r_h and a_h . The inset shows the evolution of the inverse semi-major axis of the binary in this integration, and in a second integration with roughly one-half the number of particles; the latter curve lies above the former, i.e. the decay occurs more rapidly for smaller N when $a \lesssim a_h$, due to the higher rate of star-star encounters. In the large- N limit of real galaxies, the binary hardening rate would drop to zero at $a \approx a_h$. *Lower panel:* Evolution of the mass deficit in the same two N -body integrations. Lines show least-squares fits to $t \geq 120$. (Adapted from Merritt 2006.)

i.e. t_{infall} exceeds the crossing time of the larger galaxy by a factor $\sim q^{-0.62}$. Thus for mass ratios $q \gtrsim 10^{-3}$, infall requires less than $\sim 10^2 T_{cr} \approx 10^{10}$ yr (Merritt 2000). This mass ratio is roughly the ratio between the masses of the largest ($\sim 10^{9.5} M_\odot$) and smallest ($\sim 10^{6.5} M_\odot$) known SBHs and so it is reasonable to assume that galaxy mergers will almost always lead to formation of a binary SBH, i.e. a bound pair, in a time less than 10 Gyr.

Equation (76) begins to break down when the two SBHs approach more closely than $R_{12} \approx r_h$, the influence radius of the larger hole, since the orbital energy of M_2 is absorbed by the stars, lowering their density and reducing the frictional force. Figure 23 illustrates this via N -body integrations of a $q = 0.1$ binary. In spite of this slowdown,

the separation between the two SBHs continues to quickly drop until $a \approx a_h \approx (q/4)r_h$ (Eq. 15) at which separation the binary's binding energy per unit mass is σ^2 and the binary is “hard” – it ejects stars that pass within a distance $\sim a$ with velocities large enough to remove them from the nucleus (Mikkola & Valtonen 1992, Quinlan 1996).

What happens next depends on the density and geometry of the nucleus. In a spherical or axisymmetric galaxy, the mass in stars on orbits that intersect the binary is small, $\lesssim M_{12}$, and the binary rapidly interacts with and ejects these stars. Once this has occurred, no stars remain to interact with the binary and its evolution stalls. In non-axisymmetric (e.g. triaxial) nuclei, on the other hand, the mass in stars on centrophilic orbits can be much larger, allowing the binary to continue shrinking past a_h . And in collisional nuclei of any geometry, gravitational scattering of stars can repopulate depleted orbits. These different cases are discussed independently below.

The stalling that is predicted to occur in spherical galaxies can be reproduced via N -body simulations if N is large enough to suppress two-body relaxation. One finds

$$\frac{a_{\text{stall}}}{r_h} \approx 0.2 \frac{q}{(1+q)^2}, \quad (78)$$

(Merritt 2006) with r_h the influence radius of the larger SBH, defined as the radius containing a stellar mass equal to twice M_{12} *after* infall of the smaller SBH has lowered the nuclear density. This relation was established using galaxy models with initial, power-law density profiles, $\rho \sim r^{-\gamma}$, $0.5 \leq \gamma \leq 1.5$; the coefficient in Equation (78) depends only weakly on γ . Table 1 gives predicted stalling radii for binary SBHs at the centers of the brightest Virgo cluster galaxies, based on the galaxy structural data of Ferrarese et al. (2006); all of these galaxies exhibit large, low-density cores which might have been formed by binary SBHs.

If the binary does stall at $a \approx a_{\text{stall}}$, it will have given up an energy

$$\Delta E \approx -\frac{GM_1M_2}{2r_h} + \frac{GM_1M_2}{2a_{\text{stall}}} \quad (79)$$

$$\approx -\frac{1}{2}M_2\sigma^2 + 2M_{12}\sigma^2 \quad (80)$$

$$\approx 2M_{12}\sigma^2 \quad (81)$$

to the stars in the nucleus, i.e., the energy transferred from the binary to the stars is roughly proportional to the *combined* mass of the two SBHs. The reason for this counter-intuitive result is the $a_{\text{stall}} \sim M_2$ dependence of the stalling radius (Eq. 78): smaller infalling holes form tighter binaries. Detailed N -body simulations (Merritt 2006) verify this prediction: the mass deficit (Eq. 28) is found to be

$$\frac{M_{\text{def}}}{M_{12}} \approx 0.70q^{0.2} \quad (82)$$

for nuclei with initial density slopes $1 \lesssim \gamma \lesssim 1.5$.[‡] Thus, in galaxies with pre-existing density profiles similar to those currently observed at the centers of the Milky Way and

[‡] The first N -body simulation to follow the destruction of a power-law density cusp by a massive binary was that of Milosavljević & Merritt (2001), however the number of particles used was so small that the evolution was dominated by spurious loss-cone refilling and the estimates of M_{def} accordingly

Table 1. Virgo “Core” Galaxies

Galaxy	B_T	M_\bullet	M_{def}	r_h	a_{stall} $q = 0.5$	a_{stall} $q = 0.1$
(1)	(2)	(3)	(4)	(5)	(6)	(7)
NGC 4472	-21.8	5.94	17.7	130. (1.6)	5.6 (0.070)	2.1 (0.026)
NGC 4486	-21.5	35.7	87.3	460. (5.7)	20. (0.25)	7.6 (0.095)
NGC 4649	-21.3	20.0	21.5	230. (2.9)	10. (0.13)	3.8 (0.047)
NGC 4406	-21.0	4.54	3.27	90. (1.1)	4.0 (0.050)	1.5 (0.019)
NGC 4374	-20.8	17.0	22.6	170. (2.1)	7.6 (0.094)	2.8 (0.035)
NGC 4365	-20.6	4.72	6.00	115. (1.4)	5.0 (0.063)	1.9 (0.023)
NGC 4552	-20.3	6.05	6.45	73. (0.91)	3.2 (0.040)	1.2 (0.015)

Properties of the brightest Virgo cluster galaxies. Col. (1): New General Catalog (NGC) number. Col. (2): Absolute B -band galaxy magnitude. Col. (3): Black hole mass in $10^8 M_\odot$, computed from the $M_\bullet - \sigma$ relation. Col. (4): Observed mass deficit in $10^8 M_\odot$ from Ferrarese et al. (2006). Col. (5): Black hole influence radius, defined as the radius containing a mass in stars equal to $2M_\bullet$, in pc (arcsec). Col. (6): Binary stalling radius (Eq. 78) for $q = 0.5$, in pc (arcsec), based on Equation (78). Col. (7): Binary stalling radius for $q = 0.1$.

M32, Equation (82) implies that mass deficits generated by stalled binaries should lie in the relatively narrow range

$$0.4 \lesssim \frac{M_{def}}{M_{12}} \lesssim 0.6, \quad 0.05 \lesssim q \lesssim 0.5. \quad (83)$$

Observed mass deficits are somewhat larger than this (Merritt & Milosavljević 2002, Ravindranath et al. 2002, Graham 2004, Ferrarese et al. 2006). Typical values are $M_{def} \approx M_\bullet$ and some galaxies have M_{def}/M_\bullet as large as ~ 4 (Table 1, Figure 24). These numbers should be interpreted with caution since both M_{def} and M_\bullet are subject to systematic errors, the former from uncertain M/L corrections, the latter from various difficulties associated with SBH mass estimation (§4). On the other hand, bright elliptical galaxies like M49 and M87 (the first two galaxies in Table 1) have probably undergone numerous mergers and the mass deficit should increase after each merger, even if expressed as a multiple of the final (accumulated) SBH mass. If the stellar mass displaced in a single merger is $\sim 0.5M_{12}$, then – assuming that the two SBHs always coalesce before the next SBH falls in – the mass deficit following \mathcal{N} mergers with $M_2 \ll M_1$ is $\sim 0.5\mathcal{N}M_\bullet$. N -body simulations verify this prediction (Merritt 2006, Figure 25). Mass deficits in the range $0.5 \lesssim M_{def}/M_\bullet \lesssim 1.5$ therefore imply $1 \lesssim \mathcal{N} \lesssim 3$, consistent with the number of gas-free mergers expected for bright galaxies (Haehnelt & Kauffmann 2002). This correspondence constitutes strong evidence that the cores of bright elliptical galaxies are due to heating by binary SBHs.

uncertain. Subsequent studies (Hemsendorf et al. 2002, Chatterjee et al. 2003, Makino & Funato 2004) achieved nearly “empty loss cones” around the binary by using mean-field algorithms and/or larger N , but these investigations were all based on galaxy models with pre-existing cores, again making it difficult to draw useful conclusions about the values of M_{def} to be expected in real galaxies.

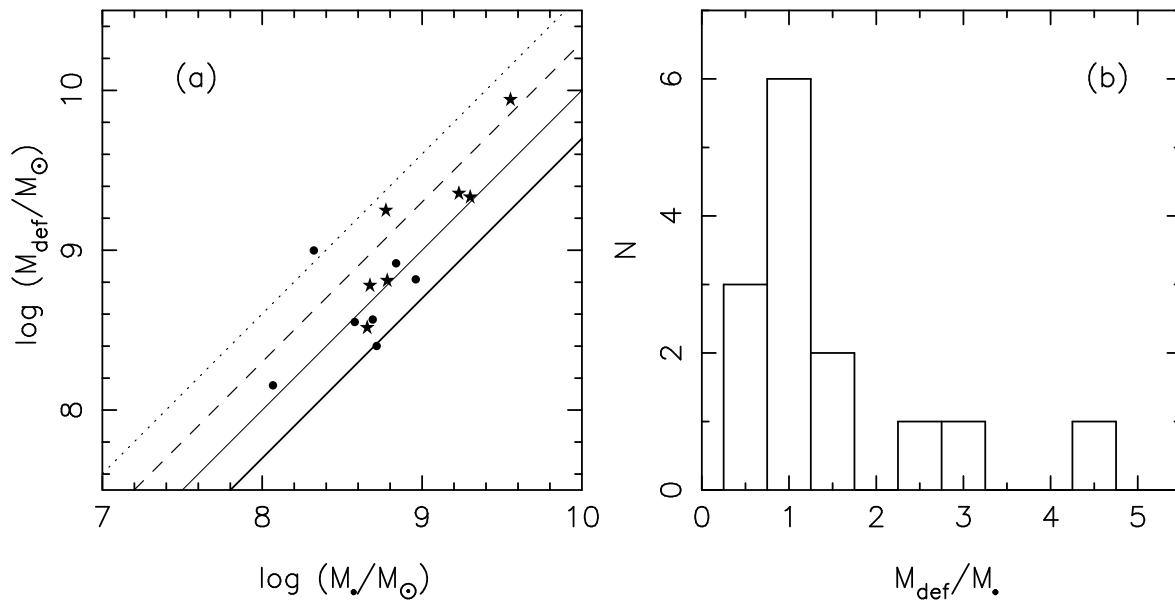


Figure 24. (a) Observed mass deficits, from Graham (2004) (filled circles) and Ferrarese et al. (2006) (stars). Thick, thin, dashed and dotted lines show $M_{\text{def}}/M_{\bullet} = 0.5, 1, 2$ and 4 respectively. (b) Histogram of $M_{\text{def}}/M_{\bullet}$ values in (a).

Mass deficits as large as those in M49 and M87 ($3 \lesssim M_{\text{def}}/M_{\bullet} \lesssim 4$; Table 1) are harder to explain in this way, although a number of additional mechanisms associated with binary SBHs can “heat” a nucleus and increase M_{def} . (a) If two SBHs fail to efficiently coalesce a binary will be present when a third SBH falls in. This scenario is conducive to smaller values of M_{\bullet} , since one or more of the SBHs could eventually be ejected by the gravitational slingshot (Mikkola & Valtonen 1990); and to larger values of M_{def} , since multiple SBHs are more efficient than a binary at displacing stars (Merritt, Piatek, Zwart & Hemsendorf 2004). Multiple-SBH interactions are discussed in more detail in §7.3. (b) The gravitational-wave rocket effect is believed capable of delivering kicks to a coalescing binary as large as $\sim 150 \text{ km s}^{-1}$ (Favata et al. 2004, Blanchet et al. 2005, Herrmann et al. 2006, Baker et al. 2006) and possibly much higher (Redmount & Rees 1989). The stellar density drops impulsively when the SBH is kicked out, and again when its orbit decays via dynamical friction. Mass deficits produced in this way can be as large as $\sim M_{\bullet}$ (Merritt, Milosavljević, Favata, Hughes & Holz 2004, Boylan-Kolchin et al. 2004). (c) Binaries might continue to harden beyond $R_{12} \approx a_h$, as discussed below, although it is not completely clear what the net effect on M_{def} would be.

7.2. Late evolution of binary SBHs and the “final-parsec problem”

The rapid phase of binary evolution discussed above is tractable using N -body codes since the mechanisms that extract angular momentum from the binary (dynamical friction from the stars, gravitational-slingshot ejection of stars by the binary) depend

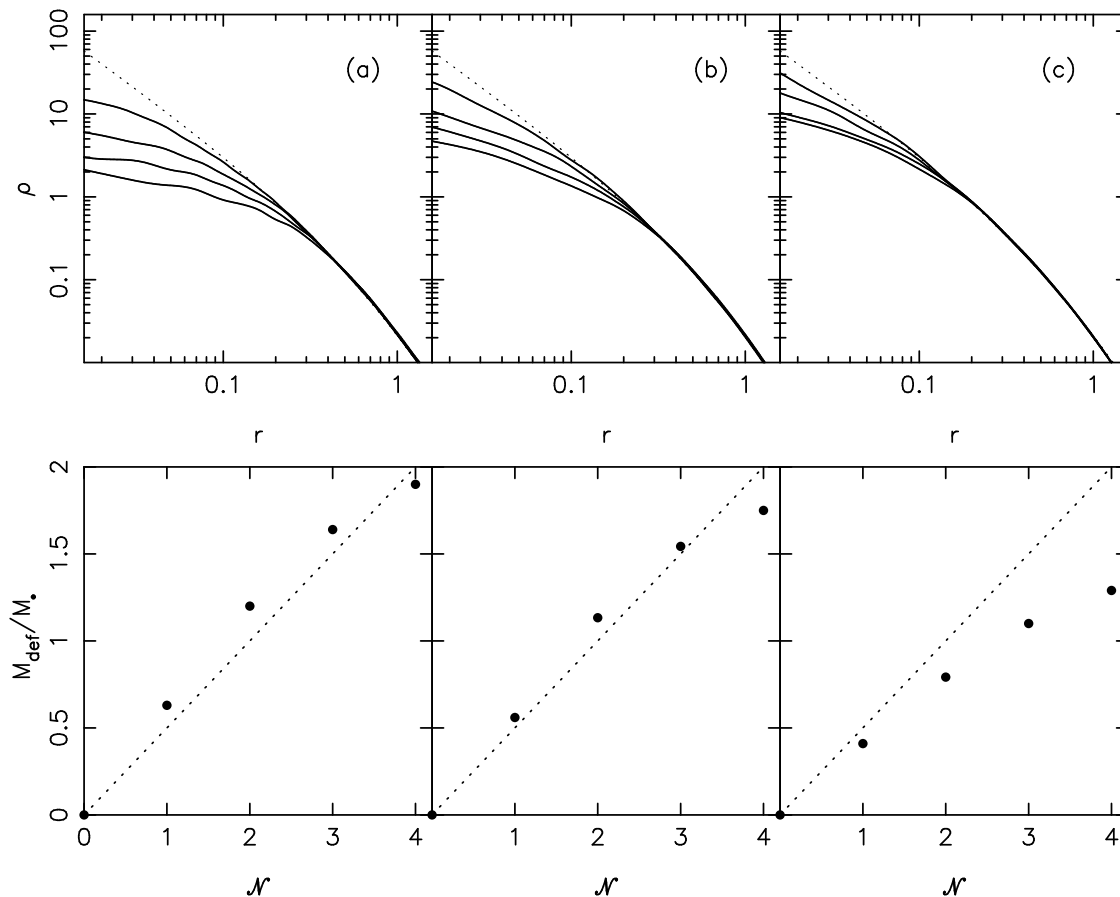


Figure 25. Density profiles (upper) and mass deficits (lower) in N -body simulations of multi-stage mergers. The initial galaxy (dotted lines, top panels) contained a central point of mass $0.01M_{gal}$; subsequent curves show density profiles after repeated infall (followed by coalescence) of a second “black hole” of mass 0.005 (a), 0.0025 (b) and 0.001 (c). In the lower panels, points show M_{def}/M_{\bullet} at t_{stall} and dotted lines show $M_{def}/M_{\bullet} = 0.5N$, where M_{\bullet} is the accumulated central mass. (From Merritt 2006.)

essentially on the mass density of the objects (stars) interacting with the binary and not on their individual masses (at least for $m_{\star} \ll M_{\bullet}$). Evolution of the binary beyond $a \approx a_h$ can be qualitatively different, and in fact N -body simulations often find that the hardening rate $(d/dt)(1/a)$ is a decreasing function of N , the number of “star” particles in the simulation, once a drops below $\sim a_h$ (Makino & Funato 2004, Berczik et al. 2005, Merritt, Mikkola & Szell 2005). Figure 26 illustrates the N -dependence for equal-mass binaries in spherical galaxy models. A straightforward extrapolation of results like these to real galaxies implies that binary SBHs would stall at separations of order 10^0 pc (Table 1) – the “final-parsec problem”.

Stalling is expected in the large- N limit since, in a fixed, smooth potential, the number of stars on orbits intersecting the binary is limited, and in fact decreases with time as the binary shrinks. Stars can interact with the binary only if their pericenters lie within $\sim \mathcal{R} \times a$, where \mathcal{R} is of order unity. Let $L_{lc} = \mathcal{R}a\sqrt{2[E - \Phi(\mathcal{R}a)]} \approx \sqrt{2GM_{12}\mathcal{R}a}$,

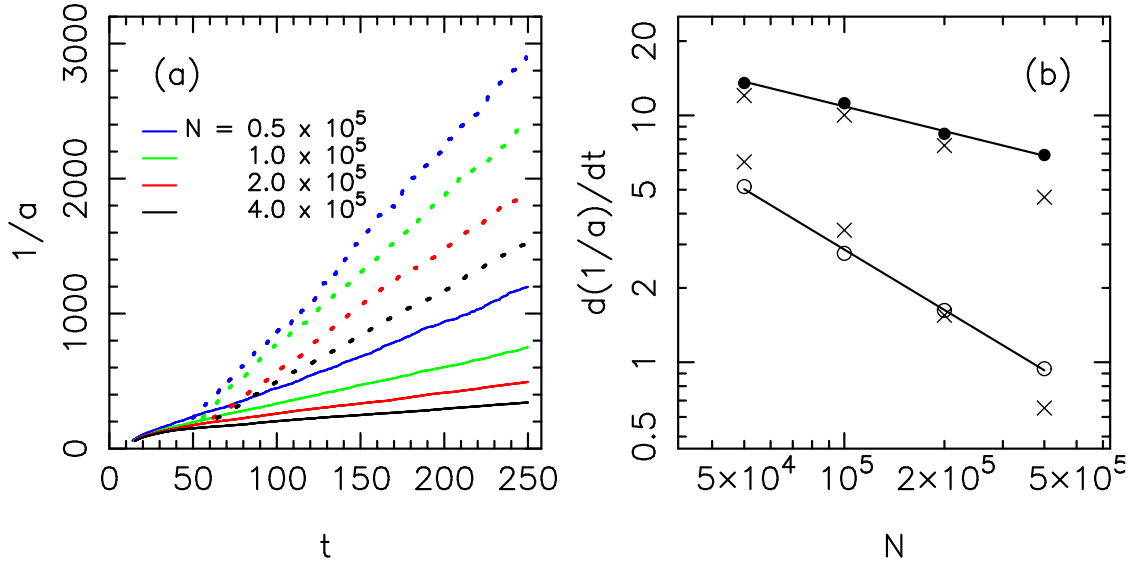


Figure 26. Long-term evolution of the binary semi-major axis (a) and hardening rate (b) in a set of high accuracy N -body simulations; the initial galaxy model was a low-central-density Plummer sphere. Units are $G = M_{gal} = 1$, $E = -1/4$, with E the total energy. (a) Dashed lines are simulations with binary mass $M_1 = M_2 = 0.005$ and solid lines are for $M_1 = M_2 = 0.02$, in units where the total galaxy mass is one. (b) Filled(open) circles are for $M_1 = M_2 = 0.005(0.02)$. Crosses indicate the hardening rate predicted by a simple model in which the supply of stars to the binary is limited by the rate at which they can be scattered into the binary's influence sphere by gravitational encounters. The simulations with largest (M_1, M_2) exhibit the nearly N^{-1} dependence expected in the “empty loss cone” regime that is characteristic of real galaxies. (Adapted from Berczik et al. 2005.)

the angular momentum of a star with pericenter $\mathcal{R}a$. The binary’s “loss cone” is the region in phase space defined by $L \leq L_{lc}$. In a spherical galaxy, the mass of stars in the loss cone is

$$\begin{aligned}
 M_{lc}(a) &= m_* \int dE \int_0^{L_{lc}} dL N(E, L^2) \\
 &= m_* \int dE \int_0^{L_{lc}^2} dL^2 4\pi^2 f(E, L^2) P(E, L^2) \\
 &\approx 8\pi^2 G M_{12} m_* \mathcal{R}a \int dE f(E) P(E).
 \end{aligned} \tag{84}$$

Here P is the orbital period, f is the number density of stars in phase space, and $N(E, L^2)dEdL$ is the number of stars in the integral-space volume defined by dE and dL . In the final line, f is assumed isotropic and P has been approximated by the period of a radial orbit of energy E . An upper limit to the mass that is available to interact with the binary is $\sim M_{lc}(a_h)$, the mass within the loss cone when the binary first becomes hard; this is an upper limit since some stars that are initially within the loss cone will “fall out” as the binary shrinks. Assuming a singular isothermal sphere for the stellar distribution, $\rho \propto r^{-2}$, and taking the lower limit of the energy integral to be $\Phi(a_h)$,

equation (84) implies

$$M_{lc}(a_h) \approx 3\mathcal{R}\mu. \quad (85)$$

The change in a that would result if the binary interacted with this entire mass can be estimated using the mean energy change of a star interacting with a hard binary, $\sim 3G\mu/2a$ (Quinlan 1996). Equating the energy carried away by stars with the change in the binary's binding energy gives

$$\frac{3}{2} \frac{G\mu}{a} dM \approx \frac{GM_1M_2}{2} d\left(\frac{1}{a}\right) \quad (86)$$

or

$$\ln\left(\frac{a_h}{a}\right) \approx 3 \frac{\Delta M}{M_{12}} \approx \frac{9\mathcal{R}\mu}{M_{12}} \approx 9\mathcal{R} \frac{q}{(1+q)^2} \quad (87)$$

if ΔM is equated with M_{lc} . Equation (87) suggests that the mass available to the binary would allow it to shrink by only a modest factor below a_h . In reality, the time scale for the binary to shrink is comparable with stellar orbital periods, and some of the stars with pericenter distances of order a_h will only reach the binary after it has shrunk to smaller separations. And in most galaxies the density profile is shallower than $\rho \sim r^{-2}$ implying smaller M_{lc} and less of a change in a .

The final parsec problem is a “problem” because it implies a low rate of SBH coalescence, which is disappointing to physicists hoping to detect the gravitational radiation emitted during the final plunge (Folkner 1998). It is also a “problem” in the sense that many circumstantial lines of evidence suggest that SBH binaries *do* efficiently coalesce. (a) Only one, reasonably compelling case for a true binary SBH exists (Rodriguez et al. 2006), even though binaries with the same projected separation (~ 7 pc, which is the expected stalling radius for a $M_{12} \approx 10^9 M_\odot$ binary; see Table 1) could be easily resolved in many other galaxies by radio interferometry. (b) Jets in the great majority of radio galaxies do not show the wiggles expected if the SBH hosting the accretion disk were orbiting or precessing. (c) Jets from Seyfert galaxies are randomly oriented with respect to the disks in their host galaxies (Ulvestad & Wilson 1984). This is naturally understood if SBH spins were randomized at an earlier epoch by binary coalescences during the merger events that formed the bulges (Merritt 2002, Kendall et al. 2003, Saitoh & Wada 2004). (d) If binary SBHs are common, mergers will sometimes bring a third SBH into a nucleus containing an uncoalesced binary, resulting in three-body ejection of one or more of the holes. But the total mass density of SBHs in the local universe is consistent with that inferred from high-redshift AGN (Merritt & Ferrarese 2001a, Yu & Tremaine 2002) implying that ejections are rare. (e) Tight, empirical correlations between SBH mass and galaxy properties (Ferrarese & Merritt 2000, Graham et al. 2001, Marconi & Hunt 2003) would also be weakened if SBH ejections were common. (f) The frequency of SBH binary coalescences estimated from X-shaped radio source statistics (Merritt & Ekers 2002) is roughly consistent with the galaxy merger rate, implying that the time for coalescence is short compared to the time between galaxy mergers.

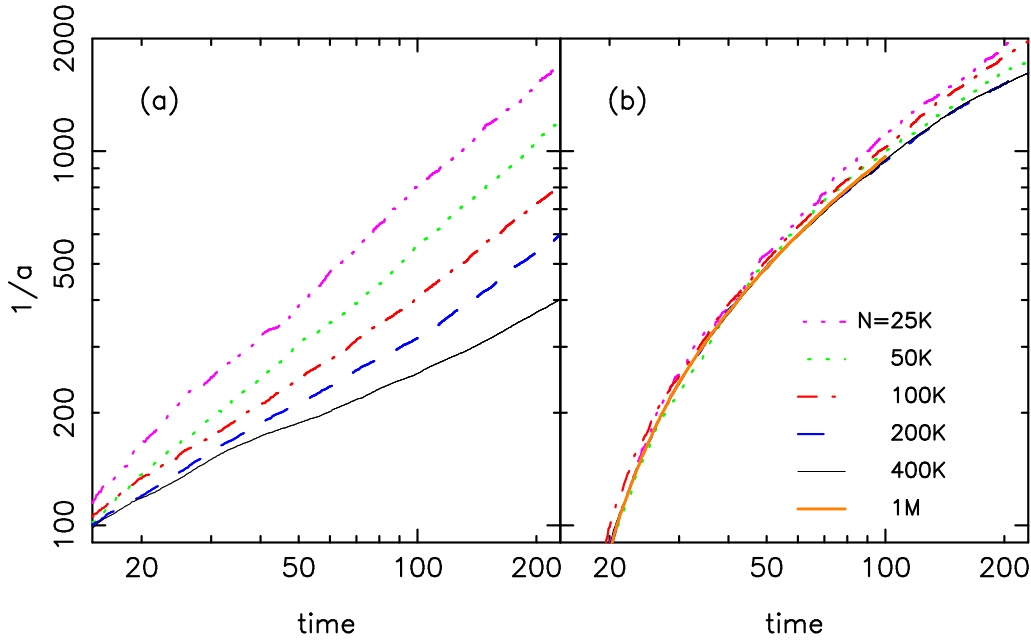


Figure 27. Efficient merger of binary SBHs in barred galaxies. Lines show the evolution of the inverse semi-major axis, $1/a$, of an equal-mass binary in N -body simulations with various N . (a) Spherical, nonrotating galaxy model. The binary hardening rate declines with increasing N , i.e. the binary would stall in the large- N limit. (b) Flattened, rotating version of the same model. At $t \approx 10$, the rotating model forms a triaxial bar. Hardening rates in this model are essentially independent of N , indicating that the supply of stars to the binary is not limited by collisional loss-cone refilling. (From Berczik et al. 2006).

A number of mechanisms have been proposed for efficiently extracting angular momentum from binary SBHS and avoiding the “final parsec problem.”

7.2.1. Non-axisymmetric geometries As discussed above (§4), steady-state, non-axisymmetric (e.g. triaxial) configurations are possible for nuclei, even in the presence of chaos induced by the SBH, and in fact departures from axisymmetry are often invoked to enhance fueling of AGN by gas (Shlosman et al. 1990). Many orbits in a triaxial nucleus are centrophilic, passing arbitrarily close to the center after a sufficiently long time (Norman & Silk 1983, Gerhard & Binney 1985). This implies feeding rates for a central binary that can be higher than in the spherical geometry and, more importantly, independent of N in the large- N limit (Merritt & Poon 2004).

The total rate at which stars pass within a distance $\mathcal{R}a$ of a central binary is

$$\dot{M} \approx a \int A(E) M_c(E) dE \quad (88)$$

where $M_c(E)dE$ is the mass on centrophilic orbits in the energy range E to $E + dE$, and $A(E)$ was defined above (Eq. 33): $A(E) \times d$ is the rate at which a single star on a centrophilic orbit of energy E experiences near-center passages with pericenter distances

$\leq d$. The implied hardening rate is

$$s \equiv \frac{d}{dt} \left(\frac{1}{a} \right) \approx \frac{2\langle C \rangle}{aM_\bullet} \int \dot{M}(E) dE. \quad (89)$$

Here, $\langle C \rangle \approx 1.25$ is the average value of the dimensionless energy change during a single star-binary encounter, $C \equiv [M_\bullet/2m_\star](\Delta E/E)$. This expression can be evaluated for a $\rho \sim r^{-2}$ galaxy using Equation (34) for $A(E)$. The result is

$$s \approx \frac{4\sqrt{6}}{9} \frac{\langle C \rangle K \bar{f}_c}{\sigma r_h^2} \int e^{-(E-E_h)/2\sigma^2} dE \approx 2.5 \bar{f}_c \frac{\sigma}{r_h^2}. \quad (90)$$

Here \bar{f}_c is an energy-weighted, mean fraction of centrophilic orbits, and the lower integration limit was set to $E_h \equiv \Phi(r_h)$. For the triaxial galaxy modelled in Figure 27, the implied value of s is $\sim 40 \bar{f}_c$, consistent with the measured peak value of $s \approx 20$.

This simple calculation, like the N -body models on which Figure 27 was based, are highly idealized, and it would be premature to draw strong conclusions about the behavior of binary SBHs in more realistic models of merging galaxies. However these results do convincingly demonstrate that binary hardening can be much more efficient in triaxial geometries than in spherical geometries due to the qualitatively different character of the stellar orbits.

7.2.2. Collisional loss cone repopulation The theory of loss cones around single black holes (§6) can be applied, with only minor changes, to binary SBHs. The orbital separation a of the SBHs in a binary is much larger than the tidal disruption radius around a single SBH:

$$\frac{a}{r_t} \approx 10^5 \times \eta^{-2/3} \left(\frac{M_\bullet}{10^8 M_\odot} \right)^{-1/3} \left(\frac{m_\star}{M_\odot} \right)^{1/3} \left(\frac{r_\star}{R_\odot} \right)^{-1} \left(\frac{a}{1 \text{ pc}} \right). \quad (91)$$

Since the physical scale of the loss cone is so large for a binary, the angular deflection of a star over one orbital period will almost always be small compared with the angular size subtended by the loss cone, implying that most stars will wander “diffusively” into the binary (Milosavljević & Merritt 2003). In the diffusive regime, the flux of stars into a sphere of radius r_t scales only logarithmically with r_t (Eq. 66b), and so the rate of supply of stars to a massive binary will be of the same order as the loss rate into a single SBH of the same mass, or (very roughly) $\sim M_{12}/T_r(r_h)$.

In the bright elliptical galaxies that exhibit clear evidence for the “scouring” effect of binary SBHs, nuclear relaxation times are always extremely long, $\gtrsim 10^{14}$ yr (Fig. 1). In these galaxies, the mass in stars scattered into a central binary in 10^{10} yr would be completely negligible compared with M_{12} . Encounter-driven loss cone repopulation is only likely to be significant in galaxies with central relaxation times shorter than $\sim 10^{10}$ yr, since in these galaxies the mass scattered into the binary over the lifetime of the universe can be comparable with the binary’s mass. Figures 1 and 17 suggest that the only galaxies in this regime are those – like the Milky Way and M32 – which exhibit steep, power-law density profiles at $r \lesssim r_h$. If binary SBHs were ever present in these galaxies, the low-density cores which they produced have since presumably “filled in”

via encounters (§5.3) or via new star formation; hence the rate of scattering of stars into the binary’s sphere of influence would have been much lower in the past than inferred from the current density profiles.

These arguments were largely confirmed by Yu (2002) in her study of the influence of collisional loss-cone refilling on binary SBH evolution in a sample of nearby galaxies. Yu (2002) made a number of simplifying assumptions. (1) The galaxy’s density profile was assumed to be fixed in time; the “scouring” effect of the binary was ignored. (2) The distribution of stars around the binary’s loss cone was assumed to be in a collisional steady state, even in galaxies with nuclear relaxation times $\gg 10^{10}$ yr. (3) The influence of stars on the binary was computed using the results of scattering experiments on isolated binaries. Thus the hardening rate of the binary was computed from

$$\frac{d}{dt} \left(\frac{1}{a} \right) = H \frac{G\rho}{\sigma} \quad (92)$$

where ρ and σ are the stellar density and velocity dispersion and $H = H(a, e, q)$ a dimensionless rate coefficient (Hills 1983, Hills 1992, Mikkola & Valtonen 1992, Quinlan 1996, Merritt 2001). (4) Only changes in orbital angular momenta of the stars were considered, even though the stellar energy distribution would also change significantly in the time $\sim T_r$ required for significant feeding of the binary. Under these assumptions, Yu (2002) found that binary hardening time scales were longer than a Hubble time in almost all galaxies, with little dependence on binary mass ratio. Yu’s more detailed conclusions about the properties of “stalled” binaries are probably too rough to be very useful because of her neglect of the influence of the binary on the density profile.

N -body techniques would seem to be better suited to the collisional-loss-cone problem since they can easily deal with the strong, early effects of the binary on the stellar distribution, and, when coupled with regularization schemes, can accurately treat binary-star interactions without the need for rate coefficients derived from scattering experiments. An example of a mechanism that is not reproduced in scattering experiments is the “secondary slingshot,” the repeated interaction of a star with a binary (Milosavljević & Merritt 2003). But unless N is very large, relaxation in N -body simulations is so rapid that the binary’s loss cone remains essentially full, and the diffusive loss cone repopulation expected in real galaxies will not be reproduced (Milosavljević & Merritt 2003).

Figure 28 shows a promising early step in this direction, using N -body models with N up to 0.25×10^6 ; the Mikkola-Aarseth chain regularization algorithm was used for close SBH-SBH and SBH-star interactions (Mikkola & Aarseth 1990, Mikkola & Aarseth 1993, Aarseth 2003b). The initial galaxy models had $\rho \sim r^{-0.5}$ near the center, somewhat shallower than expected in real galaxies, although steeper than the constant-density cores assumed in most modelling studies (e.g. Hemsendorf et al. 2002, Chatterjee et al. 2003, Makino & Funato 2004). Adopting a steeper initial profile would have produced models with essentially full loss cones; in the models of Figure 28, one can show that the loss cone defined by the binary was only partially filled for the largest N considered (Merritt, Mikkola & Szell 2005). The N -dependence of the

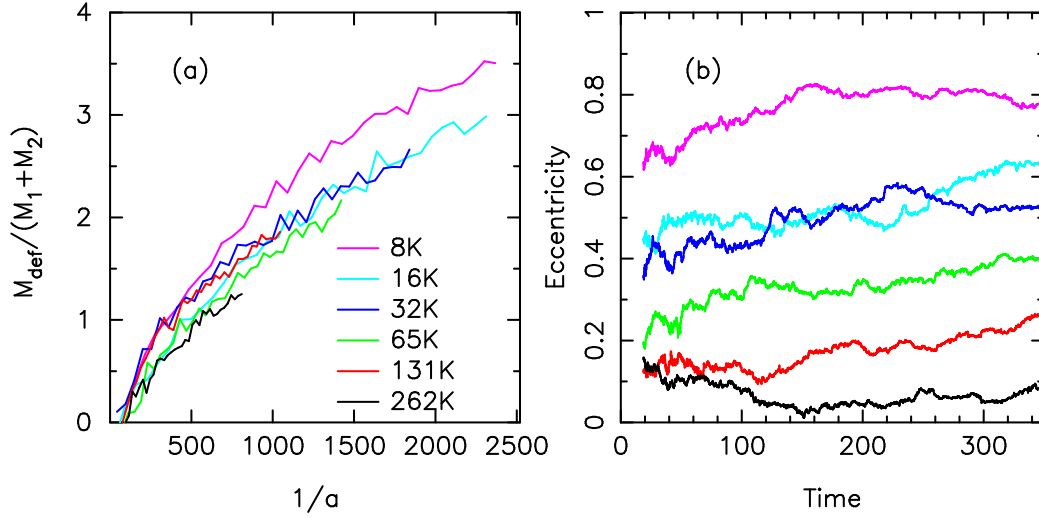


Figure 28. Results from a set of N -body integrations of the long-term evolution a massive binary in a galaxy with a $\rho \sim r^{-0.5}$ density cusp. Each curve is the average of a set of integrations starting from different random realizations of the same initial conditions. (a) Evolution of the mass deficit (Eq. 82). For a given value of binary separation a , the mass deficit is nearly independent of particle number N (b) Evolution of binary eccentricity. The eccentricity evolution is strongly N -dependent and tends to decrease with increasing N , suggesting that the eccentricity evolution in real binaries would be modest. (Adapted from Merritt, Mikkola & Szell 2005.)

Table 2. Regimes for Long-Term Evolution of Binary SBHs

Geometry	Loss-Cone Regime	Decay
Spherical/ Axisymmetric	Collisionless	$a^{-1} \propto \text{const}$ (stalls)
Spherical/ Axisymmetric	Collisional (diffusive)	$a^{-1} \propto t/N$
Spherical/ Axisymmetric	Collisional (full loss cone)	$a^{-1} \propto t + \text{const}$
Triaxial	Collisionless	$a^{-1} \propto t + \text{const}$

hardening rate was found to be $(d/dt)(1/a) \sim N^{-0.4}$, shallower than the $\sim N^{-1}$ dependence expected in real galaxies. Simulations like these can therefore still not be scaled to real galaxies, but they are useful in exploring the N -dependence of the changes induced by the binary on the galaxy. For instance, Figure 28 (a) shows that mass deficits are not strongly N -dependent when expressed as a function of the binary separation a . On the other hand, Figure 28 (b) suggests that the evolution of the binary's eccentricity is strongly N -dependent. This may explain the rather disparate results on eccentricity evolution in various N -body studies (Milosavljević & Merritt 2001, Hemsendorf et al. 2002, Aarseth 2003a).

7.2.3. Summary of Late Evolution Regimes Table 2 summarizes the different regimes of binary evolution in stellar nuclei. “Collisionless” refers here (as elsewhere in this article) to the large- N limit in which star-star gravitational encounters are inactive and stars move along fixed orbits, until interacting with the binary. Almost all galaxies are expected to be in this regime. The evolution of a real binary SBH may reflect a combination of these and other mechanisms, such as interaction with gas (Merritt & Milosavljević 2005). There is a close parallel between the final parsec problem and the problem of quasar fueling: both require that of order $10^8 M_\odot$ be supplied to the inner parsec of a galaxy in a time shorter than the age of the universe. Nature clearly accomplishes this in the case of quasars, probably through gas flows driven by torques from stellar bars. The same inflow of gas could contribute to the decay of a binary SBH in a number of ways: by leading to the renewed formation of stars which subsequently interact with the binary; by inducing torques which extract angular momentum from the binary; through accretion, increasing the masses of one or both of the SBHs and reducing their separation; etc.

7.3. Multiple Black Hole Systems

If binary decay stalls, an uncoalesced binary may be present in a nucleus when a third SBH, or a second binary, is deposited there following a subsequent merger. The multiple SBH system that forms will engage in its own gravitational slingshot interactions, eventually ejecting one or more of the SBHs from the nucleus and possibly from the galaxy and transferring energy to the stellar fluid.

If the infalling SBH is less massive than either of the components of the pre-existing binary, $M_3 < (M_1, M_2)$, the ultimate outcome is likely to be ejection of the smaller SBH and recoil of the binary, with the binary eventually returning to the galaxy center. The lighter SBH is ejected with a velocity roughly 1/3 the relative orbital velocity of the binary (Saslaw et al. 1974, Hut & Rees 1992), and the binary recoils with a speed that is lower by $\sim M_3/(M_1 + M_2)$. Each close interaction of the smaller SBH with the binary increases the latter’s binding energy by $\langle \Delta E/E \rangle \approx 0.4 M_3/(M_1 + M_2)$ (Hills & Fullerton 1980). If $M_3 > M_1$ or $M_3 > M_2$, there will most often be an exchange interaction, with the lightest SBH ejected and the two most massive SBHs forming a binary; further interactions then proceed as in the case $M_3 < (M_1, M_2)$.

During the three-body interactions, both the semi-major axis and eccentricity of the dominant binary change stochastically. Since the rate of gravitational wave emission is a strong function of both parameters ($\dot{E} \propto a^{-4}(1 - e^2)^{-7/2}$), the timescale for coalescence can be enormously shortened. This may be the most promising way to coalesce SBH binaries in the low-density nuclei of massive galaxies, where stalling of the dominant binary is likely.

This process has been extensively modelled using the PN2.5 approximation to represent gravitational wave losses (Peters & Mathews 1963) and assuming a fixed potential for the galaxy (Valtaoja et al. 1989, Mikkola & Valtonen 1990, Valtonen

et al. 1994). In these studies, there was no attempt to follow the pre-merger evolution of the galaxies or the interaction of the binary SBHs with stars. In two short non-technical contributions (submissions for the IEEE Gordon Bell prizes in 2001 and 2002), J. Makino and collaborators mention two N -body simulations of triple SBH systems at the centers of galaxies using the GRAPE-6, and (apparently) a modified version of NBODY1. Relativistic energy losses were neglected and the SBH particles all had the same mass. Plots of the time evolution of the orbital parameters of the dominant binary show strong and chaotic eccentricity evolution, with values as high as 0.997 reached for short periods. Such a binary would lose energy by gravity wave emission very rapidly, by a factor $\sim 10^8$ at the time of peak e compared with a circular-orbit binary with the same semi-major axis.

In a wide, hierarchical triple, $M_3 \ll (M_1, M_2)$, the eccentricity of the dominant binary oscillates through a maximum value of $\sim \sqrt{1 - 5 \cos^2 i/3}$, $|\cos i| < \sqrt{3/5}$, with i the mutual inclination angle (Kozai 1962). Blaes et al. (2002) estimated that the coalescence time of the dominant binary in hierarchical triples can be reduced by factors of ~ 10 via the Kozai mechanism; Iwasawa et al. (2005) recently observed Kozai oscillations in N -body simulations of galaxy models containing equal-mass triples.

If the binary SBH is hard when the third SBH falls in, the ejected SBH can gain enough velocity to escape the galaxy. If the three masses are comparable, even the binary can be kicked up to escape velocity. § One study (Volonteri et al. 2003) estimates (based on a very simplified model of the interactions) that the recoil velocity of the smallest SBH is larger than galactic escape velocities in 99% of encounters and that the binary escapes in 8% of encounters. Thus a significant fraction of nuclei could be left with no SBH, with an offset SBH, or with a SBH whose mass is lower than expected based on the $M_\bullet - \sigma$ or $M_\bullet - L_{bulge}$ relations.

There is a need for comprehensive N -body simulations of multiple-SBH systems that include gravitational loss terms, accurate (regularized) interactions between the SBH particles, and self-consistent treatment of the stars.

8. Acknowledgements

My understanding of the topics discussed here has benefited enormously over the years from discussions with many of my colleagues, including (but not limited to) D. Axon, P. Berczik, P. Coté, L. Ferrarese, D. Hoggie, P. Hut, S. Komossa, S. McMillan, M. Milosavljevic, S. Portegies Zwart, G. Quinlan, F. Rasio, A. Robinson, and R. Spurzem. This work was supported by grants AST-0206031, AST-0420920 and AST-0437519 from the NSF, grant NNG04GJ48G from NASA, and grant HST-AR-09519.01-A from STScI.

§ This idea was developed very thoroughly as a model for two-sided radio galaxies; the radio lobes were associated with matter entrained with the ejected SBHs (Valtonen & Heinämäki 2000 and references therein). While the “slingshot” model for radio galaxies has not gained wide acceptance, these papers are still an extremely valuable resource for information about the statistics of multiple-SBH interactions.

- Aarseth S J 2003a *Astrophys. Sp. Sci.* **285**, 367–372.
- Aarseth S J 2003b *Gravitational N-Body Simulations* Cambridge University Press Cambridge.
- Alexander T 1999 *Astrophys. J.* **527**, 835–850.
- Alexander T 2003 The Galactic Black Hole pp. 246–275.
- Alexander T 2005 *Physics Reports* **419**, 65–142.
- Amaro-Seoane P, Freitag M & Spurzem R 2004 *Mon. Not. R. Astron. Soc.* **352**, 655–672.
- Athanassoula E, Lambert J C & Dehnen W 2005 *Mon. Not. R. Astron. Soc.* **363**, 496–508.
- Bahcall J N & Wolf R A 1976 *Astrophys. J.* **209**, 214–232.
- Bahcall J N & Wolf R A 1977 *Astrophys. J.* **216**, 883–907.
- Baker J G, Centrella J, Choi D I, Koppitz M, van Meter J R & Miller M C 2006 *ArXiv Astrophysics e-prints*.
- Ballo L, Braitto V, Della Ceca R, Maraschi L, Tavecchio F & Dadina M 2004 *Astrophys. J.* **600**, 634–639.
- Balmaverde B & Capetti A 2006 *Astron. Astrophys.* **447**, 97–112.
- Barnes J, Hut P & Goodman J 1986 *Astrophys. J.* **300**, 112–131.
- Batsleer P & Dejonghe H 1993 *Astron. Ap.* **271**, 104–+.
- Baumgardt H, Makino J & Ebisuzaki T 2004a *Astrophys. J.* **613**, 1133–1142.
- Baumgardt H, Makino J & Ebisuzaki T 2004b *Astrophys. J.* **613**, 1143–1156.
- Baumgardt H, Makino J & Hut P 2005 *Astrophys. J.* **620**, 238–243.
- Begelman M C, Blandford R D & Rees M J 1980 *Nature* **287**, 307–309.
- Begelman M C & Rees M J 1978 *Mon. Not. R. Astron. Soc.* **185**, 847–860.
- Berczik P, Merritt D & Spurzem R 2005 *ArXiv Astrophysics e-prints*.
- Berczik P, Merritt D, Spurzem R & Bischof H P 2006 *ArXiv Astrophysics e-prints*.
- Bertone G & Merritt D 2005 *Modern Physics Letters A* **20**, 1021–1036.
- Bingeli B, Sandage A & Tarenghi M 1984 *Astron. J.* **89**, 64–82.
- Binney J J, Davies R L & Illingworth G D 1990 *Astrophys. J.* **361**, 78–97.
- Binney J & Mamon G A 1982 *Mon. Not. R. Astron. Soc.* **200**, 361–375.
- Binney J & Tremaine S 1987 *Galactic dynamics* Princeton, NJ, Princeton University Press, 1987, 747 p.
- Blaes O, Lee M H & Socrates A 2002 *Astrophys. J.* **578**, 775–786.
- Blanchet L, Qusailah M S S & Will C M 2005 *Astrophys. J.* **635**, 508–515.
- Bower G A, Green R F, Bender R, Gebhardt K, Lauer T R, Magorrian J, Richstone D O, Danks A, Gull T, Hutchings J, Joseph C, Kaiser M E, Weistrop D, Woodgate B, Nelson C & Malumuth E M 2001 *Astrophys. J.* **550**, 75–86.
- Boylan-Kolchin M, Ma C P & Quataert E 2004 *Astrophys. J.* **613**, L37–L40.
- Caon N, Capaccioli M & D’Onofrio M 1993 *Mon. Not. R. Astron. Soc.* **265**, 1013–+.
- Cappellari M & McDermid R M 2005 *Classical and Quantum Gravity* **22**, 347–+.
- Chakrabarty D & Saha P 2001 *Astron. J.* **122**, 232–241.
- Chatterjee P, Hernquist L & Loeb A 2003 *Astrophys. J.* **592**, 32–41.
- Cohn H & Kulsrud R M 1978 *Astrophys. J.* **226**, 1087–1108.
- Colgate S A 1967 *Astrophys. J.* **150**, 163–+.
- Coté P, ME X, YOU X & HIM X 2006 *ArXiv Astrophysics e-prints*.
- Crane P, Stiavelli M, King I R, Deharveng J M, Albrecht R, Barbieri C, Blades J C, Boksenberg A, Disney M J, Jakobsen P, Kamperman T M, Machetto F, Mackay C D, Paresce F, Weigelt G, Baxter D, Greenfield P, Jedrzejewski R, Nota A & Sparks W B 1993 *Astron. J.* **106**, 1371–1393.
- Cretton N & van den Bosch F C 1999 *Astrophys. J.* **514**, 704–724.
- David L P, Durisen R H & Cohn H N 1987a *Astrophys. J.* **313**, 556–575.
- David L P, Durisen R H & Cohn H N 1987b *Astrophys. J.* **316**, 505–516.
- Davidge T J, Olsen K A G, Blum R, Stephens A W & Rigaut F 2005 *Astron. J.* **129**, 201–219.
- de Vaucouleurs G 1948 *Annales d’Astrophysique* **11**, 247–+.
- Dehnen W 1995 *Mon. Not. R. Astron. Soc.* **274**, 919–932.
- Dejonghe H 1986 *Physics Reports* **133**, 217–313.

- Dejonghe H 1989 *Astrophys. J.* **343**, 113–124.
- Dejonghe H & Merritt D 1988 *Astrophys. J.* **328**, 93–102.
- Dejonghe H & Merritt D 1992 *Astrophys. J.* **391**, 531–549.
- Dokuchaev V I 1989 *Soviet Astronomy Letters* **15**, 167–+.
- Donley J L, Brandt W N, Eracleous M & Boller T 2002 *Astron. J.* **124**, 1308–1321.
- Dubinski J 1994 *Astrophys. J.* **431**, 617–624.
- Duncan M J & Shapiro S L 1983 *Astrophys. J.* **268**, 565–581.
- Eisenhauer F, Genzel R, Alexander T, Abuter R, Paumard T, Ott T, Gilbert A, Gillessen S, Horrobin M, Trippe S, Bonnet H, Dumas C, Hubin N, Kaufer A, Kissler-Patig M, Monnet G, Ströbele S, Szeifert T, Eckart A, Schödel R & Zucker S 2005 *Astrophys. J.* **628**, 246–259.
- Erwin P & Sparke L S 2002 *Astron. J.* **124**, 65–77.
- Evans N W 1994 *Mon. Not. R. Astron. Soc.* **267**, 333–360.
- Faber S M, Tremaine S, Ajhar E A, Byun Y, Dressler A, Gebhardt K, Grillmair C, Kormendy J, Lauer T R & Richstone D 1997 *Astron. J.* **114**, 1771–+.
- Fan X, Narayanan V K, Lupton R H, Strauss M A, Knapp G R, Becker R H, White R L, Pentericci L, Leggett S K, Haiman Z, Gunn J E, Ivezić Ž, Schneider D P, Anderson S F, Brinkmann J, Bahcall N A, Connolly A J, Csabai I, Doi M, Fukugita M, Geballe T, Grebel E K, Harbeck D, Hennessy G, Lamb D Q, Miknaitis G, Munn J A, Nichol R, Okamura S, Pier J R, Prada F, Richards G T, Szalay A & York D G 2001 *Astron. J.* **122**, 2833–2849.
- Fan X, Strauss M A, Schneider D P, Becker R H, White R L, Haiman Z, Gregg M, Pentericci L, Grebel E K, Narayanan V K, Loh Y S, Richards G T, Gunn J E, Lupton R H, Knapp G R, Ivezić Ž, Brandt W N, Collinge M, Hao L, Harbeck D, Prada F, Schaye J, Strateva I, Zakamska N, Anderson S, Brinkmann J, Bahcall N A, Lamb D Q, Okamura S, Szalay A & York D G 2003 *Astron. J.* **125**, 1649–1659.
- Favata M, Hughes S A & Holz D E 2004 *Astrophys. J. (Lett.)* **607**, L5–L8.
- Ferrarese et al. 2006 *ArXiv Astrophysics e-prints*.
- Ferrarese L, Cote P, Dalla Bonta E, Peng E W, Merritt D, Jordan A, Blakeslee J P, Hasegan M, Mei S, Piatek S, Tonry J L & West M J 2006 *ArXiv Astrophysics e-prints*.
- Ferrarese L & Ford H 2005 *Space Science Reviews* **116**, 523–624.
- Ferrarese L & Merritt D 2000 *Astrophys. J. (Lett.)* **539**, L9–L12.
- Ferrarese L, van den Bosch F C, Ford H C, Jaffe W & O’Connell R W 1994 *Astron. J.* **108**, 1598–1609.
- Filippenko A V & Ho L C 2003 *Astrophys. J.* **588**, L13–L16.
- Folkner W M, ed. 1998.
- Frank J & Rees M J 1976 *Mon. Not. R. Astron. Soc.* **176**, 633–647.
- Freitag M, Amaro-Seoane P & Kalogera V 2006 *ArXiv Astrophysics e-prints*.
- Freitag M & Benz W 2002 *Astron. Astrophys.* **394**, 345–374.
- Gair J R, Barack L, Creighton T, Cutler C, Larson S L, Phinney E S & Vallisneri M 2004 *Classical and Quantum Gravity* **21**, 1595–+.
- Gebhardt K, Richstone D, Ajhar E A, Lauer T R, Byun Y, Kormendy J, Dressler A, Faber S M, Grillmair C & Tremaine S 1996 *Astron. J.* **112**, 105–+.
- Gebhardt K, Richstone D, Kormendy J, Lauer T R, Ajhar E A, Bender R, Dressler A, Faber S M, Grillmair C, Magorrian J & Tremaine S 2000 *Astron. J.* **119**, 1157–1171.
- Gebhardt K, Richstone D, Tremaine S, Lauer T R, Bender R, Bower G, Dressler A, Faber S M, Filippenko A V, Green R, Grillmair C, Ho L C, Kormendy J, Magorrian J & Pinkney J 2003 *Astrophys. J.* **583**, 92–115.
- Genzel R, Pichon C, Eckart A, Gerhard O E & Ott T 2000 *Mon. Not. R. Astron. Soc.* **317**, 348–374.
- Genzel R, Schödel R, Ott T, Eisenhauer F, Hofmann R, Lehnert M, Eckart A, Alexander T, Sternberg A, Lenzen R, Clénet Y, Lacombe F, Rouan D, Renzini A & Tacconi-Garman L E 2003 *Astrophys. J.* **594**, 812–832.
- Gerhard O E & Binney J 1985 *Mon. Not. R. Astron. Soc.* **216**, 467–502.
- Gezari S, Halpern J P, Komossa S, Grupe D & Leighly K M 2003 *Astrophys. J.* **592**, 42–51.

- Ghez A M, Duchene G, Matthews K, Hornstein S D, Tanner A, Larkin J, Morris M, Becklin E E, Salim S, Kremenek T, Thompson D, Soifer B T, Neugebauer G & McLean I 2003 *Astrophys. J. (Lett.)* **586**, L127–L131.
- Ghez A M, Salim S, Hornstein S D, Tanner A, Lu J R, Morris M, Becklin E E & Duchene G 2005 *Astrophys. J.* **620**, 744–757.
- Gondolo P & Silk J 1999 *Physical Review Letters* **83**, 1719–1722.
- Gopal-Krishna, Biermann P L & Wiita P J 2003 *Astrophys. J.* **594**, L103–L106.
- Graham A W 2002 *Astrophys. J. (Lett.)* **568**, L13–L17.
- Graham A W 2004 *Astrophys. J. (Lett.)* **613**, L33–L36.
- Graham A W, Erwin P, Caon N & Trujillo I 2001 *Astrophys. J. (Lett.)* **563**, L11–L14.
- Graham A W, Erwin P, Trujillo I & Asensio Ramos A 2003 *Astron. J.* **125**, 2951–2963.
- Graham A W & Guzmán R 2003 *Astron. J.* **125**, 2936–2950.
- Graham A W, Merritt D, Moore B, Diemand J & Terzic B 2005 *ArXiv Astrophysics e-prints*.
- Haehnelt M G & Kauffmann G 2002 *Mon. Not. R. Astron. Soc.* **336**, L61–L64.
- Halpern J P, Gezari S & Komossa S 2004 *Astrophys. J.* **604**, 572–578.
- Hasan H, Pfenninger D & Norman C 1993 *Astrophys. J.* **409**, 91–109.
- Hasinger G, Miyaji T & Schmidt M 2005 *Astron. Ap.* **441**, 417–434.
- Heggie D C 1985 in J Goodman & P Hut, eds, ‘IAU Symp. 113: Dynamics of Star Clusters’ pp. 139–157.
- Heggie D C & Stevenson D 1988 *Mon. Not. R. Astron. Soc.* **230**, 223–241.
- Hemsendorf M, Sigurdsson S & Spurzem R 2002 *Astrophys. J.* **581**, 1256–1270.
- Hénon M 1961 *Annales d’Astrophysique* **24**, 369–+.
- Hénon M 1965 *Annales d’Astrophysique* **28**, 62–+.
- Hernquist L, Hut P & Kormendy J 1991 *Nature* **354**, 376–+.
- Herrmann F, Shoemaker D & Laguna P 2006 *ArXiv General Relativity and Quantum Cosmology e-prints*.
- Hills J G 1975 *Nature* **254**, 295–298.
- Hills J G 1983 *Astron. J.* **88**, 1269–1283.
- Hills J G 1988 *Nature* **331**, 687–689.
- Hills J G 1992 *Astron. J.* **103**, 1955–1969.
- Hills J G & Fullerton L W 1980 *Astron. J.* **85**, 1281–1291.
- Holley-Bockelmann K, Mihos J C, Sigurdsson S, Hernquist L & Norman C 2002 *Astrophys. J.* **567**, 817–827.
- Holley-Bockelmann K & Sigurdsson S 2006 *ArXiv Astrophysics e-prints*.
- Holley-Bockelmann K, Sigurdsson S, Mihos J C, Feldmeier J J, Ciardullo R & McBride C 2005 *ArXiv Astrophysics e-prints*.
- Hopman C & Alexander T 2006 *ArXiv Astrophysics e-prints*.
- Hudson D S, Reiprich T H, Clarke T E & Sarazin C L 2006 *ArXiv Astrophysics e-prints*.
- Hughes S A 2003 *Annals of Physics* **303**, 142–178.
- Hunter C & Qian E 1993 *Mon. Not. R. Astron. Soc.* **262**, 401–428.
- Hut P & Rees M J 1992 *Mon. Not. R. Astron. Soc.* **259**, 27P–30P.
- Ipsen J R 1978 *Astrophys. J.* **222**, 976–990.
- Iwasawa M, Funato Y & Makino J 2005 *ArXiv Astrophysics e-prints*.
- Jacobs V & Sellwood J A 2001 *Astrophys. J. (Lett.)* **555**, L25–L28.
- Jalali M A & de Zeeuw P T 2002 *Mon. Not. R. Astron. Soc.* **335**, 928–940.
- Jerjen H & Binggeli B 1997 in M Arnaboldi, G. S Da Costa & P Saha, eds, ‘ASP Conf. Ser. 116: The Nature of Elliptical Galaxies; 2nd Stromlo Symposium’ pp. 239–+.
- Jiang Z & Moss D 2002 *Mon. Not. R. Astron. Soc.* **331**, 117–125.
- Jimenez R, da Silva J P, Oh S P, Jorgensen U G & Merritt D 2006 *ArXiv Astrophysics e-prints*.
- Kalapotharakos C & Voglis N 2005 *Celestial Mechanics and Dynamical Astronomy* **92**, 157–188.
- Kalapotharakos C, Voglis N & Contopoulos G 2004 *Astron. J.* **428**, 905–923.
- Kandrup H E 1998 *Mon. Not. R. Astron. Soc.* **299**, 1139–1145.

- Kandrup H E & Sideris I V 2002 *Celestial Mechanics and Dynamical Astronomy* **82**, 61–81.
- Kandrup H E, Sideris I V, Terzić B & Bohn C L 2003 *Astrophys. J.* **597**, 111–130.
- Kandrup H E & Siopis C 2003 *Mon. Not. R. Astron. Soc.* **345**, 727–742.
- Kauffmann G & Haehnelt M 2000 *Mon. Not. R. Astron. Soc.* **311**, 576–588.
- Kendall P, Magorrian J & Pringle J E 2003 *Mon. Not. R. Astron. Soc.* **346**, 1078–1088.
- Khokhlov A & Melia F 1996 *Astrophys. J. Lett.* **457**, L61+.
- Kobayashi S, Laguna P, Phinney E S & Mészáros P 2004 *Astrophys. J.* **615**, 855–865.
- Kochanek C S 1994 *Astrophys. J.* **422**, 508–520.
- Komossa S 2002 *Reviews of Modern Astronomy* **15**, 27–+.
- Komossa S 2003 in ‘AIP Conf. Proc. 686: The Astrophysics of Gravitational Wave Sources’ pp. 161–174.
- Komossa S, Burwitz V, Hasinger G, Predehl P, Kaastra J S & Ikebe Y 2003 *Astrophys. J. (Lett.)* **582**, L15–L19.
- Komossa S, Halpern J, Schartel N, Hasinger G, Santos-Lleo M & Predehl P 2004 *Astrophys. J. Lett.* **603**, L17–L20.
- Kormendy J 1985 *Astrophys. J.* **295**, 73–79.
- Kozai Y 1962 *Astron. J.* **67**, 591–+.
- Kroupa P, Tout C A & Gilmore G 1993 *Mon. Not. R. Astron. Soc.* **262**, 545–587.
- Kuijken K 1993 *Astrophys. J.* **409**, 68–74.
- Kuijken K 1995 *Astrophys. J.* **446**, 194–+.
- Lauer T R, Ajhar E A, Byun Y I, Dressler A, Faber S M, Grillmair C, Kormendy J, Richstone D & Tremaine S 1995 *Astron. J.* **110**, 2622–+.
- Lauer T R, Faber S M, Ajhar E A, Grillmair C J & Scowen P A 1998 *Astron. J.* **116**, 2263–2286.
- Lauer T R, Gebhardt K, Richstone D, Tremaine S, Bender R, Bower G, Dressler A, Faber S M, Filippenko A V, Green R, Grillmair C J, Ho L C, Kormendy J, Magorrian J, Pinkney J, Laine S, Postman M & van der Marel R P 2002 *Astron. J.* **124**, 1975–1987.
- Li L X, Narayan R & Menou K 2002 *Astrophys. J.* **576**, 753–761.
- Lightman A P & Shapiro S L 1977 *Astrophys. J.* **211**, 244–262.
- Lynden-Bell D 1962 *Mon. Not. R. Astron. Soc.* **123**, 447–+.
- Lynden-Bell D & Inagaki S 1983 *Mon. Not. R. Astron. Soc.* **205**, 913–930.
- Macchetto F, Marconi A, Axon D J, Capetti A, Sparks W & Crane P 1997 *Astrophys. J.* **489**, 579–+.
- Madau P & Rees M J 2001 *Astrophys. J. (Lett.)* **551**, L27–L30.
- Magorrian J & Tremaine S 1999 *Mon. Not. R. Astron. Soc.* **309**, 447–460.
- Magorrian J, Tremaine S, Richstone D, Bender R, Bower G, Dressler A, Faber S M, Gebhardt K, Green R, Grillmair C, Kormendy J & Lauer T 1998 *Astron. J.* **115**, 2285–2305.
- Makino J, Fukushima T, Koga M & Namura K 2003 *Pub. Astron. Soc. J.* **55**, 1163–1187.
- Makino J & Funato Y 2004 *Astrophys. J.* **602**, 93–102.
- Marchant A B & Shapiro S L 1980 *Astrophys. J.* **239**, 685–704.
- Marconi A & Hunt L K 2003 *Astrophys. J. (Lett.)* **589**, L21–L24.
- Melbourne J, Wright S A, Barczys M, Bouchez A H, Chin J, van Dam M A, Hartman S, Johansson E, Koo D C, Lafon R, Larkin J, Le Mignant D, Lotz J, Max C E, Pennington D M, Stomski P J, Summers D & Wizinowich P L 2005 *Astrophys. J. Letts.* **625**, L27–L30.
- Merloni A, Nayakshin S & Sunyaev R A, eds 2005 *Growing black holes : accretion in a cosmological context* Springer Germany.
- Merritt D 1983 *Astrophys. J.* **264**, 24–48.
- Merritt D 1984 *Astrophys. J.* **276**, 26–37.
- Merritt D 1985 *Astron. J.* **90**, 1027–1037.
- Merritt D 1987 *Astrophys. J.* **319**, 55–60.
- Merritt D 1993 in ‘Structure, Dynamics and Chemical Evolution of Elliptical Galaxies’ pp. 275–+.
- Merritt D 1999 *Pub. Astron. Soc. Pacific* **111**, 129–168.
- Merritt D 2000 in ‘ASP Conf. Ser. 197: Dynamics of Galaxies: from the Early Universe to the Present’ pp. 221–+.

- Merritt D 2001 *Astrophys. J.* **556**, 245–264.
- Merritt D 2002 *Astrophys. J.* **568**, 998–1003.
- Merritt D 2004 *Physical Review Letters* **92**(20), 201304–+.
- Merritt D 2006 *ArXiv Astrophysics e-prints* .
- Merritt D & Ekers R D 2002 *Science* **297**, 1310–1313.
- Merritt D & Ferrarese L 2001a *Mon. Not. R. Astron. Soc.* **320**, L30–L34.
- Merritt D & Ferrarese L 2001b in ‘ASP Conf. Ser. 249: The Central Kiloparsec of Starbursts and AGN: The La Palma Connection’ pp. 335–+.
- Merritt D & Ferrarese L 2001c *Astrophys. J.* **547**, 140–145.
- Merritt D, Ferrarese L & Joseph C L 2001 *Science* **293**, 1116–1119.
- Merritt D, Mikkola S & Szell A 2005 *in preparation* .
- Merritt D & Milosavljević M 2002 in ‘Dark matter in astro- and particle physics. Proceedings of the International Conference DARK 2002, Cape Town, South Africa, 4 - 9 February 2002. H. V. Klapdor-Kleingrothaus, R. D. Viollier (eds.). Physics and astronomy online library. Berlin: Springer, ISBN 3-540-44257-X, 2002, p. 79 - 89’ pp. 79–+.
- Merritt D, Milosavljević M, Favata M, Hughes S A & Holz D E 2004 *Astrophys. J. (Lett.)* **607**, L9–L12.
- Merritt D & Milosavljević M 2005 *Living Reviews in Relativity* **8**, 8–+.
- Merritt D, Navarro J F, Ludlow A & Jenkins A 2005 *Astrophys. J. (Lett.)* **624**, L85–L88.
- Merritt D & Oh S P 1997 *Astron. J.* **113**, 1279–1285.
- Merritt D, Piatek S, Zwart S P & Hemsendorf M 2004 *Astrophys. J. (Lett.)* **608**, L25–L28.
- Merritt D & Poon M Y 2004 *Astrophys. J.* **606**, 788–798.
- Merritt D & Quinlan G D 1998 *Astrophys. J.* **498**, 625–+.
- Merritt D & Szell A 2005 *ArXiv Astrophysics e-prints* .
- Merritt D & Valluri M 1996 *Astrophys. J.* **471**, 82–+.
- Merritt D & Valluri M 1999 *Astron. J.* **118**, 1177–1189.
- Merritt D & Wang J 2005 *Astrophys. J.* **621**, L101–L104.
- Mikkola S & Aarseth S J 1990 *Celestial Mechanics and Dynamical Astronomy* **47**, 375–390.
- Mikkola S & Aarseth S J 1993 *Celestial Mechanics and Dynamical Astronomy* **57**, 439–459.
- Mikkola S & Valtonen M J 1990 *Astrophys. J.* **348**, 412–420.
- Mikkola S & Valtonen M J 1992 *Mon. Not. R. Astron. Soc.* **259**, 115–120.
- Miller G E & Scalo J M 1979 *Astrophys. J. Suppl.* **41**, 513–547.
- Miller M C & Colbert E J M 2004 *International Journal of Modern Physics D* **13**, 1–64.
- Milosavljević M & Merritt D 2001 *Astrophys. J.* **563**, 34–62.
- Milosavljević M & Merritt D 2003 *Astrophys. J.* **596**, 860–878.
- Milosavljević M, Merritt D & Ho L 2006 *ArXiv Astrophysics e-prints* .
- Milosavljević M, Merritt D, Rest A & van den Bosch F C 2002 *Mon. Not. R. Astron. Soc.* **331**, L51–L55.
- Milosavljević M & Phinney E S 2005 *Astrophys. J.* **622**, L93–L96.
- Miralda-Escudé J & Kollmeier J A 2005 *Astrophys. J.* **619**, 30–40.
- Miralda-Escudé J & Schwarzschild M 1989 *Astrophys. J.* **339**, 752–762.
- Morris M 1993 *Astrophys. J.* **408**, 496–506.
- Murphy B W, Cohn H N & Durisen R H 1991 *Astrophys. J.* **370**, 60–77.
- Navarro J F, Hayashi E, Power C, Jenkins A R, Frenk C S, White S D M, Springel V, Stadel J & Quinn T R 2004 *Mon. Not. R. Astron. Soc.* **349**, 1039–1051.
- Newton A J & Binney J 1984 *Mon. Not. R. Astron. Soc.* **210**, 711–730.
- Norman C A, May A & van Albada T S 1985 *Astrophys. J.* **296**, 20–34.
- Norman C & Silk J 1983 *Astrophys. J.* **266**, 502–515.
- Ozernoy L M 1976 *The Observatory* **96**, 67–69.
- Papaphilippou Y & Laskar J 1998 *Astron. Ap.* **329**, 451–481.
- Peebles P J E 1972a *Astrophys. J.* **178**, 371–376.
- Peebles P J E 1972b *Gen. Rel. Grav.* **3**, 61–00.
- Peng C Y, Ho L C, Impey C D & Rix H 2002 *Astron. J.* **124**, 266–293.

- Peters P C 1964 *Phys. Rev. B* **136**, 1224–1232.
- Peters P C & Mathews J 1963 *Phys. Rev.* **131**, 435–440.
- Phinney E S 1989 in M Morris, ed., ‘IAU Symp. 136: The Center of the Galaxy’ pp. 543–+.
- Poon M Y & Merritt D 2001 *Astrophys. J.* **549**, 192–204.
- Poon M Y & Merritt D 2002 *Astrophys. J. (Lett.)* **568**, L89–L92.
- Poon M Y & Merritt D 2004 *Astrophys. J.* **606**, 774–787.
- Portegies Zwart S F, Baumgardt H, Hut P, Makino J & McMillan S L W 2004 *Nature* **428**, 724–726.
- Preto M, Merritt D & Spurzem R 2004 *ArXiv Astrophysics e-prints* .
- Quinlan G D 1996 *New Astronomy* **1**, 35–56.
- Quinlan G D & Shapiro S L 1987 *Astrophys. J.* **321**, 199–210.
- Quinlan G D & Shapiro S L 1989 *Astrophys. J.* **343**, 725–749.
- Ravindranath S, Ho L C & Filippenko A V 2002 *Astrophys. J.* **566**, 801–808.
- Redmount I H & Rees M J 1989 *Comments on Astrophysics* **14**, 165–+.
- Rees M J 1984 *Annual Reviews of Astronomy and Astrophysics* **22**, 471–506.
- Rees M J 1990 *Science* **247**, 817–823.
- Richstone D O 1982 *Astrophys. J.* **252**, 496–507.
- Richstone D O & Tremaine S 1988 *Astrophys. J.* **327**, 82–88.
- Rodriguez C, Taylor G B, Zavala R T, Peck A B, Pollack L K & Romani R W 2006 *ArXiv Astrophysics e-prints* .
- Romero G E, Chajet L, Abraham Z & Fan J H 2000 *Astron. Astrophys.* **360**, 57–64.
- Roos N, Kaastra J S & Hummel C A 1993 *Astrophys. J.* **409**, 130–133.
- Safronov V S 1960 *Annales d’Astrophysique* **23**, 979–+.
- Saitoh T R & Wada K 2004 *Astrophys. J.* **615**, L93–L96.
- Salow R M & Statler T S 2001 *Astrophys. J. (Lett.)* **551**, L49–L52.
- Salpeter E E 1955 *Astrophys. J.* **121**, 161–+.
- Sambhus N & Sridhar S 2000 *Astrophys. J.* **542**, 143–160.
- Sambhus N & Sridhar S 2002 *Astron. Ap.* **388**, 766–770.
- Sanders R H 1970 *Astrophys. J.* **162**, 791–+.
- Saslaw W C 1973 *Pub. Astron. Soc. Pacific* **85**, 5–+.
- Saslaw W C, Valtonen M J & Aarseth S J 1974 *Astrophys. J.* **190**, 253–270.
- Schödel R, Eckart A, Genzel R, Merritt D, Alexander T, Ott T & Straubmeier C 2006 *ArXiv Astrophysics e-prints* .
- Schödel R, Ott T, Genzel R, Eckart A, Mouawad N & Alexander T 2003 *Astrophys. J.* **596**, 1015–1034.
- Schutz B F 2002 in M Gilfanov, R Sunyaev & E Churazov, eds, ‘Lighthouses of the Universe: The Most Luminous Celestial Objects and Their Use for Cosmology Proceedings of the MPA/ESO/, p. 207’ pp. 207–+.
- Schwarzschild M 1979 *Astrophys. J.* **232**, 236–247.
- Schwarzschild M 1981 in ‘Structure and Evolution of Normal Galaxies’ pp. 43–53.
- Schwarzschild M 1993 *Astrophys. J.* **409**, 563–577.
- Sérsic J L 1968 *Atlas de galaxies australes* Cordoba, Argentina: Observatorio Astronomico, 1968.
- Sesana A, Haardt F, Madau P & Volonteri M 2004 *Astrophys. J.* **611**, 623–632.
- Shapiro S L 1977 *Astrophys. J.* **217**, 281–286.
- Shapiro S L & Marchant A B 1978 *Astrophys. J.* **225**, 603–624.
- Shaw M, Axon D, Probst R & Gatley I 1995 *Mon. Not. R. Astron. Soc.* **274**, 369–387.
- Shields G A & Wheeler J C 1978 *Astrophys. J.* **222**, 667–674.
- Shlosman I, Begelman M C & Frank J 1990 *Nature* **345**, 679–686.
- Sigurdsson S & Rees M J 1997 *Mon. Not. R. Astron. Soc.* **284**, 318–326.
- Silk J & Rees M J 1998 *Astron. Astrophys.* **331**, L1–L4.
- Sinai Y B 1963 *Sov. Math.-Dokl.* **4**, 1818–1800.
- Spitzer L 1971 in D. J. K O’Connell, ed., ‘Pontificiae Academiae Scientiarum Scripta Varia, Proceedings of a Study Week on Nuclei of Galaxies, held in Rome, April 13-18, 1970, Amsterdam: North

- Holland, and New York: American Elsevier, 1971, edited by D.J.K. O'Connell., p.443' pp. 443–+.
- Spitzer L 1987 *Dynamical evolution of globular clusters* Princeton, NJ, Princeton University Press, 1987, 191 p.
- Spitzer L J & Saslaw W C 1966 *Astrophys. J.* **143**, 400–+.
- Spitzer L J & Stone M E 1967 *Astrophys. J.* **147**, 519–+.
- Spitzer L & Shull J M 1975 *Astrophys. J.* **201**, 773–782.
- Sridhar S & Touma J 1999 *Mon. Not. R. Astron. Soc.* **303**, 483–494.
- Statler T S, Emsellem E, Peletier R F & Bacon R 2004 *Mon. Not. R. Astron. Soc.* **353**, 1–14.
- Sunyaev R & Churazov E 1998 *Mon. Not. R. Astron. Soc.* **297**, 1279–1291.
- Syer D & Ulmer A 1999 *Mon. Not. R. Astron. Soc.* **306**, 35–42.
- Syer D & Zhao H 1998 *Mon. Not. R. Astron. Soc.* **296**, 407–413.
- Thorne K S & Braginskii V B 1976 *Astrophys. J. (Lett.)* **204**, L1–L6.
- Tonry J L 1984 *Astrophys. J. (Lett.)* **283**, L27+.
- Toomre A 1977 in B. M Tinsley & R. B Larson, eds, 'Evolution of Galaxies and Stellar Populations' pp. 401–+.
- Tremaine S 1997 in J. N Bahcall & J. P Ostriker, eds, 'Unsolved problems in astrophysics' Princeton, NJ: Princeton University Press, 1997 pp. 137–158.
- Trujillo I, Erwin P, Asensio Ramos A & Graham A W 2004 *Astron. J.* **127**, 1917–1942.
- Ulvestad J S & Wilson A S 1984 *Astrophys. J.* **285**, 439–452.
- Valluri M 1999 in 'ASP Conf. Ser. 182: Galaxy Dynamics - A Rutgers Symposium' pp. 195–+.
- Valluri M, Ferrarese L, Merritt D & Joseph C L 2005 *Astrophys. J.* **628**, 137–152.
- Valluri M & Merritt D 1998 *Astrophys. J.* **506**, 686–711.
- Valluri M & Merritt D 2000 in 'The Chaotic Universe, Proceedings of the Second ICRA Network Workshop, Advanced Series in Astrophysics and Cosmology, vol.10, Edited by V. G. Gurzadyan and R. Ruffini, World Scientific, 2000, p.229' pp. 229–+.
- Valluri M, Merritt D & Emsellem E 2004 *Astrophys. J.* **602**, 66–92.
- Valtaoja E, Teräsranta H, Tornikoski M, Sillanpää A, Aller M F, Aller H D & Hughes P A 2000 *Astrophys. J.* **531**, 744–755.
- Valtaoja L, Valtonen M J & Byrd G G 1989 *Astrophys. J.* **343**, 47–53.
- Valtonen M J 1996 *Comments on Astrophysics* **18**, 191–206.
- Valtonen M J & Heinämäki P 2000 *Astrophys. J.* **530**, 107–123.
- Valtonen M J, Mikkola S, Heinamaki P & Valtonen H 1994 *Astrophys. J. (Suppl.)* **95**, 69–86.
- van den Bergh S 1986 *Astron. J.* **91**, 271–274.
- van der Marel R P 1999a in 'IAU Symp. 186: Galaxy Interactions at Low and High Redshift' pp. 333–+.
- van der Marel R P 1999b *Astron. J.* **117**, 744–763.
- van der Marel R P 2004 in L. C Ho, ed., 'Coevolution of Black Holes and Galaxies' pp. 37–+.
- van der Marel R P, Cretton N, de Zeeuw P T & Rix H W 1998 *Astrophys. J.* **493**, 613–+.
- van der Marel R P, Evans N W, Rix H W, White S D M & de Zeeuw T 1994 *Mon. Not. R. Astron. Soc.* **271**, 99–117.
- Vandervoort P O 1984 *Astrophys. J.* **287**, 475–486.
- Verolme E K, Cappellari M, Copin Y, van der Marel R P, Bacon R, Bureau M, Davies R L, Miller B M & de Zeeuw P T 2002 *Mon. Not. R. Astron. Soc.* **335**, 517–525.
- Volonteri M, Madau P & Haardt F 2003 *Astrophys. J.* **593**, 661–666.
- Wang J & Merritt D 2004 *Astrophys. J.* **600**, 149–161.
- Wehner E & Harris W 2006 *ArXiv Astrophysics e-prints*.
- Wilson A S & Colbert E J M 1995 *Astrophys. J.* **438**, 62–71.
- Xie G 2003 *Publications of the Yunnan Observatory* **95**, 107–116.
- Young P 1980 *Astrophys. J.* **242**, 1232–1237.
- Young P J 1977 *Astrophys. J.* **215**, 36–52.
- Young P J, Shields G A & Wheeler J C 1977 *Astrophys. J.* **212**, 367–382.

Yu Q 2002 *Month. Not. R. Astron. Soc.* **331**, 935–958.

Yu Q & Tremaine S 2002 *Mon. Not. R. Astron. Soc.* **335**, 965–976.

Zhao H, Carollo C M & de Zeeuw P T 1999 *Mon. Not. R. Astron. Soc.* **304**, 457–464.

Zhao H, Haehnelt M G & Rees M J 2002 *New Astronomy* **7**, 385–394.